DEGRADATION OF COLORED INDUSTRIAL WASTEWATERS BY ADVANCED OXIDATION PROCESSES

by

Fatma Nihan DOĞAN

A thesis submitted to

the Graduate Institute of Science and Engineering

of

Fatih University

in partial fulfillment of the requirements for the degree of

Master of Science

in

Environmental Engineering

January 2012
Istanbul, Turkey

APPROVAL PAGE

I certify that this thesis satisfies all the requirements as a thesis for the degree of Master of Science.

Assist. Prof. Dr. Sami GÖREN
Head of Department

This is to certify that I have read this thesis and that in my opinion it is fully adequate, in scope and quality, as a thesis for the degree of Master of Science.

Assoc. Prof. Dr. Gökçe T. GÜYER
Supervisor

Assist. Prof. Dr. Sami GÖREN
Co-Supervisor

Examining Committee Members

Assoc. Prof. Dr. Gökçe T. GÜYER _____

Assist. Prof. Dr. Sami GÖREN _____

Assoc. Prof. Dr. Abdulhadi BAYKAL _____

Assist. Prof. Dr. Mustafa PETEK _____

It is approved that this thesis has been written in compliance with the formatting rules laid down by the Graduate Institute of Sciences and Engineering.

Assoc. Prof. Dr. Nurullah ARSLAN
Director

January 2012

DEGRADATION OF COLORED INDUSTRIAL WASTEWATERS BY ADVANCED OXIDATION PROCESSES

Fatma Nihan DOĞAN

M. S. Thesis – Environmental Engineering
January 2012

Supervisor: Assoc. Prof. Dr. Gökçe TEZCANLI GÜYER

Co-Supervisor: Assist. Prof. Dr. Sami GÖREN

ABSTRACT

The effluent of textile industry is a major source of pollution due to its high chemical oxygen demand, dark color and refractory organic compounds. Studies have shown that conventional treatment methods may not be enough for appreciable color reduction. Although it is possible to remove color via activated carbon adsorption or chemical coagulation, these treatment methods mainly transfer the pollution from liquid phase to solid phase.

Over the last decades, Advanced Oxidation Processes (AOPs) have shown to be a promising technique for decolorization and refractory compound degradation. Except Fenton processes, AOPs have also the advantage of no sludge production. Besides those advantages, AOPs have disadvantages of high operational cost due to electricity consumption in case of UV or ultrasonic generator usage. Minimization of the required irradiation (UV or sonication) time, thus, the energy consumption by optimization of the other reaction conditions, such as operational pH, frequency, chemical types, chemical concentrations, and pollutant/oxidant ratio, therefore, is very important. AOPs are based

on the hydroxyl radical (•OH) generation that attacks to organic compounds. It results as the degradation of organic matters.

The objective of this study were to investigate the effectiveness of advanced oxidation by applying UV with hydrogen peroxide, Photo-Fenton process, sonolysis, ozonation and combinations of them for decolorization of biologically treated textile industry effluents. In addition to color removal efficiency, the residual total organic carbon (TOC), phenol, Chemical Oxygen Demand (COD), Total Dissolved Solids (TDS) and toxicity has also been determined, as an important indicator of the treatment effectiveness. The effects of major process variables such as oxidant dose, pH, sonication frequency, and irradiation time on decolorization efficiency were investigated for each studied AOPs. Finally, economic analysis of each studied AOPs were conducted.

It was found that Advanced Oxidation Processes are promising technologies for the treatment of textile wastewaters. Color monitoring and Microtox toxicity experiments showed that studied AOPs efficiently decolorized the real textile wastewater without the formation of any toxic by-products.

In this study, the several experiments were carried out by using various AOPs; UV/ H_2O_2, Fenton, Photo-Fenton, US-Alone, Ozone-Alone, Ozone/ H_2O_2, Ozone/US, and Ozone/US/ H_2O_2. The 30 min color removal efficiency (%) of the studied AOPs are in the order: photo-Fenton processes > UV/H_2O_2 > US/Ozone > US/Ozone/H_2O_2 > Ozone-Alone > Ozone/ H_2O_2 > US-Alone and the corresponding % color removal are as 100%, 95%, 83%, 80%, 78% 68% and 21% respectively. The lowest operating costs were calculated for UV/ H_2O_2 and photo-Fenton processes. The operational cost of Photo-Fenton process and UV/ H_2O_2 was 1.29 Euro/m^3 and 0.64 Euro/m^3, respectively.

Keywords: Advanced Oxidation Process (AOP), textile wastewaters, COD, TOC, •OH radicals, toxicity

RENKLİ ENDÜSTRİYEL ATIKSULARIN İLERİ OKSİDASYON PROSESLERİ İLE ARITIMI

Fatma Nihan DOĞAN

Yüksek Lisans Tezi – Çevre Mühendisliği
Ocak 2012

Tez yöneticisi: Doç. Dr. Gökçe TEZCANLI GÜYER

Tez Eş-Yöneticisi: Yrd. Doç. Dr. Sami GÖREN

ÖZ

Tekstil endüstrisi atıksuları yüksek kimyasal oksijen ihtiyaçları, koyu renkleri ve degredasyona dirençli organik madde muhtevası ile çevre açısından ana kirleticilerdendir. Bir çok araştırma geleneksel arıtma methodlarının renk giderimine bir katkı sağlamadığını göstermektedir. Aktif karbon adsorbsiyonu veya kimyasal koagülasyon ile renk giderimi gerçekleştirilse de, bu methodlar sadece sıvı fazı katı faza çevirirler.

Son zamanlardaki çalışmalar ile birlikte İleri Oksidasyon Prosesleri (İOP), renk giderimi ve direçli maddelerin degredasyonu açısından umut vermektedir. Fenton prosesleri hariç İOP'lerde çamur problemi de oluşmamaktadır. Bu avatajlarının yanında, UV ve/veya ultrasonic cihazları içeren İOP'ler yüksek işletme maliyetlerine sahiptirler. Bu maliyeti minimuma indirmek için, çalışılan sistemlerde pH, frekans, kimyasal türü ve konsantrasyonu, kirletici/oxidant oranı belirlenerek optimum çalışma şartları sağlanmalıdır. İOP'ler organik maddenin degredasyonunu sağlayacak hidroksil radikali (•OH) üretim temeline dayanırlar.

Bu çalışmanın amacı ileri oksidasyon proseslerinin verimliliğini araştırmaktır. Çalışmada kullanılan İOP sistemleri UV/H_2O_2, foto-Fenton, sonoliz, ozonlama ve bunların kombinasyonundan oluşmaktadır. Çalışılan atıksu numunleri, biyolojik arıtma tesisi çıkışından alınmıştır. Renk giderme verimlerinin yanı sıra sistem arıtma verimleri toplam organik karbon (TOK), kimyasal oksijen ihtiyacı (KOİ), toplam çözünmüş madde ve toksisite açısından belirlenmiştir. Her bir İOP'nin optimum çalışma şartları oxidant miktarı, pH, ultrasonic frekansı gibi değişkenlerle ayarlanmıştır. Son olarak, çalışılan İOP'lerin ekonomik analizi yapılmıştır.

Tekstil atiksularinin ileri oksidasyon prosesleri ile arıtımı yüksek verimde gerçekleştirilmiştir. Renk giderimi ve Microtox toksisite analizleri – hiç bir ara toksik ürün oluşmamıştır- açısından değerlendirildiğinde İOP'ler ümit vadeden teknolojilerdir.

Çalışmada UV/ H_2O_2,Fenton, Photo-Fenton, US, Ozone, Ozone/ H_2O_2, Ozone/US, and Ozone/US/ H_2O_2 ileri oksidasyon prosesleri kullanılmıştır. 30 dakikalık renk giderimlerine baktığımızda, photo-Fenton > UV/H_2O_2 > US/Ozone > US/Ozone/H_2O_2 > Ozone > Ozone/ H_2O_2 > US sıralamasını sırasıyla şu yüzdeler ile görürüz: 100%, 95%, 83%, 80%, 78% 68% and 21%. İşletme maliyeti açısından en ucuz sistemler UV/ H_2O_2 ve photo-Fenton'dur. Photo-Fenton prosesi için isletme maliyeti 1.29 Euro/m^3, UV/ H_2O_2 için 0.64 Euro/m^3'dür.

Anahtar Kelimeler: İleri Oksidasyon Prosesleri (İOP), tekstil atıksuları, KOİ, TOK, •OH radikali, toksisite

DEDICATION

To my dear, precious, and esteemed family

ACKNOWLEDGEMENT

First of all, I would like to express my most sincere appreciation and gratitude to my chief supervisor Assoc. Prof. Dr. Gökçe TEZCANLI GÜYER, thank you for giving me the opportunity to work with you and for all you have done for me and for our work during the last years. Apart from improving my knowledge, you have succeeded in showing me how to plan research and, particularly, how to discuss results. Thank you for guiding me and transferring me your research methodology.

I would like to thank the head of our department and co-advisor Assist. Prof. Dr. Sami GÖREN for his precious and kind help.

I thank as well all my colleagues in the Department of Environment Engineering, for being a strong team and especially to Abdülkadir, Ramazan, Yüsra and Saida because without them it would have been much harder to develop this thesis. And I am also especially thankful to my mum, Ayşe YILDIZ to support me in my academic studies.

Most of all, I am indebted to my husband Mehmet DOĞAN for his love, friendship but also his guidance while during the thesis. My sincere warmest thanks are for him.

F.Nihan DOĞAN

TABLE OF CONTENTS

LIST OF TABLES

TABLE

LIST OF FIGURES

FIGURE

LIST OF SYMBOLS AND ABBREVATIONS

SYMBOLS/ABBREVATIONS

A	Absorbance
AEPA	Australian Environmental Protection Agency
AOP	Advanced Oxidation Process
AWWARF	American Water Works Association Research Foundation
BOD	Biological Oxygen Demand
CO_2	Carbon Dioxide
CO_3	Carbonate
COD	Chemical Oxygen Demand
DOC	Dissolved Organic Carbon
ε	Extinction Coefficient
EC_{50}	Effective Concentration
EE/O	Electrical Energy per Order
EPA	Environmental Protection Agency
ETPI	Environmental Technology Program for Industry
GC-MS	Gas Chromatography - Mass Spectrometry
H_2O_2	Hydrogen Peroxide
H_2SO_4	Sulfuric Acid
HCO_3	Bicarbonate
HPLC	High Performance Liquid Chromatography
hv	Ultraviolet irradiation
ISO	International Standards Organization
k	Kinetic Rate Constant
K	Kelvin
kHz	Kilo Hertz

kWh	Kilo Watt Hour
mM	Milimolar
MS	Mass Spectrometry
NaCl	Sodium Chloride
nm	Nanometer
NOM	Natural Organic Matters
O_3	Ozone
O&M	Operating and Maintaining
•OH	Hydroxyl radical
OP	Oxidation Potential
ppb	Part per billion
Pt-Co	Platinum-Cobalt
RES	Chromaticity Number (Renklilik Sayısı)
T	Temperature
t	Time
TDS	Total Dissolved Solids
TDS	Total Dissolved Solids
TOC	Total Organic Compounds
TREDAŞ	Tekirdağ Elektrik Dağıtım A.Ş.
TSS	Total Suspended Solids
TU	Toxicity Unit
US	Ultrasound
UV	Ultra Violet
VOC	Volatile Organic Compounds
WCQA	Water Contamination Quality Act
WHO	World Health Organization

CHAPTER 1

INTRODUCTION

The problem of wastewaters and keeping the sources gets an important challenge nowadays that we are in industrial age. The domestic use of water and industrial activities, especially in developed countries, generate high amounts of wastewater, which disposal to natural bodies causes considerable negative effects in the environment. This fact makes obligation to restore wastewaters for new uses and develop new technologies of water treatment processes.

The relationship of industrial activity and environmental problems is deeply documented. Since the effluents of some industrial wastewaters become more toxic and/or refractory, innovative oxidation technologies have been developed. These technologies are capable of transforming toxic and refractory compounds into harmless end products. Advanced oxidation processes (AOPs) are one of these technologies that gaining more importance day by day. AOPs are widely studied on the removal of color in textile, leather and yeast industries. Especially, the textile industry produces large quantities of highly colored effluents, which are generally toxic and resistant to destruction by biological methods. The discharge of these colored industries' effluents to water supplies is one of the major environmental problems. The most detrimental points of the pollution are strong color, aesthetically unwanted situation, high and unstable pH, high chemical oxygen demand (COD) and the presence of suspended solids, considerable amounts of heavy metals (e.g. Cr, Ni or Cu), chlorinated organic compounds and surfactants (Bircher et al.,1997; Ince et al., 1997). Moreover, the colored effluents reach the natural water strongly absorbs sunlight, thus impeding

photosynthetic activity of aquatic plants and seriously threatening the whole ecosystem (Kuo, 1992).

The textile industry is one of the complicated industries among manufacturing industries. Various toxic chemicals such as complexing, sizing, wetting, softening, anti-felting and finishing agents, biocides, carriers, halogenated benzenes, surfactants, phenols, pesticides, dyes and many other additives are used in wet processes which are mainly called washing, scouring, bleaching, mercerizing, dyeing and finishing processes. As a result, textile facilities produce highly toxic wastewater. Most of the dyestuffs used are complexly structured polymers with low biodegradability. The traditional treatment techniques applied in textile wastewaters such as coagulation/flocculation, membrane separation (ultrafiltration, reverse osmosis) or elimination by activated carbon adsorption, only do phase transfer of the pollutant and biological treatment is not a complete solution. Among many options, the development of processes to transform the toxic and hazardous pollutants into harmless compounds is one of the most effective solutions.

Main pollution in textile wastewater comes from dyeing and finishing processes. These processes wide range of chemicals and dyestuffs that are organic and inorganic complex structure. Conventional treatment methods with dealing this kind of wastewater are not enough to meet the limits. It has been widely reported that many dye chemicals are difficult to degrade by using conventional biological treatment units. Advanced Oxidation Processes (AOPs) appear to be a promising field of study for wastewater treatments. AOPs include several techniques such as ozonation, Fenton, photo-Fenton, photo catalysis, combined ultrasound systems, etc.

In this study, various AOPs have been investigated for textile wastewater samples from the selected industry, Ergene Basin, Turkey. Ergene Basin has become a center of industrialization due to the geographical location. Especially, eastern part of the basin has intensive industrialization. One of the biggest reasons of this intensive industrialization is closeness to Istanbul. After 1990, industrialization has brought a number of environmental problems because of unplanned and intense industrialization. A significant part of industrial facilities are located in the origin of Ergene River that centered in Corlu-Cerkezkoy sub-basin and so that, the pollution has seen in this part

markedly. Among those industries textile industry has 25% intensity that makes it the largest one of the basin. Therefore, the studied samples in this research have taken one of the textile industries, which is located in this area. The company is working on dyeing, finishing and printing processes of the textiles. The daily capacity of the plant is 2500 m^3/day. The company is in the scope of the Table 10.2 in the Water Contamination Quality Control Act (WCQA). The samples were collected from the effluent of biological treatment unit. It was noticed from the collected samples that the biological treatment had no effect on color. AOPs has applied to the samples for color removal and degradation of other organic compounds with toxicity and intermediate product determination.

This experimental work evaluates the efficiency of applying AOPs for the treatment of textile industrial wastewaters in terms of color, TOC, and COD degradation. Furthermore, it is aimed to examine the toxicity and intermediate products. Fenton, Photo-Fenton, UV/hydrogen peroxide, ozonation, ultrasound and combinations of them have been applied to textile wastewater effluents to evaluate the operation conditions for these processes and determine the optimum process. Cost analyses of each optimum system have done like real-scale applied. Since the color becomes a pollutant criteria that came into force as 280 Pt-Co limit value, the studies of decolorization of industrial wastewaters get an importance. This thesis, especially the economic part of it, aims to assist industries as well the academic world with the various combinations of AOPs.

CHAPTER 2

THEORITICAL BACKGROUND

2.1 TEXTILE INDUSTRY WASTEWATER

Textile industry employs different kinds of chemicals, depending on the nature of the raw material and products (Aslam et al., 2004). It is estimate that about 10% of them are lost in industrial wastewater (Young and Yu, 1997). The wastewater generated by the different production steps (i.e. sizing of fibers, scouring, desizing, bleaching, washing, mercerization, dyeing and finishing) has high pH and temperature. It also contains high concentration of organic matter, non-biodegradable matter, toxic substances, detergents and soaps, oil and grease, sulfide, sodas, salts and alkalinity. High salt conditions (typically up to 100 g L^{-1} sodium chloride) of the reactive dyebaths result in high-salt wastewater, which further exacerbates both their treatment and disposal (Rodriguez, 2003). The dyestuff activities create wastewaters that contain high concentration of reactive dyes (Neppolian et al., 2001; Rodríguez et al., 2002). As a result, textile industry is challenge with color removal not only for aesthetic reasons also with toxicity of chemicals used in the textile milling processing, and adverse effects of dark colored effluents to photosynthetic activity of aquatic life. These reactive dyes are highly water soluble and non-degradable under the conventional treatment methods (Neppolian et al., 2001; Rodriguez et al., 2002). Pagga and Brown (1986) reported that out of 87 dyestuffs only 47% are biodegradable.

Characteristics of textile wastewater vary from plant to plant depending upon the processes used. Textile wastewaters exhibit low Biological Oxygen Demand (BOD) to COD ratio, reflecting large amount of non-biodegradable organic matter. The

contamination observed in most of industry wastewater is higher than the limits. The current practice in textile mills is to discharge the wastewater into the local environment without any treatment. This wastewater causes serious impacts on natural water bodies and land in the surrounding area. High values of COD and BOD, presence of particulate matter and sediments, and oil and grease in the effluents causes depletion of dissolved oxygen, which has an adverse effect on the marine ecological system. Effluent from mills also contains chromium, chemicals; effluents are dark in color, which increases the turbidity of water body. This in turn hampers the photosynthesis process, causing alteration in the habitat (Rodriguez, 2003). Besides, the hazardous chemical content in textile water has some serious impacts on the health and safety of workers. Contact with chemical puts them the high risk bracket for contracting skin diseases like chemical burns, irritation, ulcers, etc. and even respiratory problems (ETPI, 2003).

Pollutants associated with dyeing may originate from the dyes themselves (e.g., toxicity, metals, color) or derive from auxiliary chemicals used during the dyeing process (e.g., salt, surfactants, levelers, lubricants, and alkalinity). Dyeing contributes essentially all of the salt and color in effluent from textiles operations (EPA, 1996).

2.1.1 Textile Dyestuffs

Textiles are dyed using many different colorants, which may be classified in several ways (e.g. according to chemical constitutions, dyeing property, solubility). The primary classification of dyes is based on the fibers to which they can be applied, and the chemical nature of each dye determines the fibers for which the dye has affinity (Tezcanli, 2003). The major dye classes and the types of fibers for which they applied can be seen in Table 2.1. The bulk of the dyes ending up in the wastewater belong to the group of azo-dyes (Wu et al., 2001). A large family of compounds all consisting of two aromatic moieties, connected with $-N=N-$ double bond. Breakage of these aromatic bonds causes decolorization. Azo bonds are the easiest oxidisable part of the dyes and therefore transformation of azo bond linkage, leading decolorization. Most of the studies results that color removal occur faster than COD removal (Ertas, 2001).

Table 2.1 Dye classes and their associated fibers (EPA, 1996)

Dye Class	Fibers
Acid	Wool and nylon (polyamide)
Basic	Acrylic, certain polyesters
Direct	Cotton, rayon and other cellulosic
Disperse	Polyester, acetate, and other synthetics
Fiber reactive	Cotton and other cellulosic, wool
Mordant	Natural fibers
Vat	Cotton and other cellulosic

2.1.2 Textile Industry Processing

The textile industry is distinguished by raw material used and this determines the volume of water required for production as well as wastewater generated. Slashing, bleaching, mercerizing, and dyeing are the major water consumption activities. Textile manufacturing operations produces wide range of pollutants due to the different characteristics of effluents. Specific water use varies from 60-400 l/kg of fabric, depending on the type of fabric (AEPA, 1998). Every process and operation within a textile dyeing and finishing plant has an environmental aspect that should be considered and for which environmental performance can potentially be improved. Table 2.2 shows the textile wet processing units and additional matters in these units.

Table 2.2 Different stages of textile wet processing (Hai et al., 2007)

Process	
Slashing/Sizing	Cotton or synthetic threads are treated with a large amount of reusable thickening agent to impart tensile strength and smoothness.
Desizing	To allow further wet processing, remove thickening agent with a weak oxidizing agent, boiling water/detergent
Scouring	Impurities in natural fibers (grease, wax etc.) or in synthetic fibers (catalysts, low molecular weight compounds etc.) are removed using caustic, - soda/ash, detergent etc.
Bleaching	Naturally occurring pigments are removed using peroxide and caustic.
Mercerizing	Cotton is treated with concentrated caustic to correct curling of fiber and reducing shrinkage and increasing dye affinity, following removal of the added chemical by warm water/detergent wash.
Weight Reduction	Polyester fiber is treated with caustic, following its removal by hot and cold-water wash, whereupon 10-20% of weight of fiber expelled as organic acid.
Dyeing and Rinsing	Different types of dyes along with wide range of dyeing-auxiliaries, e.g., electrolyte, dispersing agent, smoothing agent, surfactants etc. are applied. Hot water/detergent is applied to remove unfixed dye and auxiliaries.
Oiling	To increase the cohesion of the fibers and aid in spinning, olive oil/mineral oil with non-ionic emulsifier is sprayed on wool and washed out later on.
Fulling	Loosely woven wool from the loom is shrunk into a tight, closely woven cloth using detergent, caustic, sequestering agent, which are washed out later on
Carbonizing	Using hot concentrated acid the vegetable matter in the wool is converted to loose, charred particles, which are mechanically shaken out; finally carbonized wool is neutralized.
Printing and Rinsing	Cotton and synthetic fiber, similar to dyeing/rinsing
Finishing	Chemicals are added to render anti-bacterial deodorants, water resistance, stain proofing, glossiness etc. Involves less water and related drainage

2.2 ENVORINMENTAL PROBLEMS ASSOCIATED WITH TEXTILE EFFLUENTS

2.2.1 Sources of Color in Textile Wastewater

The term color describes the attribute of visual perception consisting of any combination of chromatic (colorful) and achromatic (colorless) content. Color derives from the spectrum of light (distribution of light power versus wavelength). The color

arises when a molecule absorbs certain wavelengths of visible light and transmits or reflects others. What this all means, an object is seen in the color of a mixture different wavelengths of light, which are reflected by that object.

Color in water may result from the presence of naturally occurring color substances or the colored industrial wastewater. In general color in water divided into true color and apparent color. The term apparent color includes both dissolved substances and undissolved suspended matters. The true color means color of water which turbidity has removed.

Color in textile wastewaters sources from dyes and pigments from printing and dyeing processes. A dye is a colored substance that can be applied in solution or dispersion to a substrate in textile manufacturing, thus giving a color appearance to textile materials. Modern textile dyes are supposed to have high degree chemical and photolytic stability in order to keep their forms and colors. For that reason the dyes are produced showing resistance to the sunshine, detergent, soap, water and treatment. Most of these dyes are not biodegradable in aerobic processes (Archibald et al., 1997).

Dyes are the principle source of color because of their low fixation capacities. Low fixation means, much of the dyes are not fixing to the textiles, that causes contaminated water with residual dyes. They should be applied properly to minimize discharge of unfixed dye residuals. Despite, their low fixing capacity, reactive dyes have the greatest consumption in dyeing process due to their bright and wide color spectra. As presented in Table 2.3, the popular reactive dye classes have low fixation (EPA, 1996). They require special concern to maximize fixation and therefore, minimize color discharge.

Treatment of color can sometimes increase the pollution risk. For instance, treating azo-dyes results in production of amines – formed as metabolites of reductive cleavage of azo bonds –, which could be a greater environmental risk than the dye itself (Yusuff, 2004). Therefore, color removal efficiency is not enough to select the optimum treatment method, the generated toxic compounds and intermediate products by treatment methods have also been investigated widely.

Table 2.3 Dye classes and their fixation ratios to the fibers (EPA, 1996)

Dye Class	Typical Fixation (%)	Fiber Applied to
Acid	80 to 93	Wool, nylon
Azoic	90 to 95	Cellulose
Basic	97 to 98	Acrylic
Direct	70 to 95	Cellulose
Disperse	80 to 92	Synthetic
Reactive	50 to 80	Cellulose
Vat	80 to 95	Cellulose

2.2.2 Salts in Textile Wastewaters

In the dyeing process textile industries generate huge quantity of salts. In Europe alone, one million tons of salt is discharged into our waterways each year. Salts aids to fix the dyes to the fabrics. The fabric is put into water, where its surface gets covered in negative ionic charges for dyeing process. The reactive dyes are used most often to dye cellulosic fabrics also develops a negative charge, so the fibers repel the dye. Dye molecules roll of the surface of the fibers and fabric does not show much color change without the salt usage. But when salt is added to the water, the solution splits into positive sodium ions (Na^+) and negative chlorine ions (Cl^-). The positive Na^+ ions then dive into the surface of the fabric to neutralize the negative charge. The dye molecules are then attracted to the fiber by weak Van der Waals forces and as the dyes get close to the fiber molecules. The concentrations to suppress those negative ions can be as high as 100 gram per liter. In the worst cases, 1 kg of salt is used to apply reactive dye to 1 kg of fabric. (O Ecotextiles, 2011) If we think the millions of fabric producing each year, the huge amounts of the salts used in textile industry can guess easily.

2.2.3 Alkalinity in Textile Wastewaters

Alkalinity of dyeing effluents is a further environmental concern. Preparation processes are generally carried out in a range of neutral pH conditions to highly alkaline conditions. Alkali is introduced to cause the reaction between the dye and the fibre, and

any reaction between the dye and the alkalinity in the water before the dyeing process will result in significant loss of dyestuff (Tezcanli, 2003).

2.2.4 Toxic Compounds in Textile Wastewaters

Dyes, photography and explosives industries have many uses for phenol although the total consumption is not very high. Some aminophenols are used as dyes and photographic developers. Trinitrophenol, for example, is used as a dye and as an explosive. Phenols are considered toxic for some aquatic life forms in concentrations superior to 50 ppb and the ingestion of one gram of phenol can have fatal consequences in humans. Its dangerousness lies in the effect that it has on the nervous system of living beings. In addition, they have a high oxygen demand, 2.4 mg O_2 per mg of phenol. Another additional effect is the capacity of phenols to combine with existing chlorine in drinking water, giving rise to chlorophenols, compounds that are even more toxic and difficult to eliminate (Rodriquez, 2003). Moreover phenols form polychlorinated compounds in bleaching effluents having high chloride contents are not easily biodegradable and are highly toxic (Agarwal, 1996).

Aromatic nitro compounds are commonly used in industrial processes (manufacture of pesticides, dyes and explosives) and as a consequence they appear as contaminants in industrial wastewaters. This substances present a high toxicity, provoking serious health problems: blood dyscrasia, eyes and skin irritations, they affect the central nervous system, etc. (Rodriquez, 2003). Several studies have shown the presence of these substances in surface waters (Howard, 1989) and ground waters (Duguet et al., 1989). One of the main ways of contamination of superficial wastewaters by nitroaromatic compounds is the residual industrial effluent.

2.3 ADVANCED OXIDATION PROCESSES

2.3.1 Introduction

Advanced Oxidation Processes were defined by Glaze (Glaze et al., 1987) as "near ambient temperature and pressure water treatment processes, which involve the generation of hydroxyl radicals in sufficient quantity to effective water purification". Hydroxyl radical is the active part that causes the degradation of pollutants (Peyton et al., 1988; Glaze and Kang, 1989; Haag and Yao, 1992; Braun et al., 1993). It is a powerful, non-selective oxidant, which acts very rapidly with most organic compounds oxidizing them into carbon dioxide and water thanks to its high standard reduction potential in Table 2.4.

Table 2.4 Oxidizing potential for conventional oxidizing agents (Metcalf and Eddy, 2003)

Oxidizing Agent	Oxidation Potential (OP), V
Fluorine	3.06
Hydroxyl radical	2.80
Oxygen (atomic)	2.42
Ozone	2.08
Hydrogen peroxide	1.78
Hypochlorite	1.49
Chlorine	1.36
Chlorine dioxide	1.27
Oxygen (molecular)	1.23

Several organic compounds as seen the Table 2.5 is susceptible to be removed or degraded by means of hydroxyl radicals (Bidga, 1995). Depending upon the nature of the organic species, two types of initial attacks are possible: i) the hydroxyl radical can abstract a hydrogen atom to form water, as with alkanes or alcohols, ii) it can add to the contaminant, as it is the case for olefins or aromatic compounds. The attack by hydroxyl radical, in the presence of oxygen, initiates a complex cascade of oxidative reactions leading to mineralization. The rate of destruction of a contaminant is approximately proportional to the rate constants for the contaminant with the hydroxyl radical.

Destruction by advanced oxidation (AO) is based on oxidative degradation by free radical attack, particularly by the hydroxyl radical (•OH), which is far more powerful as an oxidizing agent than all commonly known strong oxidants like oxygen (O_2), hydrogen peroxide (H_2O_2) and ozone (O_3) (Legrini et al., 1993). The efficiency of AO processes is directly related to the extent of hydroxyl radical yield. The rate constants for the reaction of •OH with most organic pollutants are very high as shown in Table 2.5.

Table 2.5 Reaction rate constants (k, in L $mol^{-1}s^{-1}$) of some organic pollutants with O_3 and •OH (Calgon Carbon Oxidation Technologies, 1996)

Compounds	**O_3**	**•OH**
Chlorinated Alkenes	10^{-1} to 10^{3}	10^{9} to 10^{11}
Phenols	10^{3}	10^{9} to 10^{10}
N-containing Organics	10 to 10^{2}	10^{8} to 10^{10}
Aromatics	1 to 10^{2}	10^{8} to 10^{10}
Ketones	1	10^{9} to 10^{10}
Alcohols	10^{-2} to 1	10^{8} to 10^{9}
Alkanes	10^{-2}	10^{6} to 10^{9}

There are several AOPs technologies and each one is at a different level of development and commercialization. Figure 2.1 shows the application range of some wastewater treatments depending on the flow rate and organic matter content of the effluent to be treated. According to the illustration, UV radiation and ozonation processes should be preferred at low flow rates and low organic loads. In the situation that incoming effluent contains a high organic load, incineration and wet oxidation should be employed depending on the flow rate of the effluent. On the other hand, biological treatments appear to be suitable when the flow rate of the feed is high and it has a low content of organic matter.

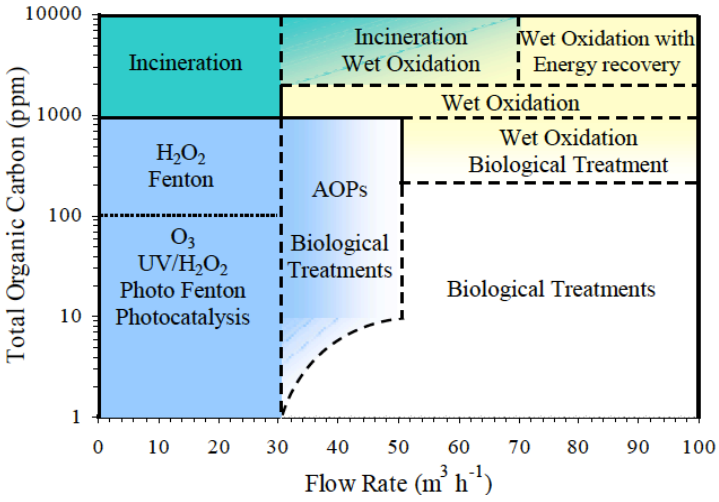

Figure 2.1 Application range of different oxidation technologies (Molina, 2006)

2.3.2 Parameters Impact on AOP Efficiency

The design of an AOP is governed by the influent contaminant concentration, target effluent contaminant concentration, desired flow rate, and background water quality parameters such as pH, alkalinity. The key design parameters for AOPs include: chemical dosages and concentrations, reactor contact time, and reactor configuration. As can be expected, higher chemical dosages and contact times are expected to result in higher removal rates; however, increasing dosages results in higher operating and maintaining (O&M) costs and possible intermediate product formation. However, in some cases, the formation of by-products and scavenger effect of some compounds can limit the AOP efficiency. There are many parameters that may impact the effectiveness of AOPs. For example, nearly all dissolved organic compound present in the source water will serve to reduce the removal efficiency of the target compound by consuming •OH (Hoigne, 1998). There is a discussion of each parameter that limit the detrimental impact of AOPs in the below:

Alkalinity: The detrimental impact of alkalinity on the effectiveness of AOPs has been extensively studied (AWWARF, 1998). As mentioned previously, the hydroxyl radical is nonselective and, thus, can be exhausted by the presence of organic or inorganic compounds other than the contaminants of concern. Both carbonate and bicarbonate will scavenge hydroxyl radicals to create carbonate radicals, which, in turn, react with other organic or inorganic compounds present, at a much slower rate (Hoigne

and Bader, 1976; AWWARF, 1998). The reaction for the scavenging of hydroxyl radicals by bicarbonate and carbonate ions is shown in Eq. (2.1) and (2.2) (Morel and Hering, 1993). The rate constants, k, for the reactions of the hydroxyl radical with carbonate and bicarbonate are 3.8 x 10^8 and 8.5 x 10^6 $M^{-1}s^{-1}$, respectively (Buxton, 1988).

$$\bullet OH + HCO_3^- \rightarrow CO_3^-\bullet + H_2O \quad (2.1)$$

$$\bullet OH + CO_3^{-2} \rightarrow CO_3^-\bullet + OH^- \quad (2.2)$$

In the presence of carbonate-bicarbonate ions part of the hydroxyl radicals react to form carbonate ions radicals, CO_3^-. According to Chen et al., (1975) carbonate radicals also react with organic compounds. These reactions are more selective than those of the hydroxyl radical and the rate constants are lower – how much lower depends on the nature of the organic compounds –.

Total Organic Carbon (TOC) and Natural Organic Matter (NOM): TOC includes the all-organic compounds present in the water; both dissolved organic carbon (DOC) and particulate organic carbon (POC). Drinking water supplies typically contain TOC concentrations ranging from <1 mg/l to >7 mg/l and include naturally occurring compounds and synthetic compounds (e.g., pesticides, gasoline components, and chlorinated compounds). NOM, a subset of TOC, is commonly used to describe large macromolecular organic compounds present in water. These macromolecules can include humic substances, proteins, lipids, carbohydrates, fecal pellets, or biological debris (Stumm and Morgan, 1996) and, while not highly reactive, often contain reactive functional groups (Hoigne, 1998). Organic matters present in the water, whether anthropogenic or natural, will scavenge hydroxyl radicals and, thus, limit the effectiveness of AOPs. The rate constants reported in the literature for hydroxyl radical reactions with NOM range from 1.9 x 10^4 to 1.3 x 10^5 $(mg/l)^{-1}s^{-1}$ (AWWARF, 1998).

Nitrates and Nitrites: Hydroxyl radicals can be formed by several mechanisms, including UV photooxidation of hydrogen peroxide. Any constituent present in the water that adsorbs UV light will decrease the formation of hydroxyl radicals. Nitrates and nitrites absorb UV light in the range of 230 to 240 nm and 300 to 310 nm and,

consequently, high nitrate (>1 mg/l) or high nitrite (>1 mg/l) concentrations have been shown to limit the effectiveness of UV technologies (Calgon, 1996).

Phosphates and Sulfates: Phosphates and sulfates are commonly present in low concentrations in natural waters; these compounds have the potential to scavenge hydroxyl radicals. However, they are extremely slow in reacting with •OH, and their scavenging effect can usually be neglected (Hoigne, 1998) for ozone/peroxide/UV systems. For TiO_2 catalytic systems, sulfates have been noted to significantly decrease the destruction rate of organic contaminants at concentrations above approximately 100 mg/l (Crittenden et al., 1996).

Iron (II), Copper (I), or Manganese (II)*:* The presence of these reduced metals in combination with NOM and hydroxyl radicals may lead to the formation of iron or copper organic complexes or the oxidation of Mn (II) to form permanganate (Hoigne, 1998; Calgon, 1996). The presence of iron (absorptivity 200 to 400 nm) and other scaling agents may result in fouling of UV systems.

Turbidity: Systems relying on UV irradiation for the oxidation of H_2O_2 or O_3 exhibit a decrease in efficiency as turbidity increases. Turbidity lowers the transmittance of the water and, thus, lowers the penetration of the UV radiation into water (National Water Research Institute, 2000). In addition, at Fenton reactions precipitated iron causes turbidity, which decreases the photoreactor's light scavenging efficiency, because part of the incident light does not enter the photoreactor but is lost due to scattering (Gernjak, 2006).

2.4 PHOTOCHEMICAL AND NON-PHOTOCHEMICAL AOPs

AOPs are generally classified with generated •OH by photochemical and non-photochemical methods that given in below. Photochemical AOPs usually include the involving ultraviolet (UV) irradiation in conjunction with an oxidant and/or catalyst. Generation of •OH can also be achieved in the absence of UV light or another source of photo by a number of AOPs that is called non-photochemical methods.

2.4.1 Photo-Chemical AOPs

Photochemical advanced oxidation means, the degradation of compounds by the assist of a light irradiation; most times it is UV light irradiation. UV is not always enough to complete degradation of compounds. The additive chemicals as H_2O_2 are needed to increase systems' efficiency. Many organic contaminants absorb UV energy in the range of 200–400 nm and decompose due to direct photolysis or become excited and more reactive with chemical oxidants. Among the AOPs, photochemical processes including the UV photolysis of H_2O_2 and the Photo-Fenton reaction (UV photolysis of H_2O_2 catalyzed by Fe^{+2} ions under acidic pH conditions) are known as the most efficient, feasible and kinetically favorable types (Alaton et al.,).

2.4.1.1 UV/H_2O_2

Hydrogen peroxide is an efficient and easy to use chemical oxidant suitable for a wide usage. It was first used to reduce odor in wastewater treatment plants, and from then on, it became widely used in the field of the wastewater technologies (EPA, 2002). However, hydrogen peroxide itself is not an efficient oxidant for many organic pollutants; it must be combined with UV light, US or ozone to produce the desired degradation results.

Under UV irradiation, H_2O_2 are photolyzed to form two hydroxyl radicals (2•OH) that react with organic contaminants (Crittenden et al., 1999). The mechanism most commonly accepted for the photolysis of H_2O_2 is the cleavage of the molecule into hydroxyl radicals and other reactive species that attack the organic molecules (Legrini et al., 1993):

$$H_2O_2 \xrightarrow{hv} 2\,HO\cdot \qquad \lambda \leq 400nm \tag{2.3}$$

Hydrogen peroxide can also react with hydroxyl radicals and the intermediary products formed thereby, according to the reaction mechanism described in a simplified way by equations (2.4) to (2.8) (Alfano et al., 2001).

$$H_2O_2 + HO\bullet \rightarrow HO_2\bullet + H_2O \quad (2.4)$$

$$H_2O_2 + HO_2\bullet \rightarrow HO\bullet + H_2O + O_2 \quad (2.5)$$

$$2HO\bullet \rightarrow H_2O_2 \quad (2.6)$$

$$2HO_2\bullet \rightarrow H_2O_2 + O_2 \quad (2.7)$$

$$HO\bullet + HO_2\bullet \rightarrow H_2O_2 + O_2 \quad (2.8)$$

High concentration of the H_2O_2 acts as a radical scavenger, while; low concentration of H_2O_2 generates not enough of hydroxyl radicals (•OH) and this leads slow rate of oxidation. If an excess of H_2O_2 is used, •OH will produce hydroperoxyl radicals, •OOH, which are much less reactive (Glaze et al., 1987). López et al., (2000) attribute this decrease in the H_2O_2/UV process yield to hydroxyl radicals reacting with excess H_2O_2, instead of reacting with the organic substrates, leading to the formation of the hydroperoxyl radical HO_2•, Eq. (2.4).

2.4.1.2 O_3/UV

Since the beginning of the 20th century, the disinfection properties of ozone have been well known. And moreover, ozone becomes to acquire an important role in the field of wastewater treatments. Its high electrochemical oxidation potential of 2.1 V (Hunsberger et al, 1977) and also due to the absence of hazardous decomposition products over the duration of the process, ozone is a potential treatment agent to transform refractory compounds into substances that can be further removed by conventional methods (Hu and Yu, 1994).

The O_3/UV process seems at present to be the most frequently applied AOP for a wide range of compounds. This is due to the fact that ozonation is a well-known procedure for water and wastewater technology. For the photolytic oxidation by ultraviolet light combined with ozone, hydroxyl radicals are generated as active species.

Ozone readily absorbs UV radiation at 253.7 nm wavelength, producing H_2O_2 as an intermediate, which then decomposes to •OH radical:

$$O_3 \xrightarrow{hv} O_2 + O(1D) \quad (2.9)$$

$$O(1D) + H_2O \rightarrow \bullet OH + \bullet OH \quad (2.10)$$

$$O_3 + H_2O \rightarrow H_2O_2 + O_2 \quad (2.11)$$

Common low-pressure mercury lamps generate over 80% of their UV energy at this wavelength. Photolysis of ozone therefore appears only to be an expensive way to make hydrogen peroxide that is subsequently photolyzed to •OH radicals. Although photochemical cleavage of H_2O_2 is conceptionally the simplest method for the production of hydroxyl radicals, the exceptionally low molecular absorptivity of H_2O_2 at 254 nm (**ε**254nm = 18.6 M^{-1} cm^{-1}) limits the •OH yield in the solution (Munter, 2001). Table 2.6 shows that photolysis of ozone yields more radicals than the UV/H_2O_2 process.

Table 2.6 Formation of OH from photolysis of H_2O_2 and O_3 (Techcommentary, 1996)

Oxidant	**ε 254nm M^{-1} cm^{-1}**	**Stoichiometry**	**•OH formed per incident photon**
H_2O_2	20	H_2O_2➔2•OH	0.09
O_3	3300	$3O_3$➔2•OH	2.00

2.4.1.3 Photo-Fenton

The reaction is based on the catalytic effect of the ferrous ions on the decomposition of H_2O_2. The main stages involved in the process are the Eq. (2.12) – (2.18) (Pera-Titus et al., 2004). The •OH radical mentioned before, once in solution attacks almost every organic compound. The Fe^{+2} regeneration can follow different paths. For Fe^{+2} the most accepted scheme is described in the following equations (Sychev and Isak, 1995):

$$Fe^{+2} + H_2O_2 \longrightarrow Fe^{+3} + HO^- + HO^{\cdot} \quad (2.12)$$

$$Fe^{+3} + H_2O_2 \longrightarrow Fe^{+2} + H^+ + HO_2^{\cdot} \quad (2.13)$$

$$Fe^{+2} + HO^{\cdot} \longrightarrow Fe^{+3} + HO^- \quad (2.14)$$

$$OH^{\cdot} + H_2O_2 \longrightarrow H_2O + HO_2^{\cdot} \quad (2.15)$$

$$Fe^{+3} + HO_2^{\cdot} \longrightarrow Fe^{+2} + H^+ + O_2 \quad (2.16)$$

$$Fe^{+3} + O_2^{\cdot} \longrightarrow Fe^{+2} + O_2 \quad (2.17)$$

$$Fe^{+2} + HO_2^{\cdot} \longrightarrow Fe^{+3} + HO_2^{-} \quad (2.18)$$

In the dark, the reaction retarded is after complete conversion of Fe^{+2} to Fe^{+3}. After H_2O_2 addition, ferrous ion concentration decreases rapidly and ferric ion is formed. After the complete disappearance of the oxidant no more Fe(II) can be consumed. The concentration of Fe(II) increases rapidly, in contrast with the dark reaction where Fe(III) can not be photoreduced to Fe (II) as shown in Eq. (2.12). The primary step is photooxidation of ferrous ions to ferric ones Eq. (2.13). In the presence of light feedback reaction takes place, Eq. (2.13). In the presence of light following reaction takes place:

$$Fe^{+3} + H_2O_2 \overset{h\nu}{\rightarrow} Fe^{+2} + \cdot OH + H^{+} \ (\lambda > 300nm) \quad (2.19)$$

And also, H_2O_2 photolysis occurs directly under UV light irradiation, Eq. (2.20):

$$H_2O_2 \overset{h\nu}{\rightarrow} 2HO^{\cdot} \ (\lambda < 300nm) \quad (2.20)$$

Walling and Weill (1974), the Fe^{+3} formed in Eq. (2.12) can react with the H_2O_2 present in the medium and be reduced to Fe^{+2} again, forming the hydroperoxyl radical, according to Eq. (2.13). This reaction, referred to by Neyens and Baeyens (2003) as Fenton-like, occurs more slowly than reaction Eq. (2.12), as reported by Pignatello (1992). The Fe^{+3} ions also react with the HO_2• and are reduced to Fe^{+2}, as shown by Eq. (2.16).

Figure 2.2 shows schematically chemical reactions for the formation of •OH radicals and oxidation of organic compound in photo-Fenton process.

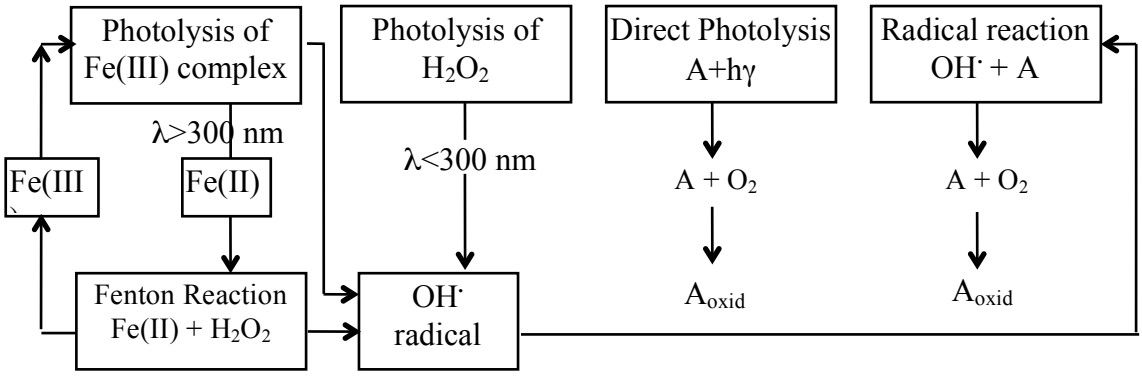

Figure 2.2 Scheme of chemical reactions in photo-Fenton process (Kim et al., 1997)

Many constituents of the waters and wastewaters can affect the reaction rates of the degradation efficiency of Fenton processes. The main parameter for Fenton reactions are given below:

Effect of pH: The reaction rate of Fenton processes efficiency high at pH 3. An increase or decrease in the pH sharply reduces the catalytic activity of the metal ion. At high pH the ferric ion precipitates as ferric hydroxide and at lower pH the complexion of Fe(III) with H_2O_2 (Eq. 2.7) is inhibited. The pH of the solution decreases rapidly by the addition of $FeSO_4$ catalyst, which typically contains residual H_2SO_4. Decrease in pH also seen by the addition of H_2O_2 and continues gradually at a rate which is largely dependent on catalyst concentration. The drop in pH is attributed to the fragmenting of organic material into organic acids (Tezcanli, 1998).

Effect of Fe:H_2O_2 ratio: The reaction rates increase with increasing H_2O_2 until a point as well Fe(II), further addition of Fe(II) and H_2O_2 becomes inefficient. It is important to establish the optimal relationship between ferrous and hydrogen peroxide ions. When higher concentrations of ferrous ions than hydrogen peroxide ions are used, the hydroxyl radicals generated by Eq. (2.12) may react with excess ferrous ions, according to Eq. (2.21), decreasing the attack of hydroxyl radicals on organic substrates (Neyens and Baeyens, 2003).

$$Fe^{+2} + HO^{\cdot} \rightarrow Fe^{+3} + HO^{-} \qquad (2.21)$$

Effect of UV light: According to Pignatello (1992), UV irradiation strongly accelerates the degradation rate of organic pollutants from Fenton's reagent, which has

the advantage of being sensitive to UV-V is radiation for wavelengths above 300 nm. Under these conditions, the photolysis of Fe^{+3} complexes enables regeneration of Fe^{+2} and the occurrence of Fenton's reaction, if H_2O_2 is available. Faust and Hoign (1990) reported that the dominant species (between pH 2.5-5) in the photo-Fenton process is the ferric complex $Fe(OH)^{+2}$, a simplified form of representing the aqueous complex $Fe(OH)(H_2O)_5^{+2}$ and the photolysis of this complex (wavelengths < 410 nm) is the largest source of hydroxyl radicals (Eq. 2.22). Other photoreactive species are also present in the reaction medium, such as $Fe_2(OH)_2^{+4}$ and $Fe(OH)^{+2}$, possibly leading to the formation of hydroxyl radicals (Faust and Hoign, 1990).

$$Fe(OH)^{+2} \xrightarrow{hv} Fe^{+2} + HO\bullet \qquad (2.22)$$

Effect of Contact Time: Malato et al., (2002) also cite the high depth of light penetration and the intense contact between the pollutant and the oxidizing agent as advantages of the photo-Fenton process, since it is a homogeneous process.

Effect of Characteristics of the Wastewater: Physical-chemical characteristics of the wastewater to be treated by this process because some substances or inorganic ions, such as Cl^-, SO_4^{-2}, $H_2PO_4^-$ /HPO_4^{-2} present in the wastewater or added as reagents ($FeSO_4$, $FeCl_3$, HCl, H_2SO_4) may interfere in the reaction mechanism of the Fenton and photo-Fenton system, inhibiting the degradation process, as reported by De Laat et al., (2004) and Nadtochenko and Kiwi (1998).

De Laat et al., (2004) suggest that the possible causes of these effects are the complexation reactions of the inorganic ion with Fe^{+2} or Fe^{+3} ions and the reactions with hydroxyl radicals that lead to the formation of less reactive inorganic radicals ($Cl\bullet^-$, $Cl_2\bullet^-$ and $SO_4\bullet^-$).

Machulek Jr et al., (2007) found that the formation of $Cl_2\bullet^-$ radical anions, due to the presence of chloride ions in the reaction medium, can be avoided by controlling pH at 3 during the reaction period, given that the degradation process of an organic substrate by the photo-Fenton process leads to the formation of acids and thus pH reduction. It occurs due to pH decrease lower than 2.5 in the presence of chlorides ions,

leading to more intense formation of ferric chloride complexes ($FeCl^{+2}$ and $FeCl^{+2}$). These complexes also undergo photolysis, thereby decreasing the amount of $Fe(OH)^{+2}$, which is the main source of hydroxyl radicals in the photo Fenton process, in addition to the formation of the $Cl_2•^-$ radical anion, which can react with Fe^{+2} (oxidizing to Fe^{+3} without the formation of hydroxyl radicals) and the organic substrate.

2.4.2 Non-Photochemical AOPs

2.4.2.1 Ozonation

When ozone is generated, the oxidation of the organic matter can occur through two different reaction pathways; direct and indirect (free radical) ozonation, leading to different oxidation products and different types of kinetics. When the direct ozonation takes place, ozone is the main oxidizing agent of the process. On the other hand, the indirect ozonation is based on the formation of hydroxyl radicals that later act as main oxidizing agent. Indirect ozonation that produces •OH radicals makes ozonation process as an advanced oxidation method. The rate constants of •OH radicals are 10^4-10^8 times faster than ozone.

2.4.2.2 Ozone/H_2O_2

Some approaches have been taken into account to improve the oxidizing power of ozonation for reducing the required time for the reaction and decreasing its energy costs. The addition of hydrogen peroxide to ozonized solutions causes rapid decomposition of ozone with high output of •OH radicals (Langlais et al., 1991). The action of ozone on organic compounds have a high molecular weight leads to sole compounds, which are refractory to ozone. So that, it is more useful to use hydrogen peroxide which is less selective than molecular ozone for this purpose. The simultaneous use of both oxidants has synergistic effects, leading to destruction of organic matter.

$$O_3 + H_2O_2 \rightarrow OH^- + O_2 + HO_2^- \quad (2.23)$$

2.4.2.3 Dark Fenton

The Fenton reaction was discovered by H.J.Fenton in 1894. In the 1930s it revealed that the effective oxidative agent in the Fenton reaction was the hydroxyl radical (Prousek, 1995).

The main reactions of dark Fenton are same as equations (2.12) – (2.18). If H_2O_2 is added to an aqueous medium containing organic compounds and excess ferrous ions (Fe^{+2}) at acidic conditions (2 < pH < 5), will generates •OH radicals as shown in below figure:

$$Fe^{+2} + H_2O_2 \rightarrow Fe^{+3} + \bullet OH + HO^- \quad (2.24)$$

$$\bullet OH + Fe^{+2} \rightarrow Fe^{+3} + OH^- \quad (2.25)$$

The main advantage of Fenton systems to the more popular homogenous AOP UV/H_2O_2 oxidation is that the process and reactor configuration is not limited by UV irradiation. However, the main disadvantage is the formation of ferric ion precipitation after pH adjustment as well as acidic conditions (pH < 5) necessary for this treatment process (Majcen-Le et al., 1997).

2.4.2.4 Ultrasound

Loomis first reported the chemical and biological effects of ultrasound at 1927s. Ultrasound spans the frequencies of 18 kHz and 10 MHz beyond human hearing. In practice, three ranges of frequencies are reported one is, low frequency or conventional power ultrasound (20-100 kHz), medium frequency ultrasound (300-1000 kHz) and high frequency ultrasound (2-10 MHz).

The application of ultrasound (US) irradiation for the degradation of organic pollutants in water has been widely described in the literature. The decomposition of pollutants by direct pyrolysis and/or oxidation by means of the reactive radicals coming from water and oxygen dissociation in the presence of US irradiation have been proposed in literature as the main degradation mechanisms. Hydrophobic pollutants

with high vapor pressure are decomposed mainly by pyrolytic degradation, whereas hydrophilic pollutants with low vapor pressure are decomposed by hydroxyl radical oxidation. However, the rate of pollutant degradation of ultrasonic irradiation is rather low to be applied in practice, especially for highly hydrophilic compounds. Hence, to improve the degradation efficiency of organic pollutants in water is to combine US irradiation with other catalysts and/or processes (Molina, 2006).

When ultrasound is introduced into liquid (e.g., water), it creates oscillating regions of positive and negative pressure. Correspondingly, the liquid molecules experience periodic compression and expansion cycles. When the pressure amplitude exceeds the tensile strength of liquid during the rarefaction of ultrasonic waves, cavitational bubbles are formed (Marachel, 2004). Cavitation is the formation of gas-filled micro bubbles or cavities in a liquid, their growth and, under proper conditions, implosive collapse (Figure 2.3). Cavitational bubbles collapse during the compression cycle of ultrasonic wave. Localized hot spots are formed, which reach temperatures and pressures around 5000 K and 500-1000 atm, respectively (Suslick, 1990; Flint and Suslick, 1991) as shown Figure 2.4, depending on factors such as ultrasonic power, frequency, hydrostatic pressure, temperature, solvent property, and dissolved gas. Three regions are postulated for the occurrence of chemical reactions: a hot gaseous nucleus, an interface between the bubble and the bulk liquid, and the bulk media.

Free radicals or/and excited states are formed from water dissociation, vapors and gases or various substrates during bubble collapse, where high temperatures and pressures provide activation energy for homolytic bond breakage. The generated radicals either react with each other to form new molecules and radicals, or diffuse into bulk liquid to serve as oxidants.

Ultrasound waves consist of expansion (rarefaction) and compression cycles (Figure 2.5). Compression cycles exert a positive pressure on the liquid and push molecules together, while expansion cycles exert a negative pressure and pull molecules apart. Cavities can be generated during the expansion of a sound wave cycle with sufficient intensity, that the distance between the molecules exceeds the critical molecular distance necessary.

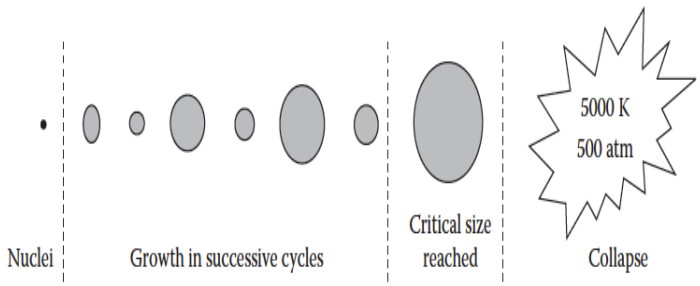

Figure 2.3 Bubble formation, growth and collapse (Chowdhury, P. and Viraraghavan, 2009)

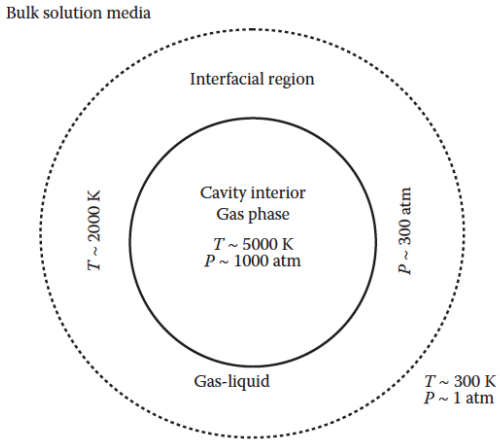

Figure 2.4 Three reaction zones in the cavitation process (Flint and Suslick, 1991)

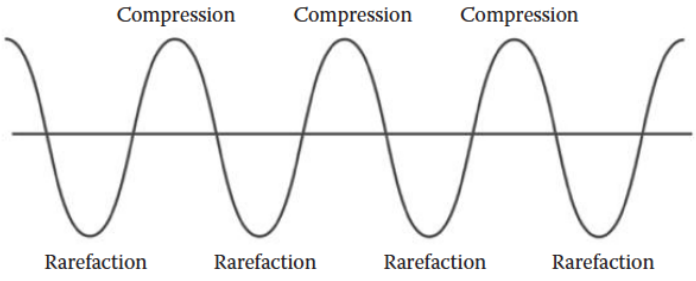

Figure 2.5 Expansions and compressions of ultrasound waves (Suslick, 1990)

Parameters, which affect cavitation and bubble collapse are;

Power Intensity: The power intensity of ultrasound is the power delivered to the liquid divided by the surface area of the ultrasonic transducer. The relationship between the ultrasonic power intensity and the acoustic pressure may be expressed as (Mason

and Lorimer, 1988);

$$I = \frac{P_0^2}{2\rho C} \tag{2.20}$$

where

I is the power intensity of a sound wave

P_0 is the acoustic pressure

ρ is the density of the liquid

C is the sound speed in the liquid

Consequently, higher acoustic pressure (amplitude of vibration), greater amounts of cavitational events, and more violent cavitational collapse happen at elevated power intensity of ultrasound. However, optimum power intensity has been observed corresponding to the highest reaction rate (Gutierrez and Henglein, 1990; Hatanaka et al., 2002). Beyond that point, a further increase in power causes a decline of the reaction rate. When a large amount of ultrasonic power enters to system, a great number of cavitation bubbles generates in the solution. They will become larger and long-lived bubbles. The bubbles will act as a barrier to the transfer of acoustic energy through the liquid. This phenomenon may be explained by bubble shielding effect. (Pace et al., 1997; Roy, 1999).

Frequency of Ultrasound: Frequency of ultrasound directly affects the generation, oscillation, the resonant size, and final collapse of cavitational bubbles in terms of both quantity (the amounts of collapse) and the quality (the violence of collapse). Generally, the cavitational threshold increases with increasing ultrasonic frequency (Mason and Lorimer, 1988). In other words, a higher acoustic pressure is required to overcome the tensile strength of liquid molecules to produce cavitation at a higher ultrasonic frequency. Lower frequency produces more violent cavitation and, as a consequence, higher localized temperatures and pressures. At very high frequency, the expansion part of the sound wave is too short to permit molecules to be pulled apart sufficiently to generate a bubble. Weak cavitation or no cavitation in megahertz range is observed.

Temperature: Higher external temperature reduces the intensity to induce cavitation due to the increased vapor pressure of the liquid. At higher external temperatures more vapor diffuses into the cavity, and the cavity collapse is cushioned and less violent. Therefore, sonochemical reactions proceed more slowly as ambient temperatures increase. The temperature near the boiling point of the liquid increases the number of bubbles, which can act as a sound barrier.

Applied Pressure: Increase in the pressure of the system will increase the intensity if cavitational collapse and consequently improves sonochemical effect (Mason, 1999). Too much pressure reduces the rate of reaction by decreasing the frequency or efficiency of bubble formations.

Dissolved Gases: Soluble gases should result in the formation of a larger number of cavitation nuclei, but the greater the solubility of the gas is the more gas molecules should penetrate the cavity. Therefore, a less violent and intense shock wave is created on bubble collapse. The thermal conductivity of the gas has significant effect on the final temperature produced during cavity collapse. Higher temperatures and pressures are generated with monoatomic gases with larger ratios of specific heat (He, Ne, Ar) than diatomics (N_2, O_2), or polyatomic gases with lower heat capacity ratios (CO_2). The gas with the higher thermal conductivity reduces the temperature achieved during the collapse.

Addition of Solid Catalysts: The addition of solid catalysts such as glass beads, ceramic disks, SiO_2, TiO_2, Al_2O_3 and talc into the reaction medium increases cavitation effects.

Property of Contaminants: Besides ultrasonic factors, the properties of contaminants such as volatility and hydrophobicity also greatly affect the degradation rate of sonication. Hydrophobic chemicals with high vapor pressures have strong tendency to diffuse into the gaseous bubble interior, so that the most effective reaction site for their destruction is the bubble-liquid interface and/or the gaseous bubble itself (Kontronarou, et al., 1991). In contrast hydrophilic compounds with low vapor pressures and low concentrations tend to remain in the bulk liquid during irradiation. The major reaction site for these compounds is the liquid medium where oxidative

degradation has occurred and that produces the hydroxyl radical are ejected into the solution during cavitational collapse (Mason, 1990).

2.5 DEGRADATION OF TEXTILE EFFLUENTS BY AOPs

Recent research studies with AOPs focused on the development of new methods for synthetic wastewater contain dyes – mainly azo dyes that are largest class of dyes in textile industry. Real wastewater effluents have not so much studied. Industrial wastewater characteristics vary not only with the industry generates them, but also within the industry. They are so different than domestic wastewaters. It is clear that studying with real wastewater is in evitable compromised by the amount and the properties. It is hard to imply the results of studied wastewaters and industries as general. Even the industries same, the characterization of wastewaters could be discrete (I.Oller, 2010). Malato et al., (2009) has mentioned it must be consider that the real wastewater contains substances that could compete with target pollutant for oxidizing agent hydroxyl radical. And also Kiwi et al., (2000) mentioned even in effluents which target pollutants are predominant, oxidation can lead to quick formation of intermediates that lower the system efficiency.

Textile wastewater includes wide variety of dyes and chemicals that make the chemical composition of textile industry effluents big problem to environment. Al-Kdasi et al., (2004) mentioned that the most of the pollution in textile industry comes from dying and finishing processes. Savin and Buntnaru (2008) characterized the textile industry with water consumption (80-100m^3/ton of finished textile), wastewater discharge (115-175 kg COD/ ton of finished textile), and wide range of chemicals, low biodegradability, color and salinity.

H_2O_2/UV is one of the AOPs that give efficiency in the color removal and organic matter decreasing. Olcay et al., (1996) documented alone H_2O_2 is not efficient to oxidize textile wastewaters at both acidic and alkali conditions. But with UV irradiation system performance becomes effective by means of decolorization and TOC, COD removal. Percowski and Kos (2003) studied with dye house wastewater and resulted 99% color reduction after 2 hours. Rosaria et al., (2002) found approximately 80% TOC

removal rate in 2 hours. By in terms of discoloration Shu et al., (1995) reported acid dyes are the easiest to decompose. Pittroff et al., said that yellow and green reactive dyes need longer discoloration times while disperse dyes are decolorized faster.

In the study of Azam et al., (2005), advanced oxidation treatment, the UV/H_2O_2 process has been applied to decolorization of the azo dye. C.I. Acid Orange 7 (AO7) in aqueous solution in a batch photo reactor. The method of study involved monitoring the rate of dye solution decolorization during irradiation by a low-pressure mercury lamp and varying gap size and volume of the reactor. The results of this study showed that the removal efficiency of AO7 is optimal with 0.3 cm gap size and 83.33 W l^{-1} of UV dosage.

Kiwi et al., (1996) documented decolorization of Orange Acid (II) achieved less than 2 hours via photo-Fenton reactions and mineralization completed to 95% in less than 8 hours. Real-scale applications of photo-fenton processes have mentioned by Vandevivere and his friends that there is several plants in South Africa using Fenton's reagent to treat textile industry wastewaters. Also commercial Photo-fenton applications can have seen in USA to treat VOCs from water (USEPA, 1998). The examples of solar driven photo-Fenton treatment plants installed in Spain are in Figure 2.6 and Figure 2.7.

Hung et al., (2005) investigated the degradation and decolorization of direct dye (Everdirect supra turquoise blue FBL), acidic dye (Isolan orange S-RL) and vat dye (Indanthrene red FBB) by Fenton and UV/Fenton processes. Fenton process is highly efficient for color removal for three dyes tested and for TOC removal of FBB and FBL. UV/Fenton showed slighter increase in treatment efficiency than that of Fenton process for both FBB and FBL dye solutions. S-RL improved much more TOC removal% by UV-irradiation.

Turhan et al., (2008) studied the decolorization of wastewater containing direct dye (Sirius Blue SBRR) by ozonation was studied in an attempt to abate pollution caused by textile dyeing houses and dye-producing plants. The rate of dye oxidation increases with increasing the air–ozone flow rate and solution pH, reaches a maximum and then decreases with a further increase in the air–ozone flow rate. The results with the direct dyestuff wastewater showed that decolorization was remarkable under the

basic condition of pH 12. A large amount of bubbles was formed at high ozone–air flow rate. After 26 min of ozone treatment, decolorization was completed.

Alaton et al., (2005) investigate the COD removal of biodical finishing effluent by ozonation and the other AOPs. Photo-Fenton (20mM H_2O_2- 5mM Fe(II)- pH:3 time:30minutes) process has 80% COD removal, whereas Fenton has 37%. With 800 mg/h applied ozone at pH:12, the result is 52% in terms of COD removal.

The study of Koprivanac et al., (2006) involves comparative investigations of the efficiency of several ozone- and/or UV-based processes: O_3, O_3/H_2O_2, UV/H_2O_2, UV/O_3 and $UV/H_2O_2/O_3$, for the minimization of phenol as a model hazardous pollutant in wastewater. For all applied AOPs the best experimental conditions concerning selected varied process parameters, initial pH and H_2O_2 dosage, were determined. Different AOPs were evaluated on the basis of their eco-effectiveness; by the means of phenol decay and TOC value decrease, and their cost-effectiveness. It was established that the complete phenol removal can be achieved by adjusting the pH and H_2O_2 dosage. The overall mineralization extent depended on the type of process, number and type of oxidants and/or UV light, and their studied processes parameters as well. The highest overall mineralization extent, 58.0% TOC removal, was achieved by $UV/H_2O_2/O_3$ process. From the aspect of both eco- and cost- effectiveness, $UV/H_2O_2/O_3$ was shown as the most suitable process.

Nilsun et al., (2004) compared the degradation of azo dyes by 520 kHz ultrasonic irradiation and its combinations with ozone and/or ultraviolet light (UV) was investigated using a probe dye C.I. Acid Orange 7. UV irradiation, however, was found to induce a catalytic effect when applied in combination with either ultrasound or ozone schemes. The study reported herein has shown that while ultrasound may render decolorization of textile azo dye solutions, overall dye degradation or ultimate mineralization of the dyes is not possible unless it is used in combination with O_3 and/or UV irradiation.

Arslan and Balcıoglu (1999) investigated ozonation; hydrogen peroxide coupled with ozone, and UV irradiated processes for the treatment of synthetic dye bath effluents containing six reactive dyestuffs and their assisting chemicals. They observed

rapid and complete decolorization for all systems with optimum H_2O_2 dose and reaction pH. The increase in pH from acidic conditions to basic conditions yielded 41 per cent enhancement in ozone absorption rate. Total decolorization of synthetic dye bath effluent was achieved after 20 minutes of ozonation (33 mg O_3) at pH=11.5.

Huang and Shu (1994) assessed the decolorization and mineralization of textile wastewater containing the direct dyes Black 22 and Blue 199 by the sequential application of O_3 and H_2O_2/UV. The effects of pH and H_2O_2 dose were also investigated. Fastest decolorization was achieved at neutral pH and an initial optimum concentration of 1 per cent w/w H_2O_2.

Lin and Lin (1993) investigated the treatment of low, medium and high strength textile waste effluents by ozonation and chemical coagulation. It was observed that ozone is highly effective in removing color of these effluents but relatively ineffective in reducing the COD especially for the high and medium strength effluents. The COD reduction was improved to a maximum of 70 per cent after a proceeding chemical coagulation.

Vajnhandl et al.,(2007) studied with C.I Reactive Black 5, known as non-biodegradable azo-dye, at ultrasonic irradiation 20, 279 and 817 kHz. Experiments carried out with low frequency probe type and high frequency probe type transducer at 50, 100 and 150 kW of acoustic power and within 5-300 mg/l dye concentration range. 50% TOC degradation has found after 6 hours treatment that indicates low efficiency of TOC removal with ultrasound alone. Discoloration as well as radical production increased with increasing frequency, acoustic power and irradiation time. After 6 hours, the discoloration rate is 98.7%.

Nilsun et al., (2010) described the degradation of two azo dyes at low (20kHz) and high (577,861, 1145 kHz) frequency ultrasound (US) to compare their reactivity and to assess the impacts of frequency, OH•, chemical structure and soluble/non-soluble additives. Low frequency US alone was found totally ineffective for bleaching the dyes even after 2-h irradiation, while high frequency provided significant color decay in 30-min contact.

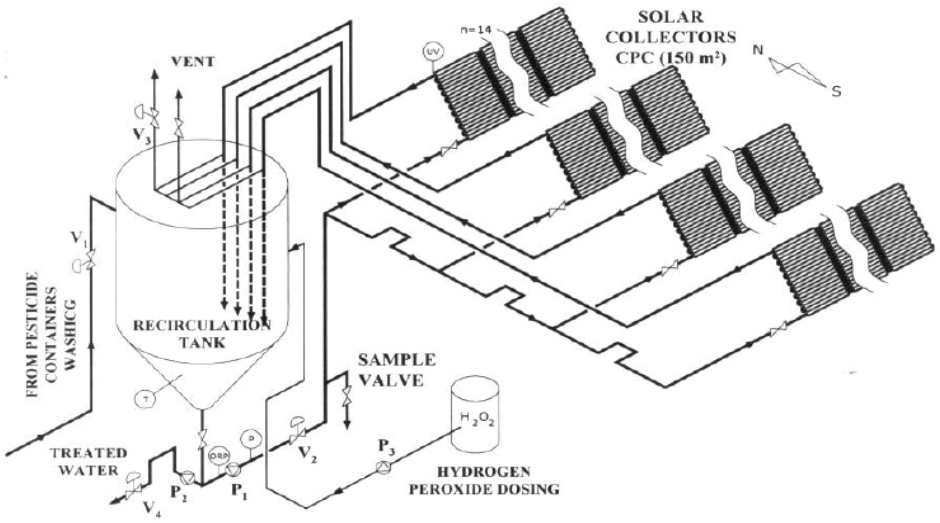

Figure 2.6 Schematic diagram of solar driven H_2O_2 plant in Spain (Malato et al., 2004)

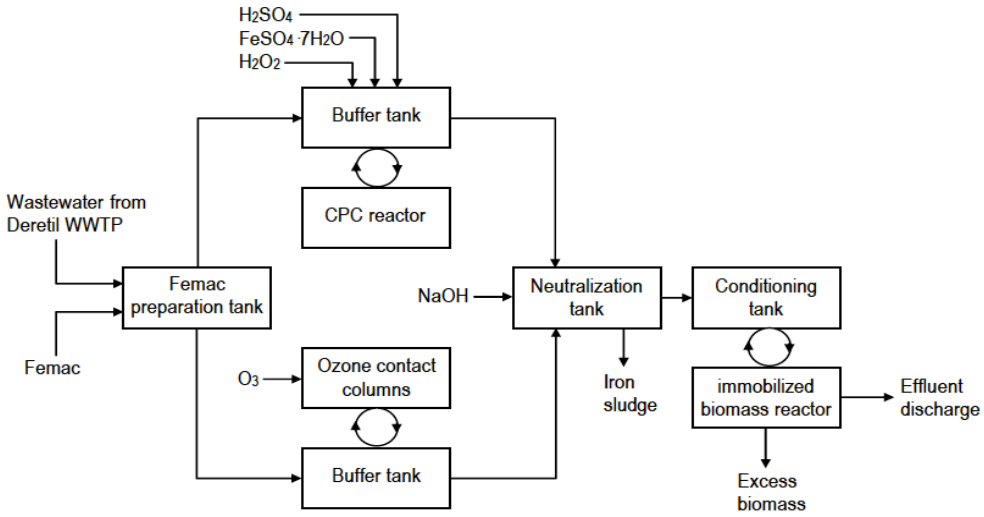

Figure 2.7 The flow diagram of Fenton process in Deretil, Spain (Malato et al.,2004)

CHAPTER 3

MATERIALS AND METHODS

3.1 MATERIALS

3.1.1 SAMPLES

Textile wastewater samples were studied in the each set of experiments. The samples were taken from the one of the textile industry that located Ergene Basin, Tekirdag. The company is working on dyeing, finishing and printing processes of the textiles. The daily capacity of the treatment plant is 2500 m^3/day. The company has biological treatment plant. The experiments performed with the effluents of the biological treatment unit.

The company is in the scope of the Table 10.2 in the Water Contamination Quality Control Act (WCQA). The characterization of the wastewater has given Table 3.1 with the WCQA limit values. The samples have studied immediately after taken to avoid the degradation and oxidation.

Table 3.1 Physical-chemical characterization of studied textile industry sample

Parameters	Influent	Effluent	WCQC limit values (Table 10.2)
Temperature (^{0}C)	36.5	30.6	-
pH	12.01	7.85	6-9
Conductivity (µS/cm)	7500	5915	-
TSS (mg/l)	333	76	100
COD (mg/l)	1763	300	300
Phenol (mg/l)	5.15	3.06	0.5
T.Crom (mg/l)	1.00	0.1	1
Color (Pt-Co)	1600	1600	280
Sulfide (mg/l)	30	7.32	-
Alkalinity (mg/l)	-	2000	-

3.1.2 LABORATORY EQUIPMENT

UV Reactor: The irradiation setup was a 1200 ml continuous steel photoreactor with a 40W low-pressure mercury vapor sterilization lamp (Light Tech) in a quartz jacket. UV lamp is emitting short wave ultraviolet radiation at 253.7 nm. During a typical run, 800 ml sample solution was continuously circulated through the reactor with a peristaltic pump (Behr) that adjust the flow rate. The picture of experimental set-up is presented in Figure 3.1.

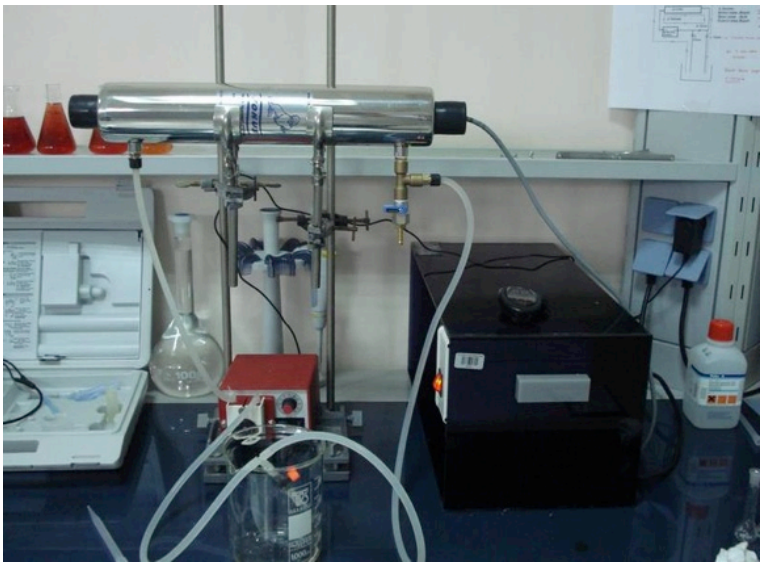

Figure 3.1 The picture of the UV/H_2O_2 AOP system

Ozone Generator: During ozonation and ultrasound coupled ozonation experiments ozone has supplied to the system through an OPAL-OG-400 model generator (100W). The dissolved ozone concentration in solution was determined by indigo method (Standard Methods 4500-B) and found as approximately 0.220 mg/l. The ozone is given to the reactor with bubbling through out the experiments to enhance the ozone dissolution.

Figure 3.2 The picture of the Ozone Generator

Ultrasonic Reactor: The system consists of 1500 ml glass reactor surrounding by cooling jacket to keep the temperature constant at 20±0.5^{0}C. Piezoelectric transducer is emitting at three frequencies, 582, 860 and 1136 kHz. 250-Watt generator converts the electrical power input into mechanical energy (Meinhardt). The active acoustical vibration area is 22cm^2 (Figure 3.3).

An ultrasonic system transforms electrical power into vibrational energy, i.e. mechanical energy, which is then transmitted into the sonicated reaction medium. The power supplied from the generator to into the reactor has measured by calorimetry, which involves a measurement of the initial rate of heating produced when a system is irradiated by ultrasound (Mason, 1999).

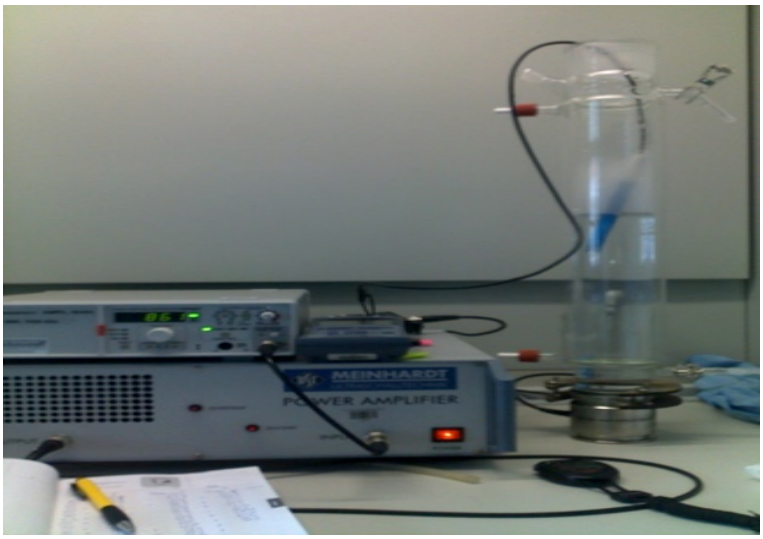

Figure 3.3 The picture of the Ultrasound Reactor

Spectrophotometer: HACH DR5000 UV-Visible spectrophotometer was used to determine the absorption spectra of the samples at 436, 525, 620 nm and Pt-Co scale. The degradation of color was monitored by measuring the reduction in the absorbencies. Hydrogen peroxide was measured spectrophotometrically and ozone determination has done spectrophotometrically at 600nm.

Figure 3.4 The picture of the Spectrophotometer

3.1.3 MATERIALS

Reagent grade Hydrogen Peroxide, H_2O_2 (30%, Merck) was obtained from Merck. Ferrous sulfate heptahydrate, FeSO4.7H2O, (99.5%, Fluka) was used for preparing Fenton reagent. Sodium Hydroxide (97.5%, Fluka) and sulfuric Acid (95-98%, Fluka) has used for pH adjustments.

3.1.4 ANALYTIC METHODS

Chemical Oxygen Demand (COD)*:* The COD is the indirect measurement of the oxygen needed for the complete oxidation of all the compounds present in solution – organic or inorganic-. It is an indirect measurement because oxidation is carried out by a strong oxidizing agent, potassium dichromate. It is usually taken as an estimation of the organic matter content in solution, in spite of the possible interference of non-organic reduced species contained in the sample (Cl-, Fe^{+2}, NO_2^-, sulphurs, etc.).

The analytical part comprises the heating to the temperature (148 ºC) of a known sample volume (2.5 mL) with an excess of potassium dichromate $K_2Cr_2O_7$ (1.5 mL of digestion solution) in presence of sulphuric acid (3.5 mL catalyst solution, Ag_2SO_4/H_2SO_4) for a period of time of two hours in sealed glass tubes. During this time, the organic matter is oxidized (Tchobanoglous and Burton, 1991).

Color Analyses*:* Wastewater from industries does not show sharp and distinguished absorption maxima. Characterization of the intensity of color of a water sample can be defined by measuring the absorption of light. Different colors cause maximum absorption at different wavelengths of the incident radiation. Although there are several color determination methods, in this study two most pronounced color determination methods are used. They are i) Chromacity number (RES), and ii) Pt-Co methods.

i) According to International Standard, the color of the water is determined by using photometer or spectrometer at least three different wavelengths distributed over the range of the visible spectrum:

λ(1)=436 nm λ(2)=525nm λ(3)=620nm

Absorbance of filtrated samples measured in their true color with a spectrophotometer according to ISO EN 7758. Measurements have performed at 436, 525 and 620 nm against optically pure water. Then, Chromaticity Number of the specified wavelength (α) calculated with the aid of Eq. (3.1):

$$\alpha(\lambda) = \frac{A}{d} \times f \qquad (3.1)$$

where:

A is the absorbance of the water sample at the wavelength λ;
d is the optical path lenght, in millimeters, of the cell;
f is a factor used to give the spectral coefficient, in reciprocal meters (f=1000)

As defined in ISO EN 7758, the limit discharge values for are 7, 5, 3 m^{-1}, for the wavelengths 436 nm, 525 nm, and 620 nm, respectively.

ii) Pt-Co is a color standard, made from dilutions of a Pt-Co solution by A.Hazen in American Chemical Journal, in 1892, adopted in Standard Methods For the Examination of Water and Waste Water, made by APHA. HACH DR 5000 UV-Vis spectrophotometer was used for the examination of color in terms of Pt-Co color unit. The stored program in spectrophotometer is calibrated in color units based on the APHA-recommended standard of 1 color unit being equal to 1 mg/l platinum as chloroplatinate ion. Test results (Programs 125) are measured at 465 nm. Prior to measurements, all samples are filtrated (0.45μm filter paper) to avoid interferences by undissolved matters.

Acccording to the current Turkish Water Pollution Control Regulation, color discharge limit for the related textile industry (Table 10.2) was given as 280 Pt-Co. In the near future, The Ministry of Environment is planning to define new standard, that is RES, for color examination.

HPLC (High Performance Liquid Chromatography) Analysis: The identification of the chemical constituents of the textile industrial wastewaters analysis was done by means of high-performance liquid chromatography (HPLC). The phenol and phenolic compounds was investigated for all samples during 30 minutes treatment by applied AOPs. Analyses have performed with Shimadzu Prominence LC-20A (Figure 3.5).

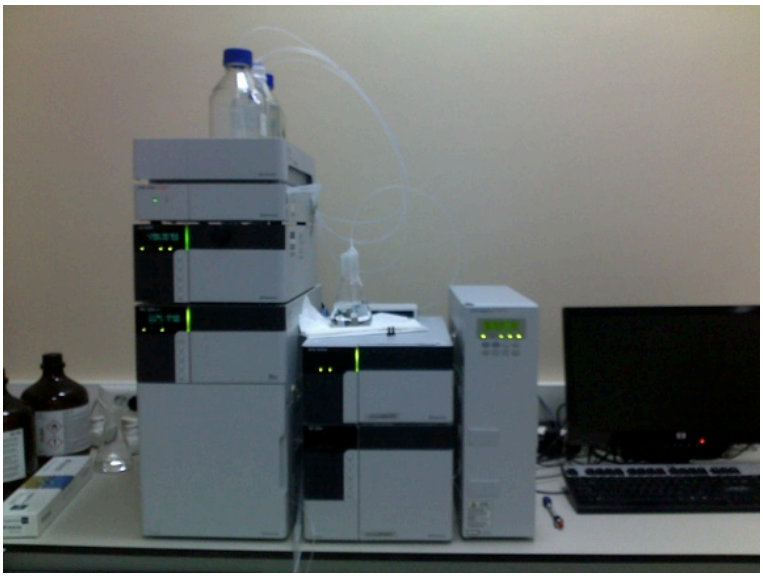

Figure 3.5 The picture of the HPLC

The column presented the following characteristics:

- Packing: Mediterranea Sea18
- Particle size: 5 μm
- Length: 10 cm
- Inner diameter: 0.46 cm

The mobile phase used was a mixture acetonitrile:water (80:20 %), isocratically delivered (constant composition and flow rate) by a pump at a flow rate of 1.5 ml/min^{-1}. The wavelength of the UV detector was selected from the absorption spectra of phenol and phenolic compounds. Maximum absorption of phenol was found 270 nm, and phenolic compounds, hydroquinone, resorcinol, catechol are 290, 275 and 275 nm, respectively. Injected volume of each sample was 20 μL. Temperature was set at 25ºC. Under these conditions, retention time for phenol, hydroquinone, resorcinol, catechol is

4.56 min, respectively. Integration was performed from the peaks area and the calibration was done by means of phenol standards.

TOC Analyses: Organic load is a key parameter in wastewaters control. For our analysis, we used both the total organic carbon (TOC) method, as well as the chemical oxygen demand (COD) method to determine the organic charge present. Basically, in the TOC analysis, the sample undergoes combustion until all carbon is in the CO_2 form. Next the carbon dioxide is quantified by IR detection.

The total organic carbon (TOC) technique is a quantification of all the carbon contained in the organic matter present in the water sample. The TOC analysis does not differentiate between the carbons of different organic compounds, but does distinguish between organic and inorganic carbon. Consequently, TOC does give a measure of the mineralization of the samples independent of the type of intermediates, which appear. Additionally, TOC is more accurate than COD. COD quantification must be carried out under strict conditions in order to have comparative results and could present interferences from some non-organic reducing species contained in the sample. The total carbon analyses of the samples generated during the degradation experiments gave us the mineralization rate of the processes in a simple and quick analysis. Total organic carbon of samples was determined with a Shimadzu TOC-VCPn analyzer.

Microtox Analysis: Toxicity of the samples was determined using a Microtox Model 500 Analyzer (Figure 3.6), which utilizes freeze-dried luminescent bacteria (*V. fisheri*) as test organisms.

Figure 3.6 The picture of the Microtox

3.1.5 Kinetic Studies

The degradation of color in all test samples was pseudo-first order with respect to the absorbance of the dye in the visible band. The analysis of absorbance versus time data by non-linear regression showed that absorbance decays exponentially:

$$\frac{A}{A0} = e^{-kt} \tag{3.2}$$

where A and A_0 are the maximum absorbance of the effluent at time t and zero, respectively, and k is the decay constant (min^{-1}).

CHAPTER 4

RESULTS AND DISCUSSIONS

4.1 UV/H_2O_2 PROCESS

4.1.1 Optimum H_2O_2 Dosage

Various concentrations (10, 25, 50 and 80 mM) of H_2O_2 was studied in the experiments. 800 ml of sample was fed to UV reactor by 40 ml/min flow rate with studied concentrations of H_2O_2. The experiments were conducted in the presence of UV light for 30 minutes. To determine the optimum dosage, kinetic rate constants k (min^{-1}) were calculated by monitoring the absorbance decays. Kinetic rate constants followed exponential decay as mentioned in section 3.1.5 and calculated for RES absorbance wavelengths, 436 nm, 525 nm and 620 nm, respectively. The experiments were performed at natural pH of the effluents that is 7-8 and at room temperature (20±0.5). The results of the experiments are given below as A/A_0 versus time.

The rise in the initial concentration of H_2O_2 increases the color degradation up to 25mM H_2O_2 concentration, after that, it begins to decline with the increase in H_2O_2 concentration (80mM H_2O_2). This decrease in the H_2O_2/UV process can be attributed to the scavenging effect of excess H_2O_2 (with hydroxyl radicals) as can be seen in (Equation 2.4). Excess hydrogen peroxide readily reacts with hydroxyl radicals, leading to the formation of the hydroperoxyl radical HO_2•, which is less powerful than OH•. Also, via this scavenging reaction, less amount of OH• will be left in solution for further dye degradation/decolorization. At low concentration of H_2O_2 (10mM), relatively low concentration of hydroxyl radicals was formed for dye oxidation, which results in low decolorization rate.

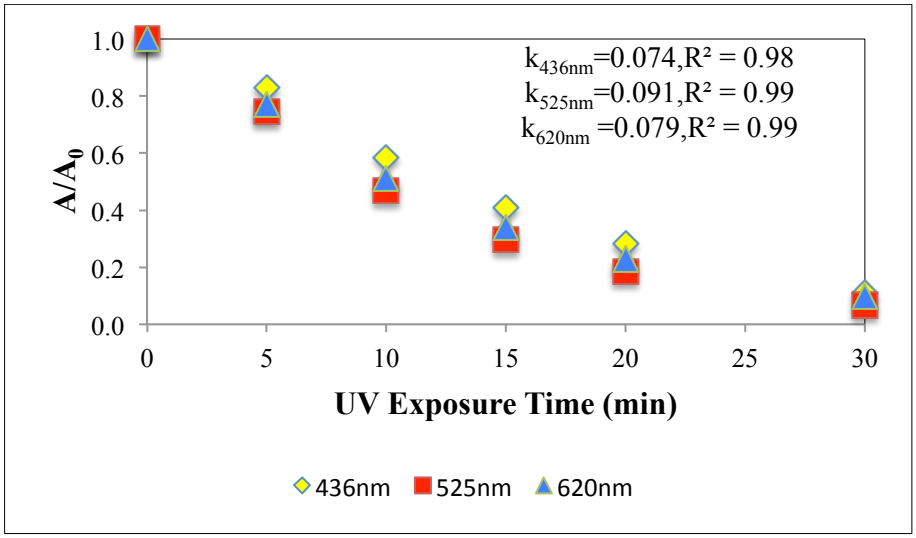

Figure 4.1 Rate of color removal for 10mM H_2O_2

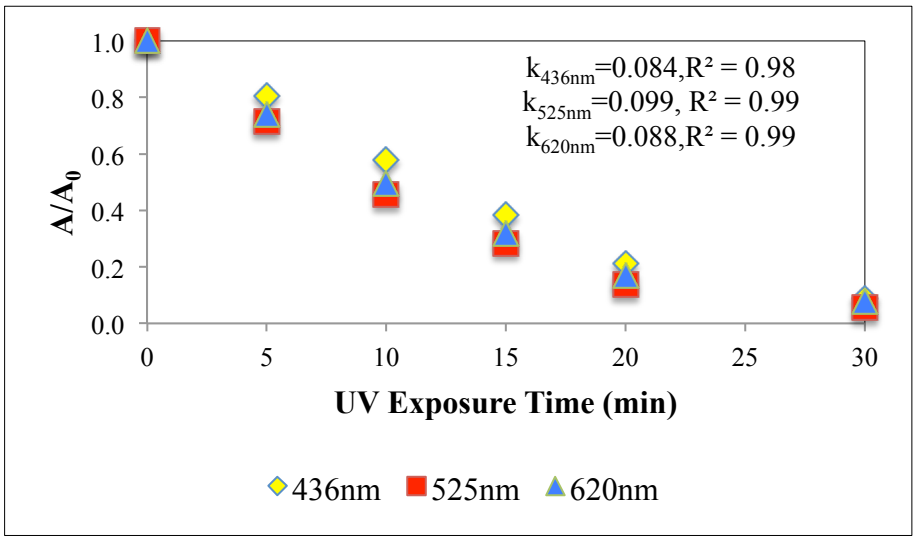

Figure 4.2 Rate of color removal for 25mM H_2O_2

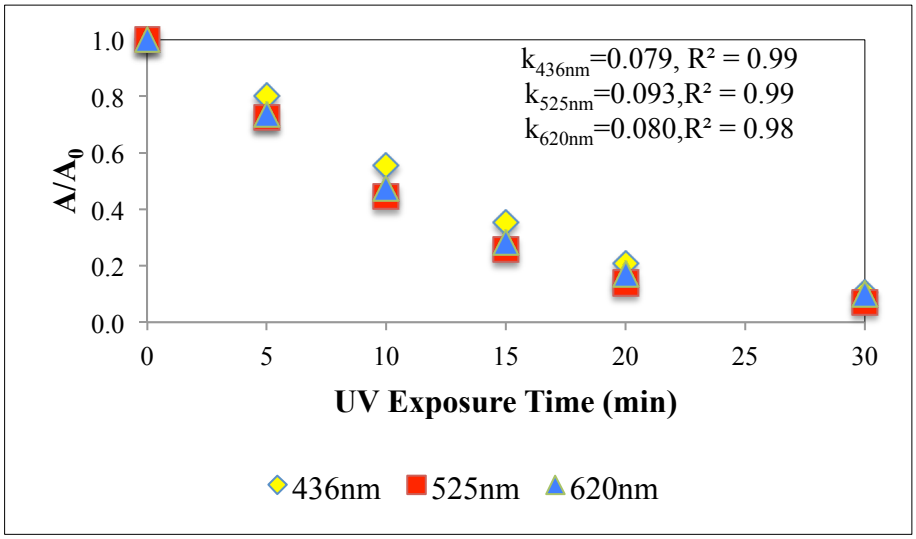

Figure 4.3 Rate of color removal for 50mM H_2O_2

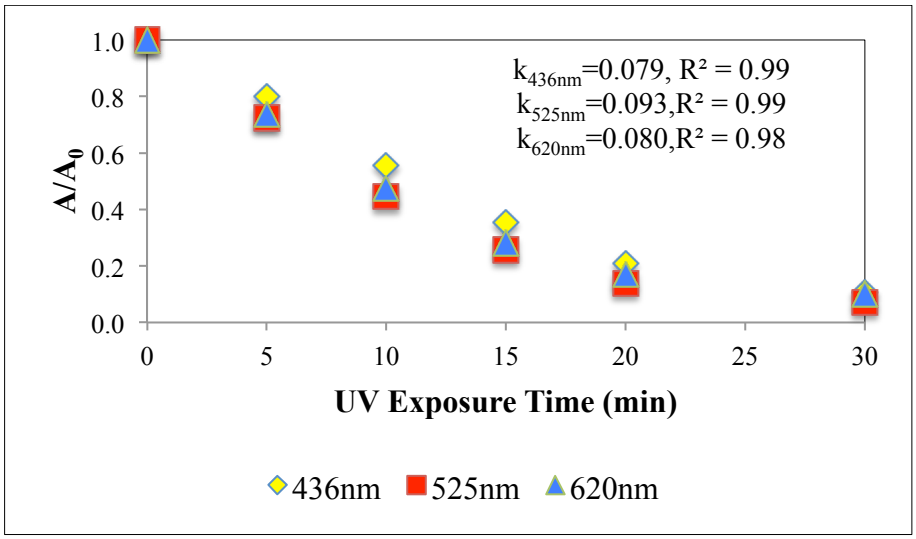

Figure 4.4 Rate of color removal for 80mM H_2O_2

The optimum H_2O_2 dosage was selected as 25 mM from the kinetic rate constants, k (min^{-1}). The fastest degradation of the pollutants has occurred at 25 mM H_2O_2/UV for k values of the three wavelengths. Table 4.1 shows the reaction rates at various H_2O_2 concentrations for UV/H_2O_2 process.

Table 4.1 Kinetic Rate Constants, k (min^{-1}) values

H_2O_2 Conc. (mM)	Kinetic Rate Constants (k min^{-1})		
	436nm	**525nm**	**620nm**
10	0.0748	0.0908	0.0789
25	**0.0837**	**0.0994**	**0.0876**
50	0.0786	0.0930	0.0804
80	0.0637	0.0782	0.0707

4.1.2 Effect of pH

The influence of pH on the rate of decolorization of the effluent samples by UV/ 25mM H_2O_2 process was investigated at two different pH values: 3.0 and natural pH 7-8 during 30 minutes of treatment time and 40 ml/min flow rate with 800ml sample. The pH was adjusted with concentrated H_2SO_4. The Figure 4.5 depicts the color removal rate at 436, 525 and 620 nm wavelengths at pH 3. The results showed that the degradation rate increased when pH increased from 3 to 7-8 (Figure 4.6). Increase in pH could improve the formation of hydroperoxide anion (HO_2^-) to generate more ·OH, since the molar extinction coefficient of HO_2^- (240 $mol^{-1}L\ s^{-1}$) was higher than that of H_2O_2 (19.6 $mol^{-1}L{\cdot}s^{-1}$), and the reaction rate of HO_2^- with OH• was faster than that of H_2O_2. The reaction rate of HO_2^- with OH is 7.5 10^9 M^{-1} s^{-1} while as H_2O_2 is 2.7 10^7 M^{-1} s^{-1} (Eq. 4.1 and 4.2).

$$OH\cdot + H_2O_2 \rightarrow O_2^- + H_2O + H^+ \quad (k = 2.7\ 10^7\ M^{-1}s^{-1}) \tag{4.1}$$

$$OH\cdot + HO_2^- \rightarrow O_2^- + OH^- + H^+ \quad (k = 7.5\ 10^9\ M^{-1}s^{-1}) \tag{4.2}$$

Additionally, by acidifying the solution, amount of added conjugated bases increased (Cl^-, NO_3^-, SO_4^{-2}, PO_4^{-3}) anions. These anions are able to react with hydroxyl radicals leading to inorganic radical ions, which show a much lower reactivity than OH•, so that to avoid this anions to compete with OH•, even though they have slow reactions rates, the pH adjustment has not done. It is preferred to study at neutral conditions. There is also a drastic competition between the wastewater and the anions with respect to HO• (Mitrovic et al., 2001). At higher pH values, the adverse effect of alkalinity (scavenging effect of CO_3^{-2} with OH•, and less reactive carbonate radical

formation) did not play an important role for decolorization. Probably alkalinity scavenging reactions is not dominant at pH 7-8. The reverse effects of alkalinity could occur at high pHs than 7-8. When the hydroxyl radicals are scavenged by bicarbonate or carbonate ions, the products may be carbonate ion radicals that in turn may react with the organic compounds; however, these new radicals are more selective and have lower rate constants species (Tuhkanen, 2004). On the other hand, bicarbonate and carbonate do not adsorb UV light, they simply react readily with hydroxyl radicals (Wang et al., 2000), and thus they do not compete for UV irradiation during UV-based AOPs.

Therefore, to avoid the adverse effect of acidification of samples, the natural pH (7-8) is selected as optimum pH level. And also, the results presented in this experiment sets indicates the reaction rates constant of pH:7-8 is higher than pH:3 (Table 4.2).

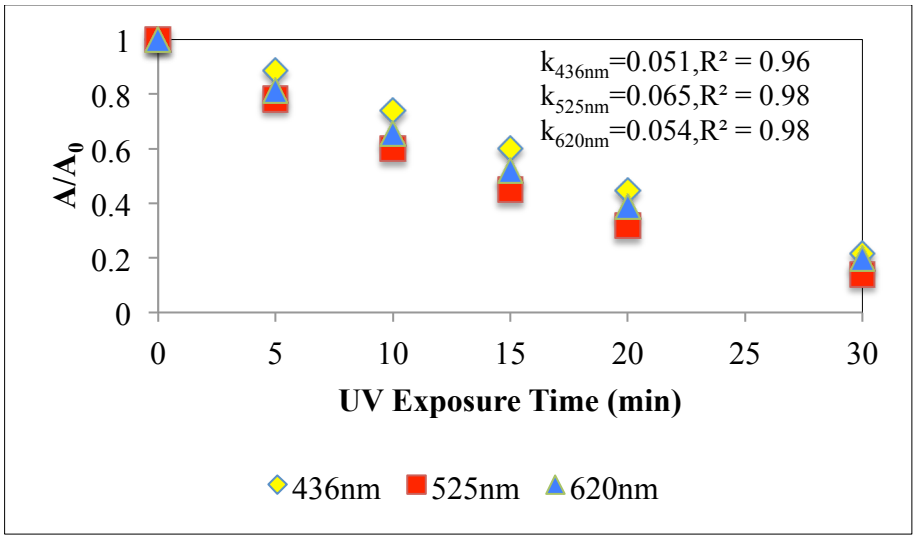

Figure 4.5 Rate of color removal at pH:3 for 25mM H_2O_2/UV

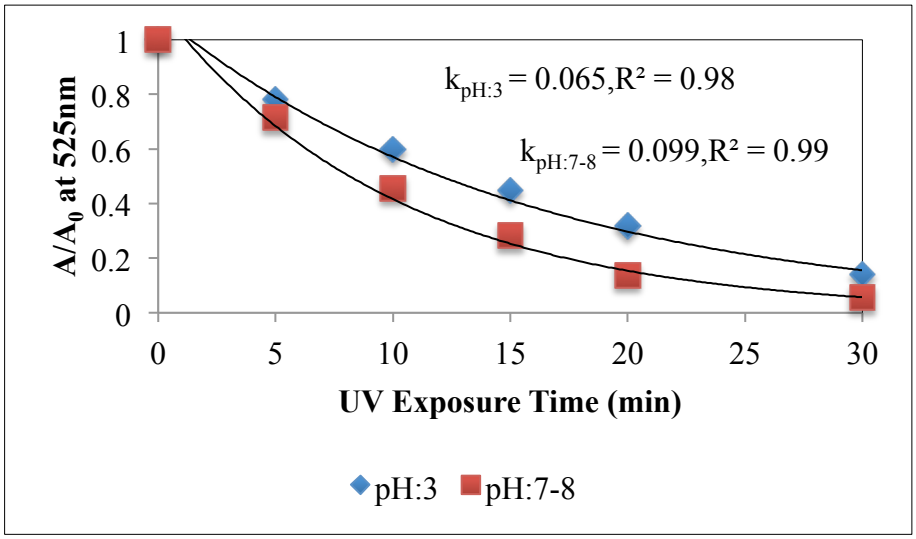

Figure 4.6 Comparison of color removal rate at pH:3 and pH:7-8 for 25mM H_2O_2/UV

Table 4.2 Kinetic Rate Constants k (min^{-1}) values pH:3 and pH:7-8

pH	Kinetic Rate Constants (k min^{-1})		
	436nm	525nm	620nm
3	0.051	0.065	0.054
7-8	0.083	0.099	0.097

4.1.3 Effect of Flow Rate

All experiments were performed at 40 ml/min flow rate. Additionally 90 ml/min flow rate has tried to compare flow rate factor. Optimal conditions (original pH and 25mM H_2O_2) have used.

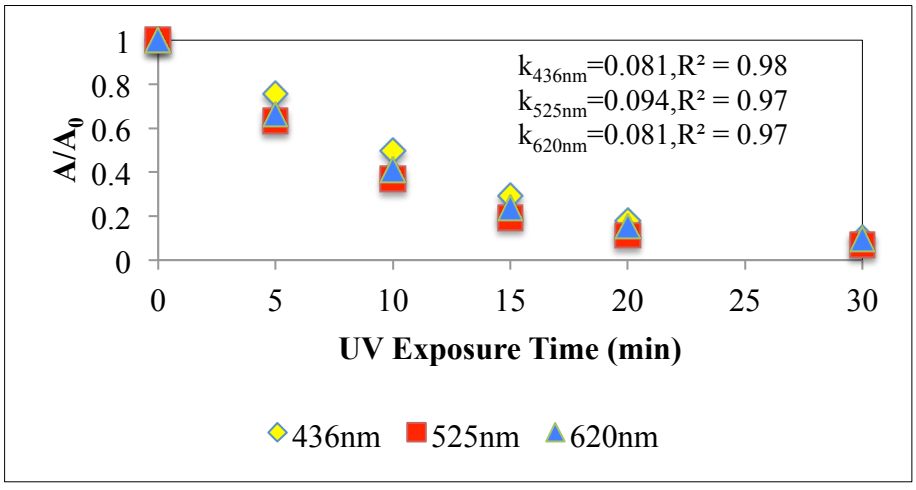

Figure 4.7 Color removal rate at 90 ml/min flow rate

There is no clear difference between two flow rates as seen Table 4.3. Kinetic rate constants are almost the same. 40 ml/min has chosen as optimum flow rate.

Table 4.3 Kinetic rate constants of flow rates, 40 and 90 ml/min

Flow Rate (ml/min)	Kinetic Rate Constants (k min^{-1})		
	436nm	525nm	620nm
40	0.08	0.09	0.09
90	0.08	0.09	0.08

4.2 PHOTO-FENTON AND FENTON PROCESSES

4.2.1 Optimum Fe^{+2} Concentration

Photo-Fenton processes were performed with optimum H_2O_2 concentration (25mM) and various ferrous concentrations (0.01, 0.1, 0.5 and 1 mM Fe^{+2} solutions). Sample pH was adjusted to 3 where Fenton reactions have the highest decolorization yields as discussed in Chapter 2, then 25mM H_2O_2 has added to 800ml sample. At the end of the experiments, samples pH was adjusted to nearly 8 with 1 N NaOH, followed by 90 ml/min centrifuge for 5 minutes. The ferrous sludge was discarded from the clear phase for color analysis. The same procedure was conducted for dark Fenton process.

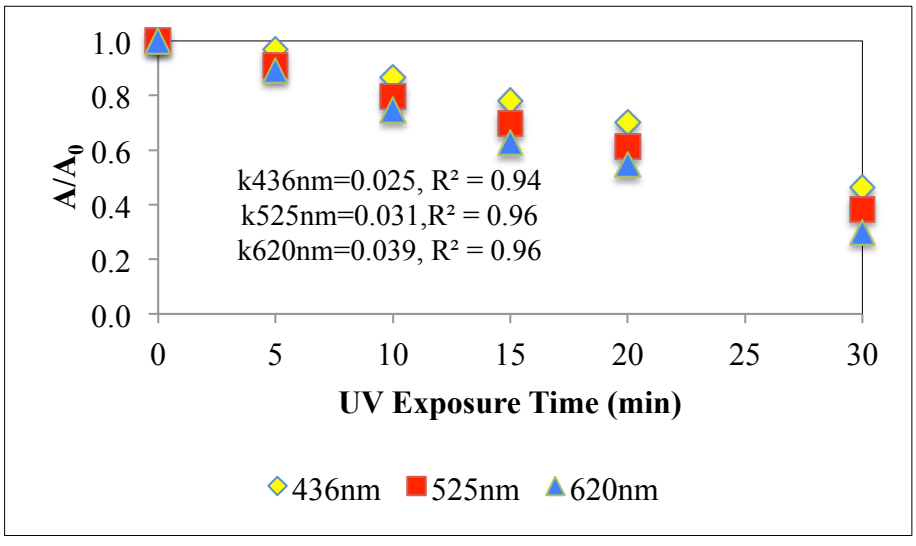

Figure 4.8 Rate of color removal for 0.01mM Fe(II)/25mM H_2O_2/UV

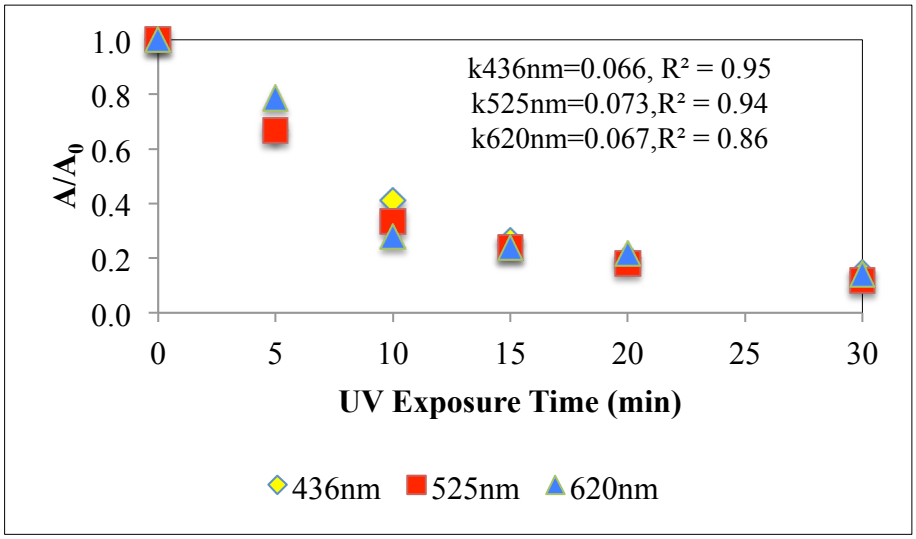

Figure 4.9 Rate of color removal for 0.1mM Fe(II)/25mM H_2O_2/UV

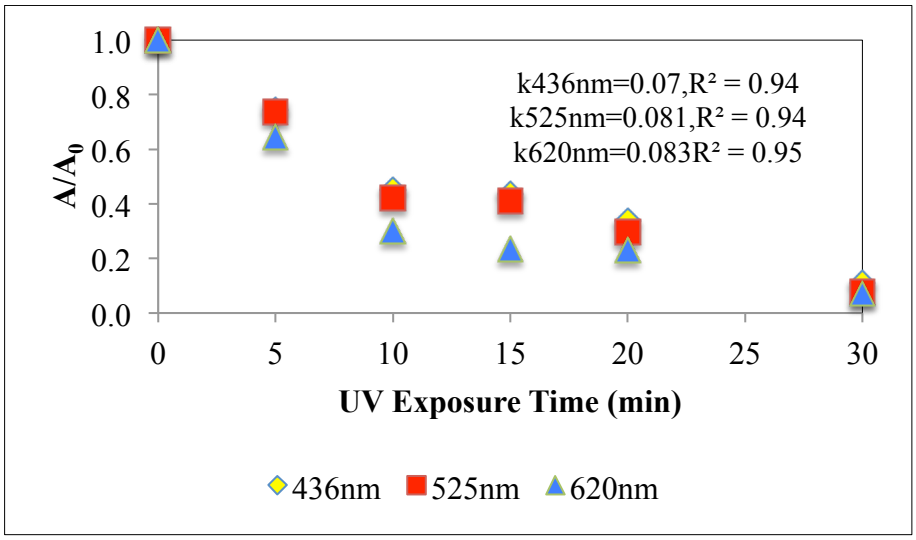

Figure 4.10 Rate of color removal for 0.5mM Fe(II)/25mM H_2O_2/UV

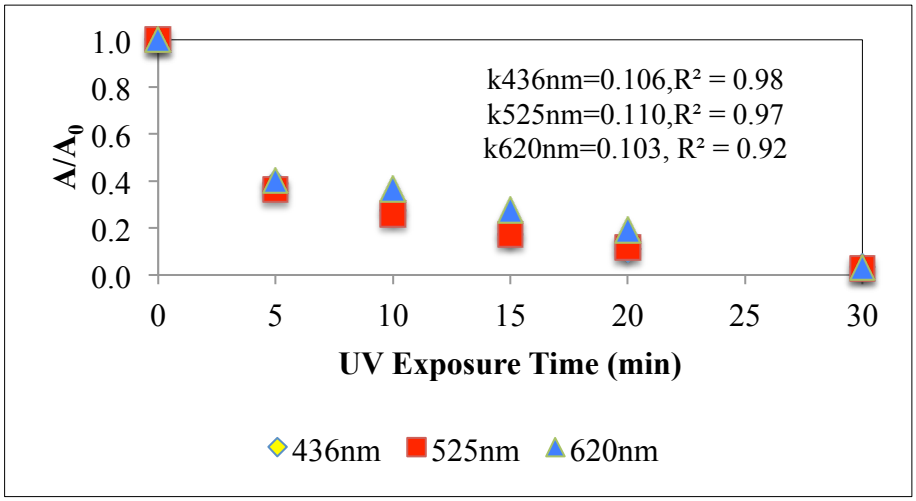

Figure 4.11 Rate of color removal for 1mM Fe(II)/25mM H_2O_2/UV

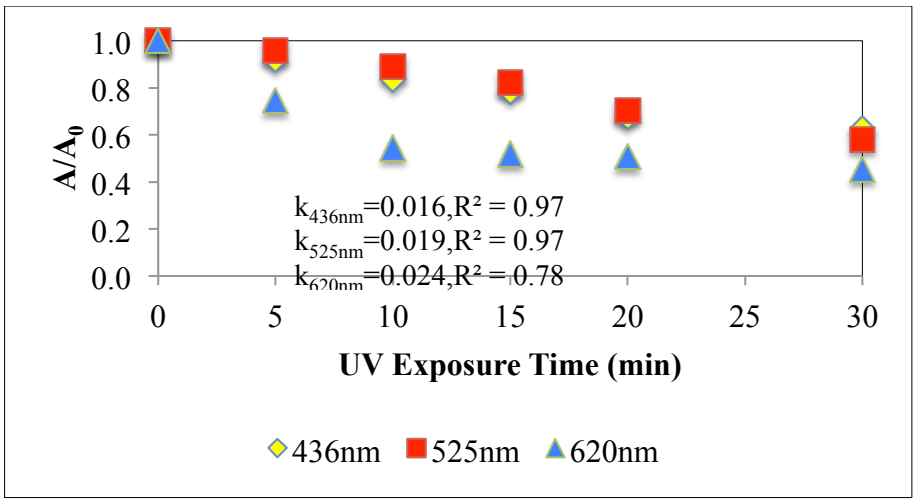

Figure 4.12 Rate of color removal for 0.1mM Fe(II)/25mM H_2O_2

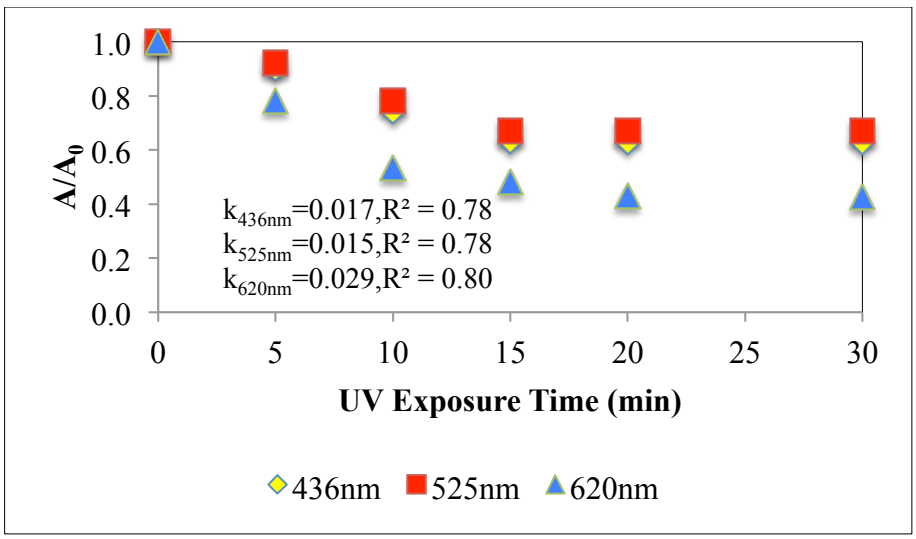

Figure 4.13 Rate of color removal for 1mM Fe(II)/25mM H_2O_2

Degradation efficiency by Fenton process is affected by Fe^{+2} ions concentration addition, which catalyze hydrogen peroxide decomposition resulting in $OH^{\cdot}$ radical production and consequently the degradation of organic molecules. The effect of Fe^{+2} concentration on color removal was examined by changing the Fe^{+2} concentration between 0.01 to 1mM while keeping the concentration of H_2O_2 and pH constant ($[H_2O_2]$=25mM, pH 3.0).

Fenton oxidation is known as a highly pH dependent process since pH plays an important role in the mechanism of OH radical production in the Fenton's reaction. At high pH (pH > 4), the generation of OH radical gets slower because of the formation of the ferric hydroxo complexes. The complexes would further form $[Fe(OH)_4]$ when the pH value is higher than 9 (Gulkaya et al., 2006). On the other hand, at very low pH values (<2.0) hydrogen ions acts as OH radical-scavengers. The reaction is slowed down due to the formation of complex species $[Fe(H_2O)_6]^{+2}$, which reacts more slowly with peroxide compared to that of $[Fe(OH)(H_2O)_5]^{+2}$. Therefore, the samples' pH adjusted to 3 to increase the efficiency of the systems.

The degradation rates increased with increasing the amount of Fe^{+2} for Fenton and photo-Fenton processes see Figures 4.8-4.13. In Fenton process addition of Fe^{+2} from 0.1mM to 1mM increases rate constant of reaction. The reaction rate for 1mM Fe^{+2} is higher than 0.1mM. In photo-Fenton process the k (min^{-1}) values are much greater than dark Fenton processes. Due to its slow dissociation rate in the dark, the generation of hydroxyl radicals was reduced. It is obvious that UV irradiation affects the efficiency of destruction effluent samples. It will react with hydrogen peroxide to produce the hydroxyl ions and radicals, and effectively promote the Fenton reaction.

Comparison reaction rates of Fenton and photo-Fenton processes have given Table 4.4. Fenton reactions are significantly slower than photo assisted reactions. In the same Fe^{+2} concentration (1mM), photo-fenton process is 100 times faster than dark fenton reaction.

The high removal efficiency of Fenton and photo-Fenton method can be explained by the fact that oxidation reaction are coupled to coagulation occurring due to

the presence of ferrous/ferric cations, thus these metallic ions play a double role as a catalyst and a coagulant in the process (Abo-Farha,2010).

Table 4.4 Kinetic rate constants for photo-Fenton and Fenton reactions

PHOTO-FENTON PROCESS			
Fe^{+2} Conc. (mM)	**Kinetic Rate Constants (k min^{-1})**		
	436nm	**525nm**	**620nm**
0.01	0.02	0.03	0.03
0.1	0.06	0.07	0.07
0.5	0.06	0.08	0.08
1	0.10	0.11	0.10
FENTON PROCESS			
Fe^{+2} Conc. (mM)	**Kinetic Rate Constants (k min^{-1})**		
	436nm	**525nm**	**620nm**
0.1	0.01	0.01	0.02
1	0.01	0.01	0.02

4.3 OZONATION PROCESS

4.3.1 Ozone-Alone Process

Ozone was introduced to 500 ml sample for 30 minutes at pH 3, 7-8 (original) and 10 to study the effect of pH on decolorization rate. O_3 was supplied by an air-ozone generator through a pump with a diameter of 40 mm and length of 300mm. The generated ozone amount has determined by indigo colorimetric method described in Standard Methods for the Examination of Water and Wastewater (APHA, 1989) (APPENDIX A). Ozone is transferred to the sample by porous diffusers to improve efficiency.

The temperature was kept constant at 20°C in this study keeping in mind that the higher the temperature, the lower the ozone solubility and stability. But, the temperature increase from 0 to 30°C will enhance the ozonation rate and this enhancement will

exceed all the other effects of ozone instability and lower solubility. It is generally accepted that increasing temperature by 10°C increases the reaction rate by a factor of 2 or 3. (Faroq et al ., 1991), and the ozone reaction rate increases (Guendy, 2007).

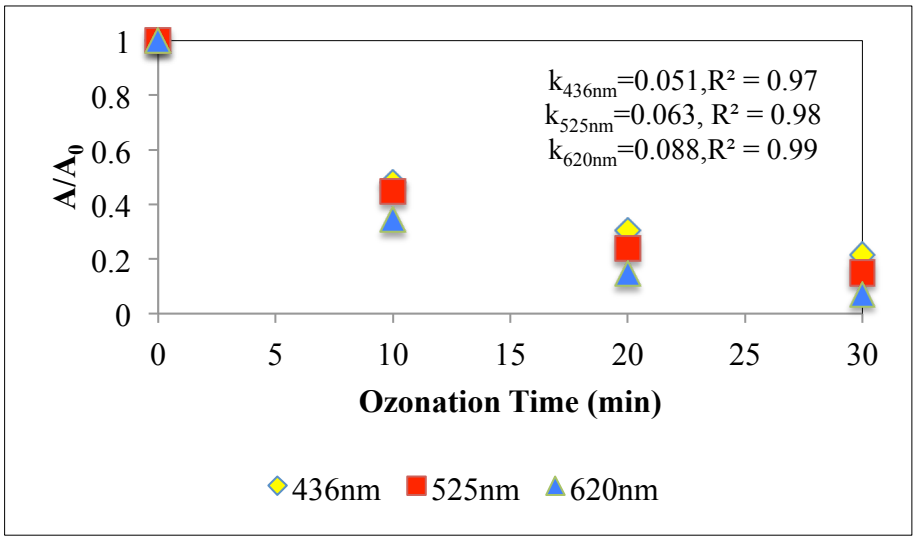

Figure 4.14 Rate of color removal at pH:3

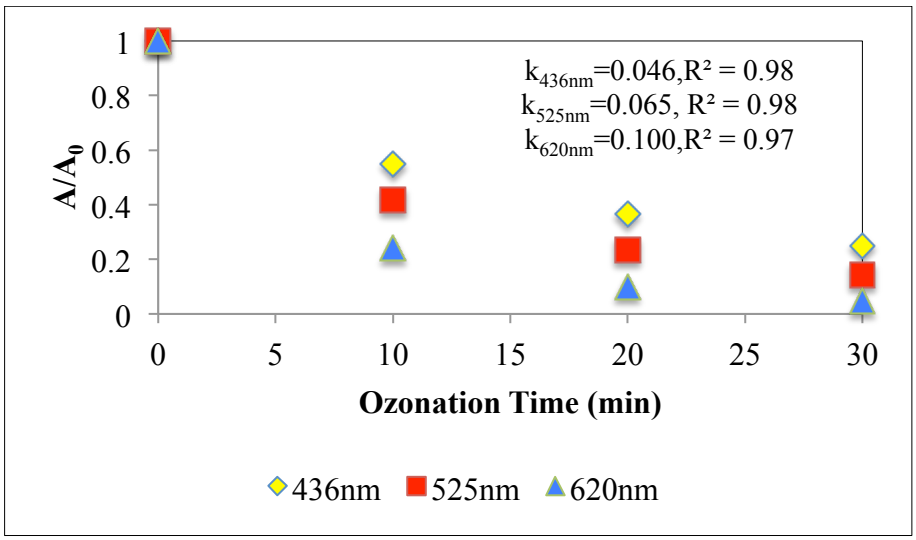

Figure 4.15 Rate of color removal at pH:7-8

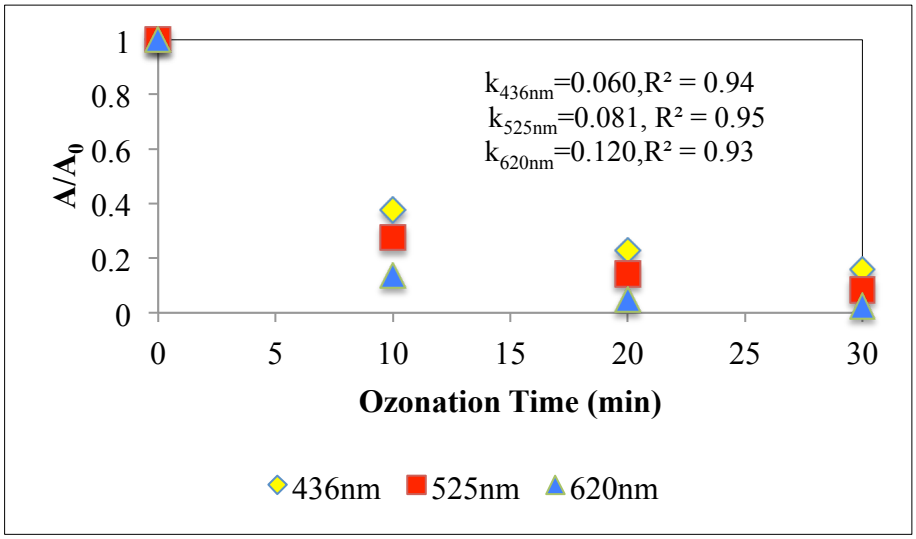

Figure 4.16 Rate of color removal at pH:10

The pH of the solution will alter the chemical composition of the ozone; for example, hydroxyl radicals were formed from ozone decomposition at high pH, while the molecular ozone remains as the main oxidant at low pH. Since hydroxyl radicals have a higher oxidizing ability than ozone, higher pHs should be favorable for dye and color oxidation (Michelsen, 1992). At low pH level (pH 3), it reacts primarily as the O_3 molecule by selective and sometimes relatively slow reactions. Ozone at elevated pH 10 it rapidly decomposes into hydroxyl free radicals, which react very quickly and hence, the reaction rates at pH 10 is higher than the other studied pH values. Hydroxyl radical produced due to decomposition of ozone explains the increased dissociation of ozone with increasing alkalinity.

Table 4.5 Kinetic rate constants for ozonation process

OZONATION	Kinetic Rate Constants (k min^{-1})		
	436nm	**525nm**	**620nm**
pH:3	0.051	0.063	0.088
pH:7-8	0.046	0.065	0.100
pH:10	0.060	0.081	0.120

4.3.2 Ozone/H_2O_2 Process

The effect of H_2O_2 addition to O_3 oxidation was investigated by adding 25mM H_2O_2 at original wastewater pH and the wastewater was ozonated for 30 min with the same O_3 flow rate at ozone-alone process.

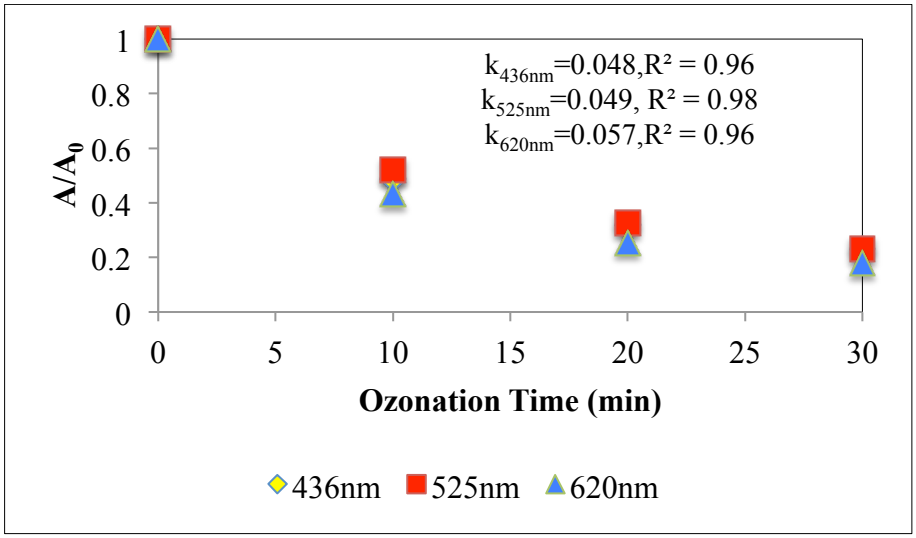

Figure 4.17 Rate of color removal at pH:7-8, Ozone/25mM H_2O_2

Color removal was monitored at pH 7,8 (natural pH of the wastewater) and presented in Figure 4.17. Decolorization decay rate constants did not enhanced (even decreased at the abundant color wavelength, 525 and 620 nm) by the addition of H_2O_2. This result may be explained by the oxidation of inorganic species ozone and scavenging effect of H_2O_2 at the studied concentration . Inorganic compounds can react much faster with ozone than organic compounds. The variation in direct rate constants for inorganic compounds, however, spans a much wider range- more than 12 orders of magnitude compared to 6- with exceptions- for organic compounds. Likewise, the reaction is faster with ionized or dissociated inorganic compounds. The reaction rate for O_3/H_2O_2 is dependent on the initial concentration of ozone/hydrogen peroxide (Gunten, 2003).

$$H_2O_2 \leftrightarrow HO_2^- + H^+ \quad pK_{a=}11.8 \tag{4.3}$$

$$HO_2^- + O_3 \rightarrow HO_2^- + O_3^- \quad K_{a=}2.2\times10^6 M^{-1}s^{-1} \tag{4.4}$$

The reaction of ozone with the undissociated hydrogen peroxide, which would lead to a loss of ozone and hydrogen peroxide, is negligible:

$$H_2O_2 + O_3 \rightarrow H_2O + 2O_2 \quad k < 10^{-2}M^{-1}s^{-1} \tag{4.5}$$

The hydroperoxyl radical $HO_2^-\bullet$ and the ozonide anion $O_3^-\bullet$ produced in Equation (4.4) then enter the chain reaction of indirect pathway to produce OH radical. Comparison of the initial reaction of ozone with HO_2^- (2.2×10^6 M^{-1} s^{-1}) and to that of ozone with OH^- (k=70 M^{-1} s^{-1}) shows that in the O_3/H_2O_2 system the initation step by OH^- is negligible. Whenever the concentration of hydrogen peroxide is above 10^{-7}M and the pH value less than 12, HO_2^- has a greater effect than OH^- has on the decomposition rate of ozone in water.

4.4 ULTRASOUND PROCESSES

In sonochemical systems, optimization of input power and the reactor configuration is the most important strategy to achieve maximum reaction yields. An ultrasonic system transforms electrical power into vibrational energy, i.e. mechanical energy, which is then transmitted into the sonicated reaction medium. Part of it is lost to produce heat, and another part produces cavitation, but not all of the cavitational energy produces chemical and physical effects. Some energy is reflected and some is consumed in sound re-emission (Mason, 1999). Hence, there can be significant differences between the power supplied from the generator and that delivered into the reactor. In a pure liquid, one might assume that almost all the mechanical energy (acoustic energy) is transformed to heat by absorption. Of the methods available to measure the amount of ultrasonic power entering a sonochemical reaction medium, the most common and easiest is calorimetry, which involves a measurement of the initial rate of heating produced when a system is irradiated by ultrasound (Mason, 1999). The method involves the measurement of the temperature rise T against time t for about 30 seconds, using a thermocouple placed in the reaction vessel. From T versus t data, the temperature rise at zero time, dT/dt, can be estimated either by curve-fitting the data to a polynomial in t, or by constructing a tangent to the curve at time zero. The ultrasonic power (P) actually entering the system can then be calculated by substituting the value

of dT/dt into equation 4.1. (Mason, 1999; Mason and Cordemans, 1998; Mason *et al*., 1992):

$$\text{Power} = (dT/dt).C_p.M \qquad (4.1)$$

where

C_p= heat capacity of water (~4.1840-4.1790 J $g^{-1}.ºC^{-1}$),

(dT/dt)= the temperature rise at zero time,

M= total mass of water in the reaction vessel (g).

After calculating the power in the reaction medium, the efficiency of the system can be determined either by calculating the ultrasonic intensity which is equal to total (determined) power per unit emitting area (W cm^{-2}), or by ultrasonic density (W mL^{-1}), i.e. total power per total mass of the solvent (water) in the reactor.

In general, the generator power should not automatically be turned to a maximum, because a relatively small amount of energy is often sufficient. In most cases, the increase in power leads to the creation of more bubbles in the bulk liquid, which lowers the effective reaction yield by absorbing the acoustic energy. Decoupling can also result from a reduction of the area of the emitter surface due to the greater number of bubbles.

4.4.1 System Optimization

Calorimetric tests were performed at various power settings during 10 min sonication of 500, 800, 1000 and 1250 mL of deionized water. The power input was calculated from the change in temperature by the calorimetric measurements. Ultrasound system has different amplitude degrees start from 1 to 7. The experiments performed at three different amplitude degrees, 5-6-7 to determine the optimum conditions. Temperatures during 10 minutes sonication at various amplitudes and volumes have given APPENDIX B. The example calculations have done below;

Table 4.6 Increase of temperature by the time
(500ml sample, 860kHz, amplitude degree 7)

Time (min)	**0**	**0.30**	**1**	**1.5**	**2**	**2.5**	**3**	**3.5**	**4**	**4.5**	**5**
T (^{0}C)	22.5	23.8	24.7	25.6	26.8	27.7	28.9	29.8	30.9	32.1	33.0
Time (min)	**5.5**	**6**	**6.5**	**7**	**7.5**	**8**	**8.5**	**9**	**9.5**	**10**	
T (^{0}C)	34.0	35.2	36.0	37.0	37.8	38.9	39.9	40.8	41.8	42.7	

From T (temperature) versus t (time) data plotted in Figure 4.18, the temperature rise at zero time, (dT/dt), was calculated by curve-fitting the data to a polynomial in t.

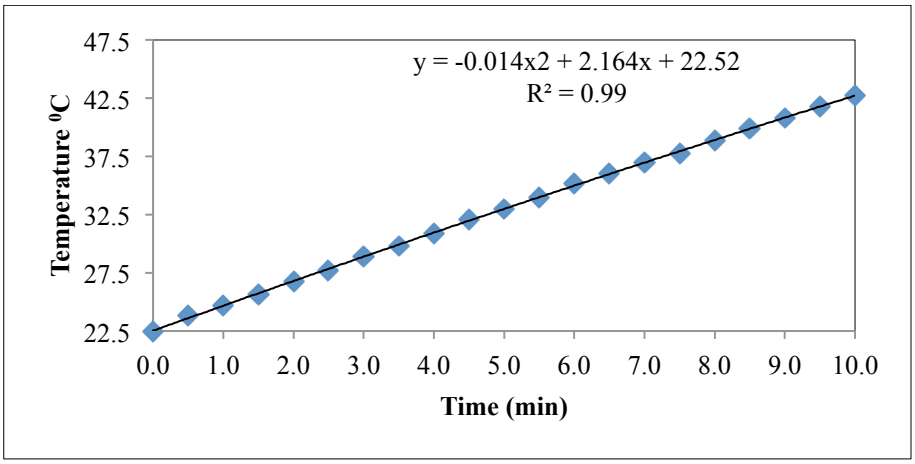

Figure 4.18 Temperature rise by the time
(500 ml sample at 860 kHz and amplitude degree 7)

The power input is calculated by substituting the value of dT/dt into Eq. (4.1):

C_p = 4.178 J g^{-1} $ºC^{-1}$(average of the heat capacity of water in between 19 – 23 ºC) (Weast and Astle, 1983), M = 500 g, dT/dt= (2.164/60) = 0.036 ºC sec^{-1}

Thus, Power = 0.036 (ºC sec^{-1}) × 4.178 (J g^{-1} $ºC^{-1}$) × 500 (g) = 75 W and the corresponding power density value is 0.15= (75/500) W mL^{-1}.

The maximum power density was obtained when the solution volume was 500 mL. The power density reduced as the volume of water was increased. The maximum power density is 0.15 as seen the Table 4.7 As a result, optimum conditions are 500 mL at 7 degree amplitude and 860 kHz.

Table 4.7 Colorimetric measurements of power input and power densities at various amplitudes and reaction volumes

Frequency	582kHz					
Amplitude	5		6		7	
Volume (ml)	Power Input (W)	Power Density (W/ml)	Power Input (W)	Power Density (W/ml)	Power Input (W)	Power Density (W/ml)
500	14.64	0.03	33.47	0.07	56.48	0.11
800	13.39	0.02	26.78	0.03	73.64	0.09
1000	16.74	0.02	33.47	0.03	66.94	0.07
1250	15.69	0.01	36.61	0.03	62.76	0.05
Frequency	860kHz					
Amplitude	5		6		7	
Volume (ml)	Power Input (W)	Power Density (W/ml)	Power Input (W)	Power Density (W/ml)	Power Input (W)	Power Density (W/ml)
500	20.92	0.04	37.66	0.08	73.22	0.15
800	16.73	0.02	33.47	0.04	70.29	0.09
1000	25.10	0.03	37.66	0.04	79.50	0.08
1250	20.92	0.02	41.84	0.03	88.91	0.07
Frequency	1136kHz					
Amplitude	5		6		7	
Volume (ml)	Power Input (W)	Power Density (W/ml)	Power Input (W)	Power Density (W/ml)	Power Input (W)	Power Density (W/ml)
500	12.52	0.03	27.19	0.05	58.58	0.12
800	20.08	0.03	33.47	0.04	70.29	0.09
1000	12.55	0.01	33.47	0.03	58.58	0.06
1250	26.15	0.02	36.61	0.03	67.99	0.05

4.4.2 Rate of Hydrogen Peroxide

In an attempt to determine correlation between system performances in terms of chemical effects, the production of hydrogen peroxide was monitored in deionized water as an indirect indicator of free radical production (Hydrogen peroxide is produced during the sonolysis of water by the recombination of •OH at the cooler bubble interface as •OH + •OH → H_2O_2).

Pre-aerated deionized water was sonicated for 30 minutes at optimized conditions (maximum conditions) and samples were withdrawn from the reactors at 10 minute intervals to analyze hydrogen peroxide concentration in the effluents. The analysis was made by the triiodide method (Klassen *et al*., 1994) accordance with Standard Methods, details of which are given in APPENDIX C together with calibration curve.

H_2O_2 concentrations for 500 ml deionized water at 582, 860 and 1136 kHz have calculated by the aid of H_2O_2 calibration curve. H_2O_2 production at 582 and 860 kHz is almost same and two times faster than 1136 kHz.

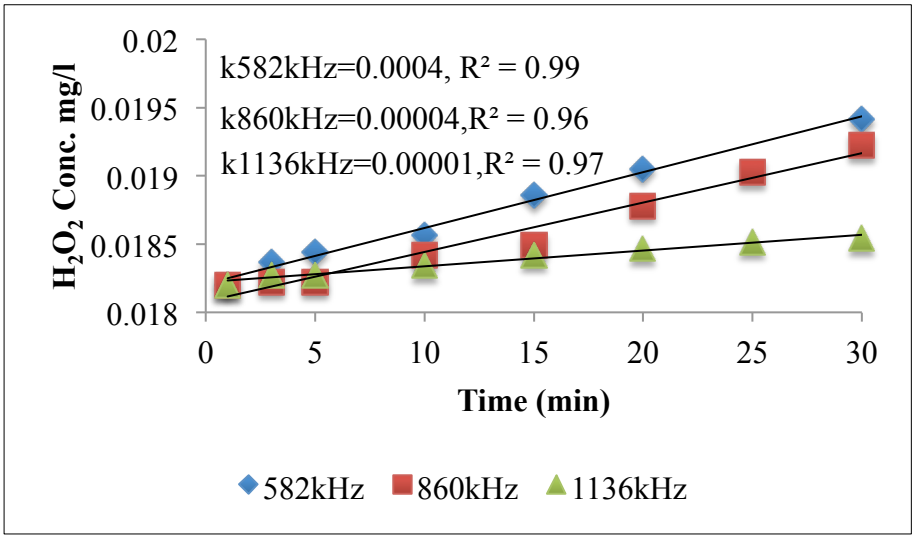

Figure 4.19 H_2O_2 concentration during 30 minutes ultrasonic irradiation

4.4.3 Ultrasound Processes

4.4.3.1 US-Alone System

The one hour pre-aerated 500 ml samples were irradiated at 860 kHz in the presence of aeration. The reactor was cooled with water circulation to keep the temperature constant. Absorbance measurements were done with filtrated samples. The results are shown in Figure 4.20.

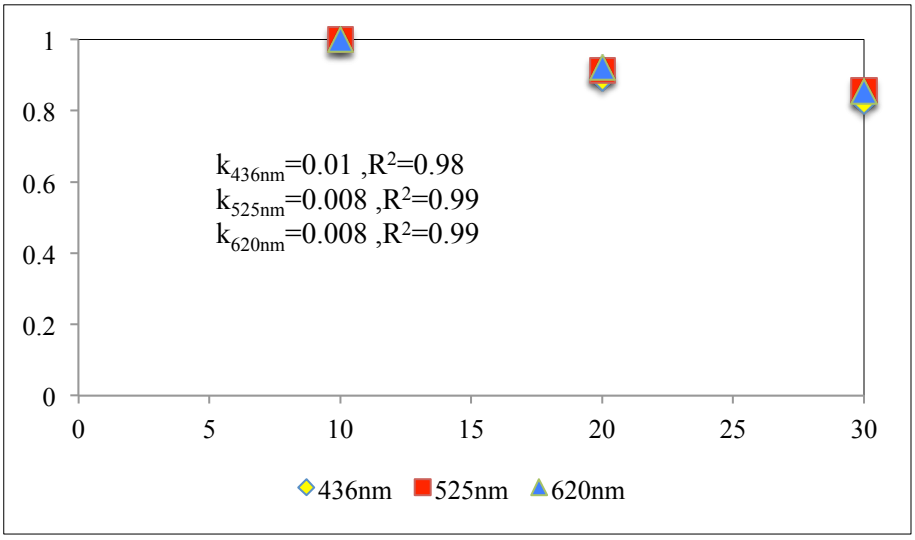

Figure 4.20 Color Removal Rate for US-Alone Process at 436, 525 and 620nm

The reaction rates of US-Alone process are slower than the other studied AOPs. The color removal has not achieved during 30 minutes sonication. It is easy to say that US-Alone process is not efficient for and should be coupled with other oxidants or catalysts to enhance the decolorization yield.

4.4.3.2 Combined US Processes

At least one hour pre-aerated 500ml of sample were used for US/Ozone and US/Ozone/H_2O_2 processes. The experiments were carried out at original pH of the samples. H_2O_2 concentration was 25mM. Ultrasound frequency was 860 kHz. Ozone was given to US reactor with diffusers to dissipate the ozone effectively.

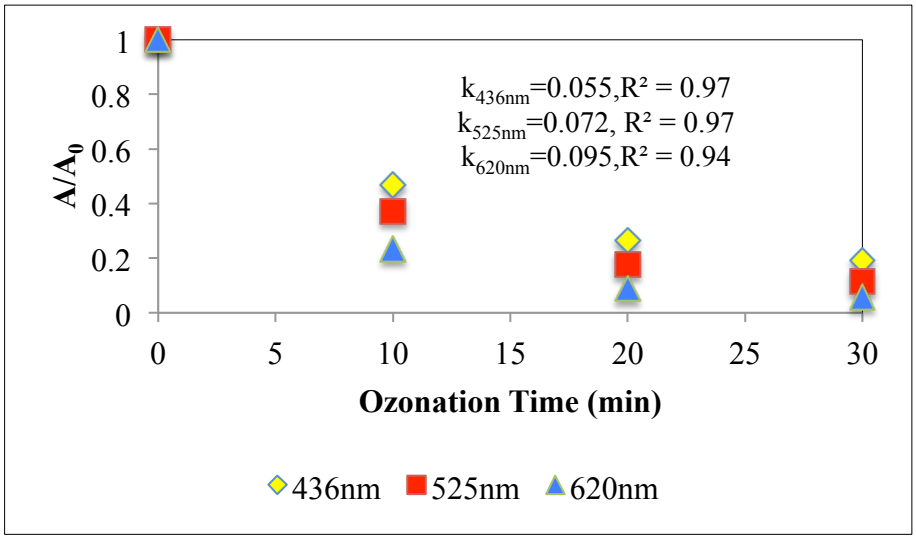

Figure 4.21 Color Removal Rate for US/Ozone Process

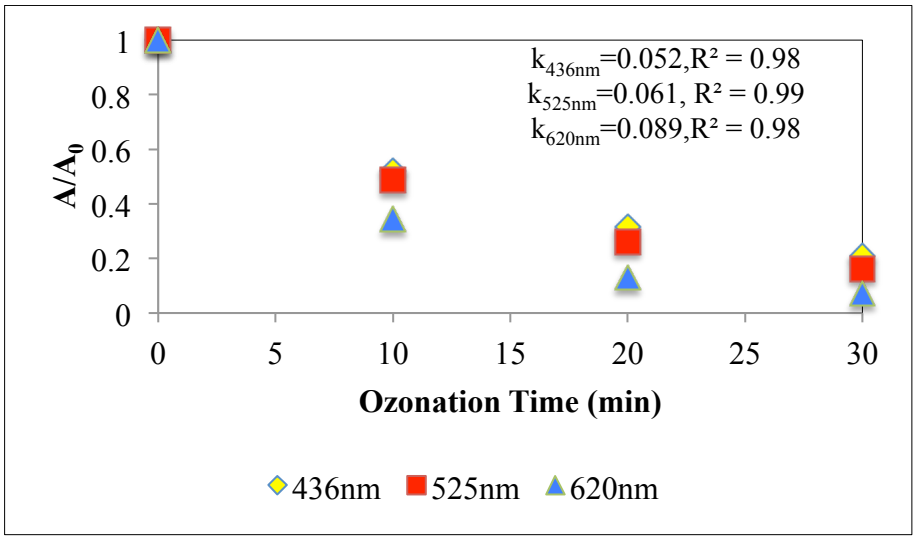

Figure 4.22 Color Removal Rate for US/Ozone/H_2O_2 Process

Figure 4.21-4.22 shows the absorbance decay of US and combined US processes. US-Alone process is not efficient by means of color removal. There is no slight absorbance decay as seen the Figure 4.21-4.22. And the reaction rates are too slow than the combined US processes. US/Ozone and US/Ozone/H_2O_2 have almost the same kinetic rate constants. Ozone and H_2O_2 could induce the effect on decolorization as in Ozone/ H_2O_2. Combination of ozone and H_2O_2 may be effective for oxidation of impurities and inorganic contents (See Section 4.3.2).

Table 4.8 Kinetic Rate Constants of US and combined US processes

AOPs	Kinetic Rate Constants (k min^{-1})		
	436nm	**525nm**	**620nm**
US-Alone	0.01	0.008	0.008
US/Ozone	0.055	0.072	0.095
US/Ozone/H_2O_2	0.052	0.061	0.089

4.5 COMPARISON OF THE OPTIMUM AOPs

4.5.1 Comparison by Decolorization Rates

Color removal kinetic constant rates were determined by using the pseudo-first kinetic model (Eq. 3.1). All the rate constants values calculated as the slope of the absorbance decay graphs given as tables in the former sections. The decolorization rates were determined at 436, 525 and 620 nm in Figure 4.23. Pt-Co measurements for all studied AOPs have given in Figure 4.24.

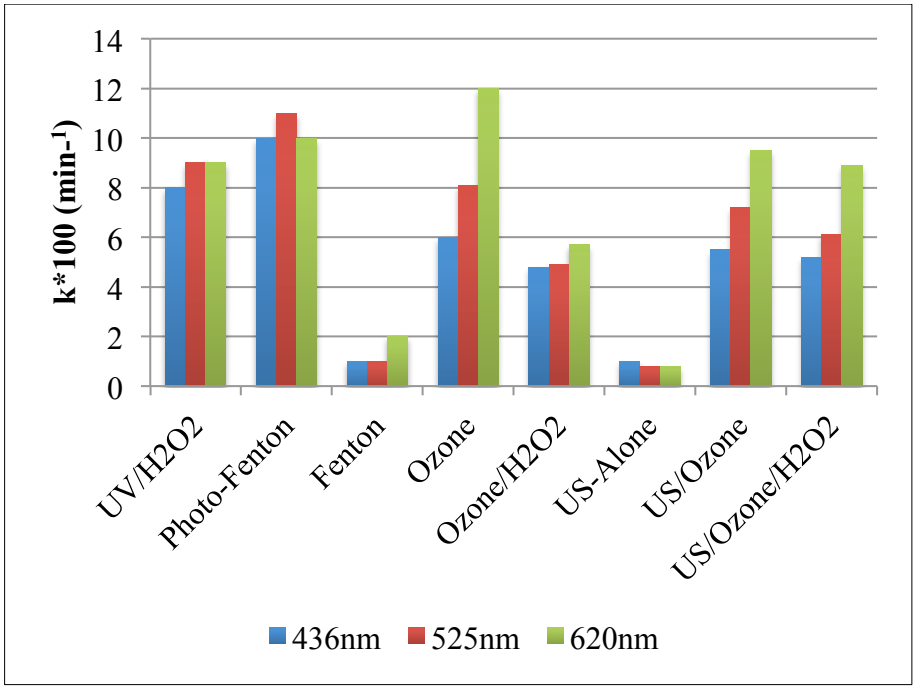

Figure 4.23 Kinetic rate constants, k*100 (min^{-1}) for studied optimum AOPs

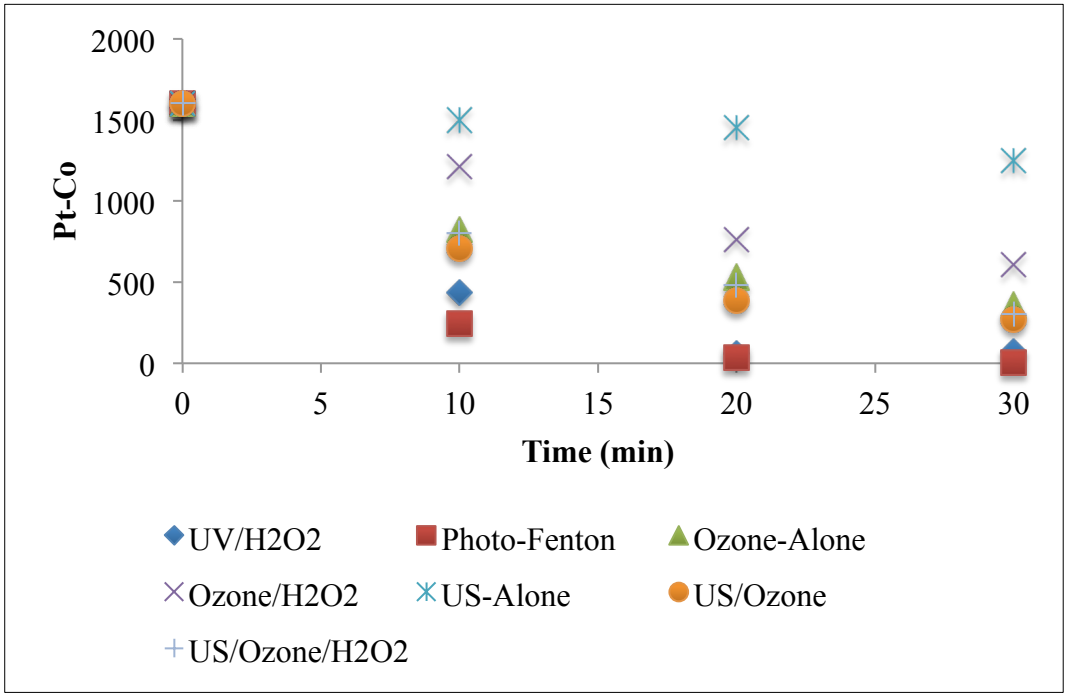

Figure 4.24 Pt-Co values for studied optimum AOPs

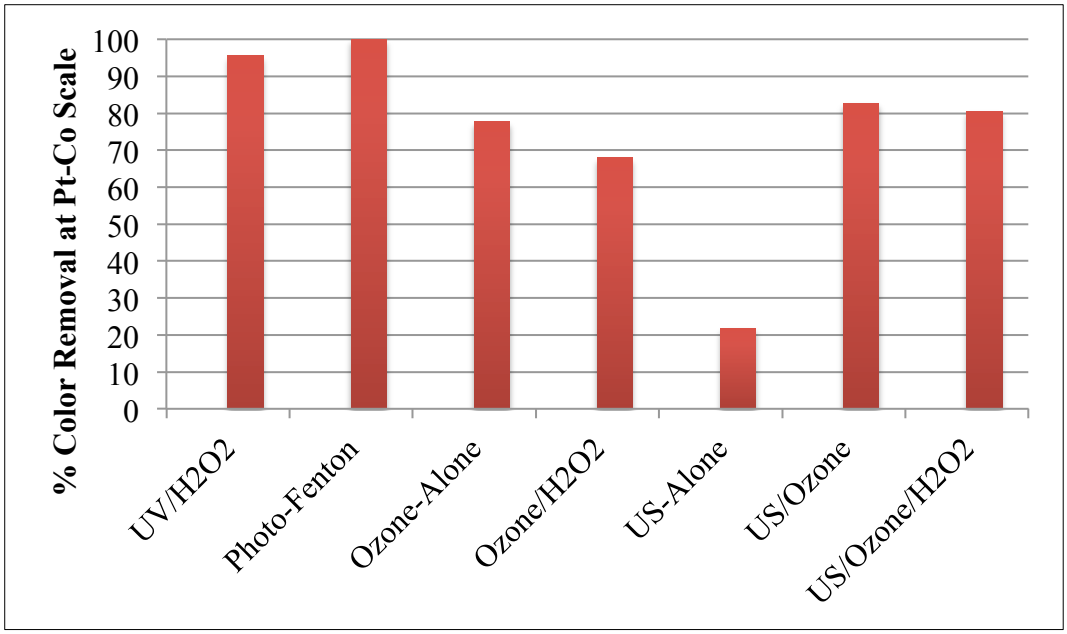

Figure 4.25 Color removal rates as %, for studied optimum AOPs

Most of the Advanced Oxidation Processes are suitable for color removal as seen the Figure 4.23, 4.24 and 4.25. At three different RES wavelengths gives the different kinetic rate constants. The highest decolorization rate was observed at 620 nm, which represents the blue color. This can be attributed to the blue color, which is the

predominant color of the wastewater. 436 nm refers yellow color scale as well as 525 nm red and 620 nm blue.

UV/H_2O_2 and photo-Fenton processes showed good efficiency on the color removal as seen the above figures. Unless US-Alone process is not coupled with any catalysis and/or chemicals, it is not efficient for color removal. Photo-Fenton followed 100%, UV/H_2O_2 95%, Ozone-Alone 78%, Ozone/H_2O_2 68%, US/Ozone 83%, US/Ozone/H_2O_2 80% color removal efficiency while US-Alone followed 21% color removal rates in Pt-Co color unit.

4.5.2 Comparison by Organic Content Removal

The impact of oxidation on degradability can be characterized by the relative TOC and COD degradation after AOPs. These two parameters commonly used to characterize the efficiency of the advanced oxidation process. The comparison between these values, measured at the commencement and at the end of the reaction, allows the knowledge of the degree of mineralization of the process or in other words, the amount of organic matter transformed into CO_2, which is normally one of the main objectives to be accomplished.

UV based processes are the most efficient AOP for color removal. Therefore, the TOC and COD analyses were performed for these processes. The TOC contents of the samples during 2 hours irradiation are given Figure 4.26. The initial TOC content of the biotreated effluent sample is 41.58 mg/l. COD concentration of the sample is 310 mg/l. COD measurements were conducted after 30 minutes irradiation.

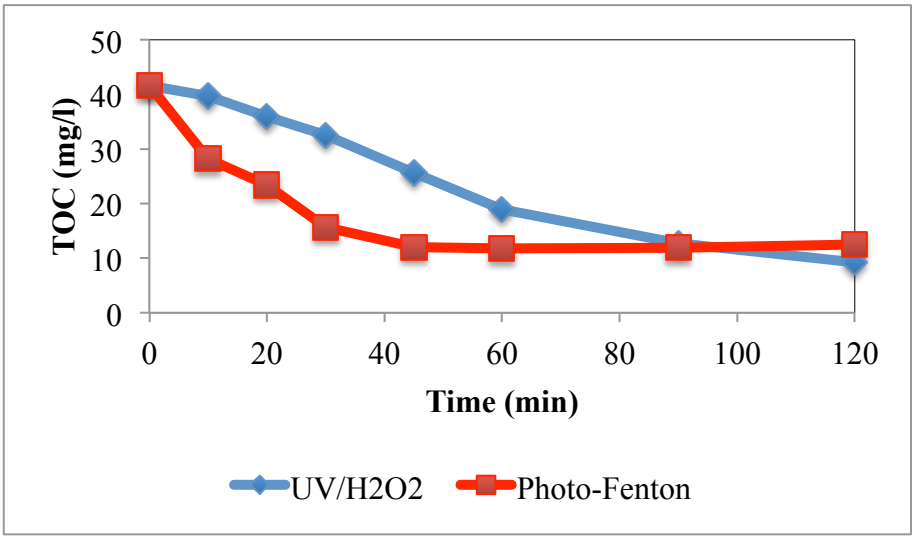

Figure 4.26 TOC values for most efficient AOPs

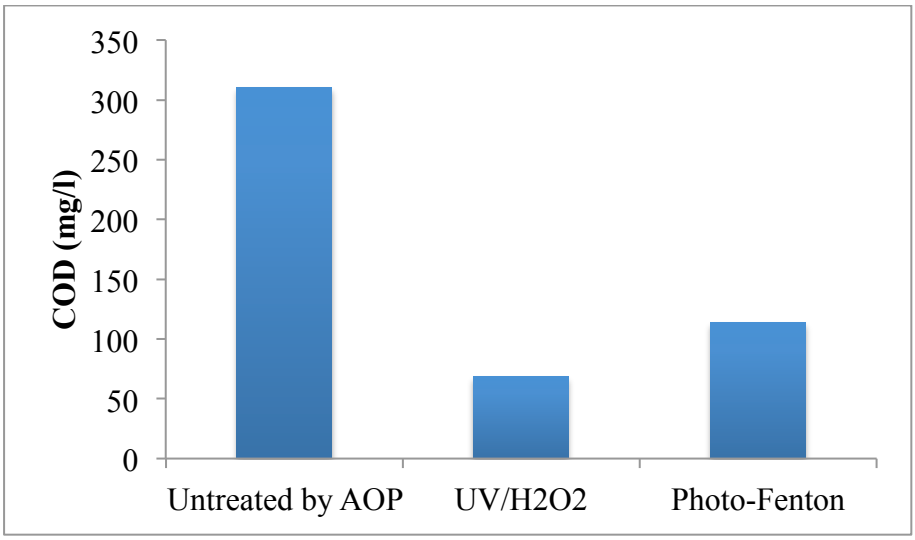

Figure 4.27 COD concentrations for most efficient AOPs after 30 min irradiation

UV/H_2O_2 and Photo-Fenton and processes are the two best efficient systems for mineralization as well the color removal, they reached the 78 and 70 % TOC removal rates at end of 2 hours for UV/H_2O_2 and Photo-Fenton processes, respectively. COD removal rates are 78% for UV/H_2O_2 and 63% for photo-Fenton process. UV/H_2O_2 process has higher mineralization rate than photo-Fenton. However, when we check the 30 minutes irradiation results, mineralization by photo-Fenton process has much higher removal rates in TOC (Figure 4.28). As seen the Figure 4.25 reaction rate of UV/ H_2O_2 increases after one hour irradiation while as photo-Fenton reaction starts to slow down.

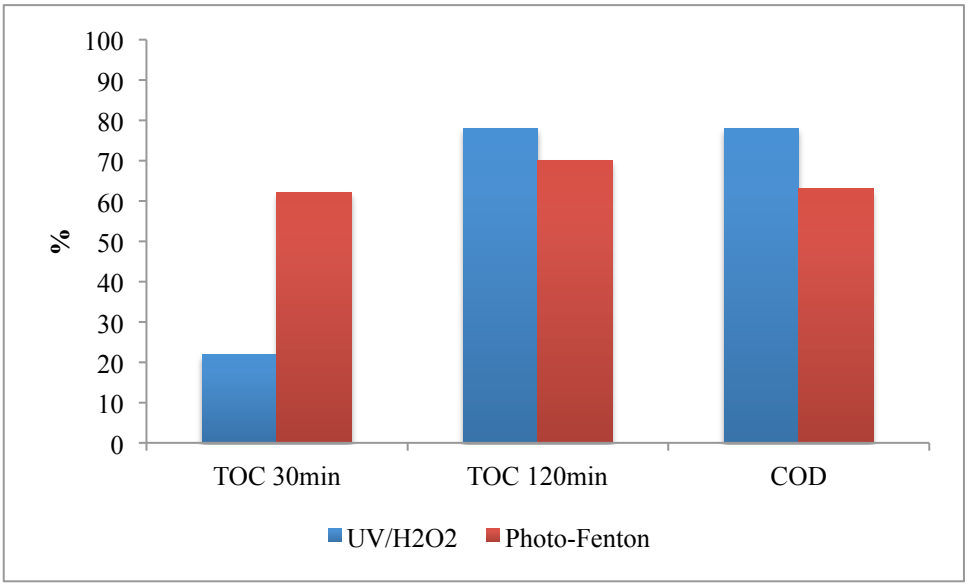

Figure 4.28 Comparison of UV/H_2O_2 and photo-Fenton process after 30 minutes irradiation

4.5.3 Comparison by Toxicity

Toxicity is the ability or property of a chemical, substance or sample to disrupt or inhibit a biochemical process within a living thing. Toxicity of the samples was determined using a Microtox Model 500 Analyzer, which utilizes freeze-dried luminescent bacteria (*V. fisheri*) as test organisms. The test system is based on the principle that bacterial luminescence is tied directly to cell respiration, so that any inhibition of cellular activity (due to toxicity) results in a reduction in the degree of luminescence. The Microtox analyzer is made of an array of sample wells for holding dilutions of bacterial suspensions, and a photometer to measure the light output of *V. fisheri* at 5 and 15 min after contact with the toxicant. Light readings are compared to those of control bacteria (healthy) to determine the inhibition of light emission, and to estimate the EC_{50} of the sample. (EC_{50} is defined as the effective concentration of the toxicant- expressed as percentage relative to the original sample strength- that causes a 50 per cent reduction in the light output of the test organisms during the designated time interval.) Sample preparation, osmotic adjustment and serial dilution procedures were carried out by reference to the Basic Protocol of the Microtox assay (Microtox Manual, 1992). Toxicity Unit (TU) value was calculated by using EC_{50} ($100/EC_{50}$, expressed as volume percentage).

Dye solutions had color, which could interfere with bacterial luminescence. So, those samples were re-analyzed according to the color correction test. The raw wastewater, 30 minutes treated samples by UV/H_2O_2 and photo-Fenton was studied for toxicity analyses. And additionally, toxicity test was performed for US-Alone, Ozone-Alone. The results are represented as Toxicity Unit (TU) in Table 4.9.

Table 4.9 Toxicity analyses of optimum AOPs after 30 minutes irradiation

Samples	Toxicity Unit (5min)	Toxicity Unit (15min)	EC_{50} for 15 min
Untreated	4.97	3.69	27.10
Photo-Fenton	3.48	2.69	37.17
UV/H_2O_2	2.97	2.00	50.00
US-Alone	1.31	1.50	66.66
Ozone-Alone	0.36	0.81	-

As seen the results, optimum systems; photo-Fenton and UV/H_2O_2 decreased the toxicity of the untreated samples. Ozone-Alone system almost has no toxicity effect, which is already used as disinfection. US process also have high toxicity removal rate. The toxicity of the untreated sample is not in a critical condition, so that the toxicity removal by AOPs.

4.5.4 Comparison by Total Dissolved Solids

Total dissolved solids (TDS) comprise inorganic salts (principally calcium, magnesium, potassium, sodium, bicarbonates, chlorides and sulfates) and some small amounts of organic matter that are dissolved in water. The textile wastewater uses high content of salts during textile milling activities. The effluents have high alkalinity. The initial TDS concentration of studied sample is 5323 mg/l. It shows that biological treatment has no effect on dissolved solids –especially salts- removal. Table 4.10 represents the TDS concentrations with UV/H_2O_2 and photo-Fenton processes after 30 minutes irradiation.

Table 4.10 TDS removal rates for optimum AOPs after 30 minutes irradiation

Samples	TDS (mg/l)	TDS Removal (%)
Untreated Sample	5313	-
UV/H_2O_2	2322	56
Photo-Fenton	4338	18

AOPs are not effective for TDS removal as seen the Table 4.10. UV/H_2O_2 process has better TDS removal than photo-Fenton. Although, the ferrous ions separated by centrifuging, the residual ones in sample may cause increase in TDS concentration. High amounts of salts are involved the textile manufacturing processes. These salts decrease the efficient of the treatment plants, and undesirable for water reuse.

4.5.5 Comparison by HPLC Analysis

The detection of the phenol and phenolic compounds (resorcinol, catechol and hydroquinone) has performed with HPLC. Phenol standard curve has given Figure 4.30. Maximum absorption of phenol was found 270 nm, and phenolic compounds, hydroquinone, resorcinol, catechol are 290, 275 and 275 nm, respectively. Retention times of the compounds are given in Table 4.11.

Table 4.11 Retention times for phenol and phenolic compounds

Compounds	Wavelength (nm)	Retention Time (min)
Phenol	270	4.6
Catechol	275	2.29
Resorcinol	275	1.75
Hydroquinone	290	1.36

As seen the Figures 4.29-4.33, phenol and phenolic compounds have not observed in the untreated and treated samples. But, with the aid of the chromatograms, it is seen a pure peak in the untreated sample at 0.69 minutes that have maximum wavelength of approximately 290 nm. In some AOPs, the concentration of this compound is decreasing, in the some of the AOPs it is increasing. It could not detected by HPLC, mass spectrometry should be use for the detection of this compound as a

future work. The figures includes the chrotogram for UV/H_2O_2 process, the other studies are documented in APPENDIX D.

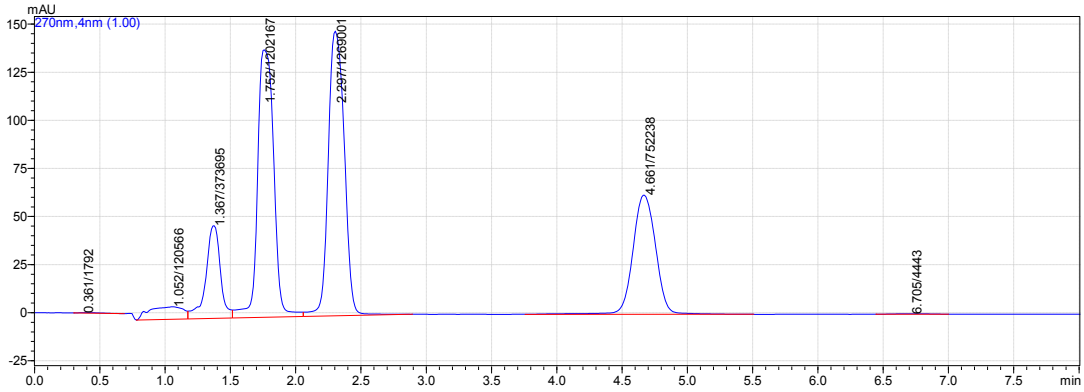

Figure 4.29 Chrotogram of the phenol standard

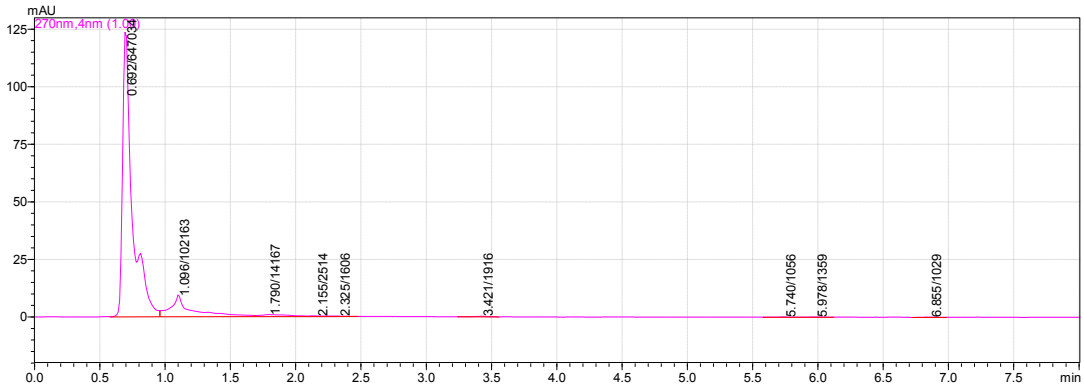

Figure 4.30 Chrotogram of the untreated sample

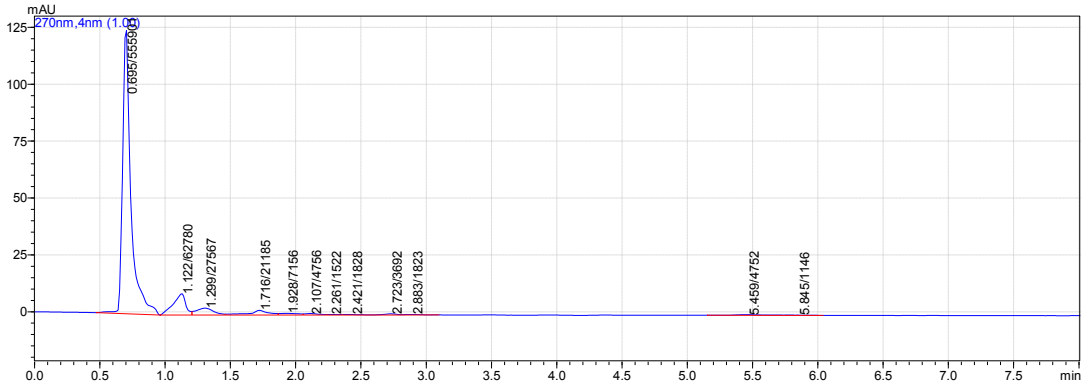

Figure 4.31 Chrotogram of the 10 minutes treated sample by UV/H_2O_2

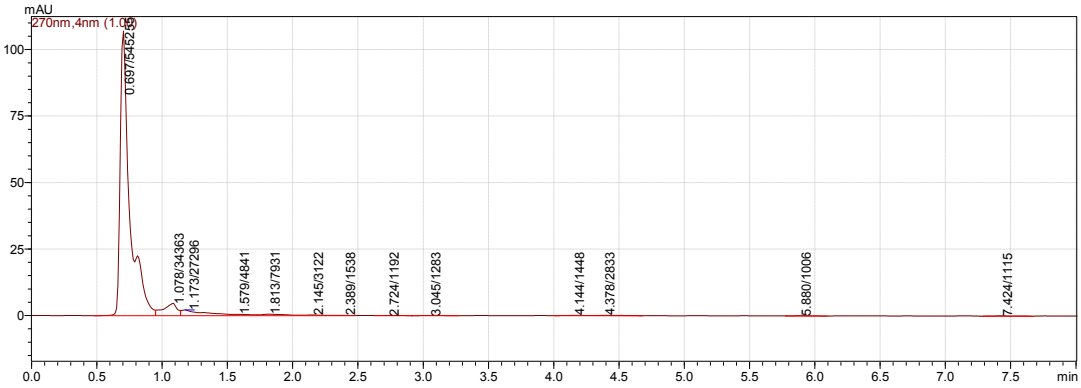

Figure 4.32 Chromatogram of the 20 minutes treated sample by UV/H_2O_2

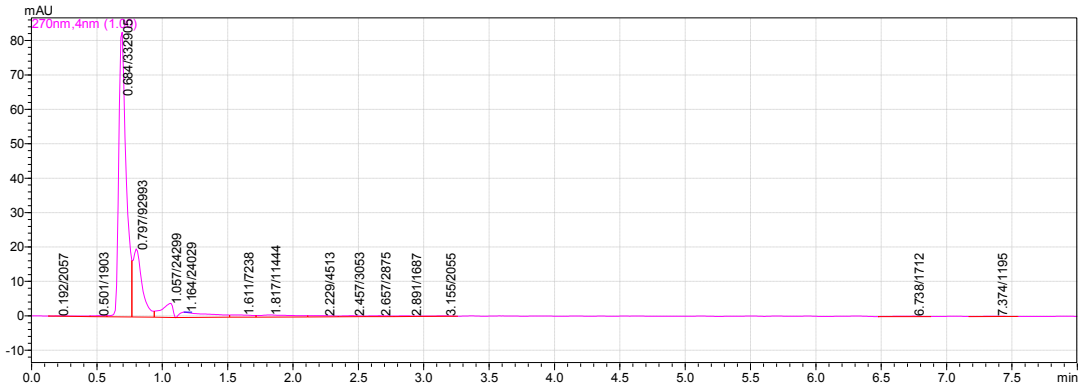

Figure 4.33 Chromatogram of the 30 minutes treated sample by UV/H_2O_2

CHAPTER 5

ECONOMIC ANALYSIS

5.1 COST OF ENERGY REQUIREMENTS

Operating costs are directly affected by treatment performances of the applied processes. To ease up comparison of reaction efficiencies, powerful scale-up parameters called EE /O (that is the electrical energy required to re move a pollutant by one order of magnitude in one m^3 of wastewater) values have been calculated by applying the following empirical formula:

$$\mathrm{EE/O}\left(\frac{\mathrm{kWh}}{\mathrm{m3}}\right) = \frac{P\ t\ 1000}{V\ 60 \log\left(\frac{Cinf}{Ceff}\right)} \tag{5.1}$$

where P (kW) is the power input, t is the oxidation time (in min), V is the volume of the effluent sample (in liter) and Cinf and Ceff are the initial and final concentrations of the contaminant (Bolton et al., 1996, Azbar et al., 2004, Yasar et al., 2006).

In our study, it is not possible to determine concentration of wastewater samples. Log (A_0/A) can gives the same reduction for decolorization. So, the color values were used instead of concentration values. The rate constants (Table 5.1) were then used to calculate the time required for 85% color degradation of the pollutant. For the studied textile wastewater sample, 85 % color reduction was sufficient to achieve the effluent discharge limit value of 280 Pt-Co, which was given by Turkish Water Pollution Control Regulation. The Pt-Co values of the biotreated effluent samples averagely 1600 mg/l Pt-Co, with the 85% color degradation, we can reach the 280-limit value. Therefore, t_{85} (time required to degrade 85 % of the initial color) was

assumed as the residence time for AOP studies. The cost estimation was performed for 1 m^3 water.

Since the color degradation obeys the first order kinetics, k values of all AOPs are required to calculate t_{85}. The summary of first order color degradation decay constants are presented below:

Table 5.1 Color degradation constants

Process	k (min^{-1})
UV/H_2O_2	0.113
Photo-Fenton	0.240
US-Alone	0.009
Ozone-Alone	0.049
Ozone/H_2O_2	0.039
US/Ozone	0.059
US/Ozone/H_2O_2	0.054

Using k to denote the rate constant for degradation and t85 for time required for 85% degradation of the pollutant, the first-order degradation of pollutants is given by (Fogler, 2004):

$$ln\frac{Ainf}{Aeff} = k * t \tag{5.2}$$

For 85% degradation, this equation is converted to

$$t_{85} = \frac{1.897}{k} \tag{5.3}$$

By using the Equation (5.3), calculated t_{85} values are presented below:

Table 5.2 Required times for 85% color degradation

Process	t_{85} (min)
UV/H_2O_2	17
Photo-Fenton	8
US-Alone	210
Ozone-Alone	39
Ozone/H_2O_2	49
US/Ozone	32
US/Ozone/H_2O_2	35

As can be seen from the above table, the lowest detention time to achieve the required color limit value (280 Pt-Co) was observed for Photo-Fenton process. Besides achieving the required discharge limits, low operational costs are desirable for industrial application of the system in large scale. Therefore, it is important to achieve the desired effluent limits within the shortest detention times for lower operational costs. EE/O parameter calculated by the equation (5.1) results are presented below:

Table 5.3 Energy requirement for one m^3 water treatment

Process	Power Input (W)	Volume of Sample (ml)	t_{85} (min)	EE/O (kWh/m^3) for 620nm
UV/H_2O_2	40	800	17	18.7
Photo-Fenton	40	800	8	8.8
US-Alone	250	500	210	2314.8
Ozone-Alone	100	500	39	171.9
Ozone/H_2O_2	100	500	49	216.0
US/Ozone	350	500	32	493.8
US/Ozone/H_2O_2	350	500	35	540.1

The samples have taken from the wastewater treatment unit in Tekirdag. Electrical consumption cost in Tekirdag for the industries have taken from the TREDAS (Tekirdag Elektrik Dagitim A.S) data. The cost of the electricity consumption is approximately 0.17lira/kWh= 0.068Euro/kWh. Electrical energy cost per m^3 of wastewater for each studied AOPs are presented below:

Table 5.4 Energy requirement cost

Process	Energy Cost (Euro/m^3)
UV/H_2O_2	1.27
Photo-Fenton	0.59
US-Alone	157.4
Ozone-Alone	11.6
Ozone/H_2O_2	14.6
US/Ozone	33.5
US/Ozone/H_2O_2	36.7

It should be kept in mind that, ferrous ions should be removed after Photo-Fenton and Fenton processes before discharge to aquatic media. Ferrous iron can be removed by precipitation at pH>8, and the produced ferrous sludge should be discarded from the system. This means the additional chemical/electrical cost for photo-Fenton process. The separation in the study has performed with 5 minutes centrifuging with addition of 0.5 ml of 1M NaOH. The energy requirement for centrifuging and chemical addition has to be taken into account for the real scale applications. In this study, it is ignored.

5.2 COST OF CHEMICAL REQUIREMENTS

The chemical costs include the costs of consumables such as hydrogen peroxide, ferrous and chemicals involved with the AOP. The price of hydrogen peroxide (30%) was considered to be 6.8 euro per liter (Macrol). The price of Fe(II)Sulphate was considered as 1.42 Euro per kg (Basak Kimya). The chemicals were used in UV/H_2O_2, photo-Fenton, Ozone/H_2O and US/Ozone/H_2O_2 processes.

H_2O_2 consumption is 3.19 ml/L for all H_2O_2 based processes. Ferrous salt consumption is 17.5 ml/L for photo-Fenton process.

Table 5.5 Chemical consumptions and cost of the chemicals

Process	H_2O_2 Consumption ml/l	Ferrous Salt Consumption mg/l	Cost of Chemicals Euro/m^3
UV/H_2O_2	3.19	-	0.022
Photo-Fenton	3.19	17	0.046
Ozone/H_2O_2	3.19	-	0.022
US/Ozone/H_2O_2	3.19	-	0.022

5.3 TOTAL OPERATING COST

The total operating cost is the sum of consumed energy and chemical costs (Table 5.6).

Table 5.6 Total Operating Cost

Process	Total Cost (Euro/m^3)
UV/H_2O_2	1.29
Photo-Fenton	0.64
US-Alone	157.4
Ozone-Alone	11.6
Ozone/H_2O_2	14.7
US/Ozone	33.5
US/Ozone/H_2O_2	36.7

As seen in the above table, UV based AOPs are the most feasible techniques by means of cost effectiveness. Photo-Fenton process has the lowest operational cost (0.64 Euro/m^3) to achieve the regulation decolorization discharge limits. UV/ H_2O_2 system is also cost effective with its 0.262 Euro/m^3 operational cost. US systems are

not cost effective and still should be coupled with other AOP techniques to lower the operational costs.

CHAPTER 6

CONCLUSIONS AND RECOMMENDATIONS

In this study, the several experiments were carried out by using various AOPs;

- UV/ H_2O_2
- Fenton
- Photo-Fenton
- US-Alone
- Ozone-Alone
- Ozone/ H_2O_2
- Ozone/US
- Ozone/US/ H_2O_2

System performances were determined in accordance to experimentally calculated first order decolorization rates. Since the current Turkish Water Pollution Control Regulation requires the color discharge limit values as 280 Pt-Co, biologically treated textile wastewater color was determined by Pt-Co examination method. Because The Ministry of Environment is planning to define color discharge limit as in ISO EN 7880, color degradation of the samples were monitored at 436, 525 and 620 nm wavelengths. The measurement at 436 nm is the obligation for natural waters that stated in ISO Standard. 525 and 620 nm represents the general maximum absorption wavelengths of the industrial wastewaters. Depending on the manufacturing capacity of the industry, the characteristics of industrial wastewaters change day by day, even hour by hour. Therefore, for a good color characterization of the textile industry wastewater, it should be monitored at all wavelengths: 436, 525

and 620 nm, which represent the yellow, red and blue color, respectively. Economic analysis of studied AOPs that are based on the regulational color discharge limit value of 280 Pt-Co, are also conducted.

The first conclusion reached from the experimental work of this study is that Advanced Oxidation Processes are promising technologies for the treatment of textile wastewaters. Color monitoring and Microtox toxicity experiments showed that studied AOPs efficiently decolorized the real textile wastewater without the formation of any toxic by-products.

Phenol or its intermediate compounds were not observed (in raw wastewater or in treated wastewater samples) during HPLC analysis. According to chromatograms, pure peaks at 290 nm and 0.69 min were observed. Depending on the applied AOP treatment, the area of this peak enhanced or decreased. It was not possible to detect this compound by HPLC itself. The related compound cannot be defined unless GC-MS or HPLC-MS is used.

Among the studied AOPs, UV based AOPs (UV/H_2O_2 and Photo Fenton) are the most efficient techniques in the terms of decolorization, mineralization and cost effectiveness.

The color degradation of the textile industry wastewater follows first order kinetics.

In UV/H_2O_2 experiments, H_2O_2 concentration up to 25mM increase the color degradation then it begins to decline with increasing oxidant concentration (80mM) due to the scavenging effect of excess H_2O_2 with hydroxyl radicals. The highest decolorization was observed at the natural pH of the wastewater (pH 7-8).

In photo Fenton process, optimum operating conditions are H_2O_2/Fe^{+2} (25:1) mM/mM concentrations at pH 3.

The highest decolorization rate for ozonation is observed at pH $\geq$ 10. When ozone is coupled with H_2O_2, a decrease in decolorization rate was observed.

US-Alone process did not decolorize of the wastewater in test time (30 min) and 21% decolorization was observed. US was coupled with other AOP techniques to enhance the decolorization efficiency. US/Ozone coupled system's decolorization rate was higher than the single systems, which was attributed to the enhanced mass transfer of ozone with ultrasonic irradiation. Addition of H_2O_2 to US/ozone system had adverse effect on decolorization.

First order decolorization kinetic constants were found to be highest for photo-Fenton and UV/ H_2O_2 techniques.

The 30 min color removal efficiency (%) of the studied AOPs are in the order: photo-Fenton processes > UV/H_2O_2 > US/Ozone > US/Ozone/H_2O_2 > Ozone-Alone > Ozone/ H_2O_2 > US-Alone and the corresponding % color removal are as 100%, 95%, 83%, 80%, 78% and 68% respectively.

High TOC removal achieved after 2 hours degradation. UV/H_2O_2 had 78% TOC and 78% COD removal, while photo-Fenton process had 70% TOC and 63% COD removal.

It was observed that the biological treatment plant of the studied textile industry did not achieve decolorization. Therefore, AOPs can be applied as a post treatment to the textile industry wastewater for efficient decolorization.

The lowest operating costs were calculated for UV/ H_2O_2 and photo-Fenton processes. The operational cost of Photo-Fenton process and UV/ H_2O_2 was 1.29 Euro/m^3 and 0.64 Euro/m^3, respectively. But as mentioned in the Section 5.1 the photo-Fenton process has sludge problem due ferrous ions precipitation. Ferrous ions should be settled down at high pH, then separating with centrifuging, filtration etc. It means more energy and chemical cost. And moreover, the pH of the solution had to be adjusted 6-9 after separation to meet the limit pH value in the legislation.

TDS measurements indicate the salt content of the wastewater. Biological treatment plant also could not treat TDS.

As photo-Fenton and UV/H_2O_2 process has shown to be very effective in degradation of color and mineralization, it is interesting to carry out these processes in a more practical way. This can be achieved by:

- using solar irradiation instead of artificial light sources (UV)
- identifying the contaminants intermediates to establish a possible mechanism of reaction and to obtain enhancement in degradability.
- examining the effect of other operating conditions (temperature, wastewater characteristics, alkalinity) in reactor performance
- applying various combinations of processes (US/UV, Ozone/ H_2O_2 /UV)

APPENDIX A

OZONE DETERMINATION

Ozone concentration in deionized water was carried out according to the indigo colorimetric method described in Standard Methods for the Examination of Water and Wastewater (APHA, 1989). This method is quantitative, selective, and simple; it replaces methods based on the measurement of total oxidant. The method is based on the decolorization of indigo by ozone in acidic solution. The decrease in absorbance is linear with increasing ozone concentration.

For the preparation of indigo stock solution, 770 mg potassium indigo trisulfonate ($C_{16}H_7N_2O_{11}S_3K_3$) and 1 ml conc. phosphoric acid was added to a volumetric flask and filled to 1 L with deionized water. The stock solution is stable for about 4 months when stored in the dark, and should be discarded when absorbance at 600 nm of a 1:100 dilution falls below 0.16/cm. For the preparation of indigo reagent, 100 mL indigo stock solution, 10 g sodium dihydrogen phosphate (NaH_2PO_4), and 7 mL conc. phosphoric acid were added to a volumetric flask and filled to 1 L with deionized water. Then 10 ml indigo reagent and 5 mL sample were mixed and diluted to 100 mL with deionized water. Blank sample was prepared in the absence of sample. The absorbance of both solutions were measured at 600 nm and the ozone concentration was prepared by the following equation:

$$\text{mg } O_3 / \text{L} = \frac{100 \times \Delta A}{0.42 \times b \times V}$$

where

ΔA is the difference in absorbance (600 nm) between blank and sample, b is the path length of cell, cm (1 cm), V is the volume of the sample, ml, and the

proportionality constant at 600 nm is 0.42 ± 0.01/cm/mg/L ($\Delta \varepsilon$= 20 000/M. cm) compared to the ultraviolet absorption of pure ozone of ε= 2950/M. cm at 258 nm).

The absorbance values at 600 nm were recorded and samples taken within time intervals, and given in Table A.1. The fed ozone concentration to deionized water was calculated by substituting the absorbance value at 600 nm into the above equation.

Table A.1 Results for the fed ozone concentration to deionized water

	Deionized Water	
Time (min)	A_{600}	O_3 (mgL^{-1})
0	0.000	0.000
5	0.082	0.238
10	0.081	0.261
20	0.083	0.214
30	0.085	0.166

APPENDIX B

ULTRASOUND SYSTEM OPTIMIZATION

Temperatures during 10 minutes sonication at various amplitudes and volumes have given below as mentioned section 4.4.1.

Table B.1 Temperature rise by the time for 500 ml dionized water

V=500ml									
Frequency	582kHz			860kHz			1136kHz		
amplitude	5	6	7	5	6	7	5	6	7
time(sec)									
0	21.5	21.8	22.5	21.7	21.9	22.5	21.7	21.8	22.3
30	22.4	22.8	23.8	22.3	22.6	23.8	22.2	22.4	23.0
60	22.5	23.2	24.2	22.6	23.1	24.7	22.3	22.8	23.7
90	22.7	23.6	24.7	23.0	23.6	25.6	22.5	23.2	24.5
120	22.9	24.0	25.8	23.3	24.2	26.8	22.7	23.5	25.3
150	23.2	24.4	26.5	23.5	24.7	27.7	22.8	24.0	26.1
180	23.5	24.8	27.2	23.8	25.2	28.9	23.0	24.4	27.0
210	23.6	25.3	27.9	24.1	25.8	29.8	23.2	24.7	27.8
240	24.0	25.8	28.7	24.4	26.3	30.9	23.3	25.1	28.6
270	24.1	26.2	29.2	24.7	26.9	32.1	23.5	25.5	29.4
300	24.2	26.5	30.6	25.0	27.4	33.0	23.8	26.0	30.1
330	24.3	27.1	31.3	25.2	28.0	34.0	23.9	26.3	30.9
360	24.6	27.6	32.0	25.6	28.5	35.2	24.1	26.7	31.7
390	24.9	27.9	33.0	25.8	29.0	36.0	24.2	27.1	32.4
410	25.3	28.2	33.8	26.1	29.6	37.0	24.4	27.5	33.3
440	25.7	28.7	34.6	26.4	30.0	37.8	24.6	27.9	34.1
470	25.9	29.0	35.1	26.7	30.8	38.9	24.8	28.3	34.9
500	26.2	29.3	35.9	26.9	31.2	39.9	25.0	28.7	35.3
530	26.5	29.7	36.2	27.3	31.8	40.8	25.1	29.1	36.0
560	26.7	30.0	36.9	27.5	32.2	41.8	25.4	29.5	36.6
590	27.0	30.3	37.6	27.7	32.7	42.7	25.5	29.9	37.3

Table B.2 Temperature rise by the time for 800 ml dionized water

V=800ml									
Frequency	582kHz			860kHz			1136kHz		
Amplitude	5	6	7	5	6	7	5	6	7
Time (sec)									
0	21.9	22.0	22.6	20.4	21.0	21.0	21.0	20.8	21.1
30	22.2	22.6	24.3	20.8	21.5	22.0	21.5	21.5	21.9
60	22.3	22.8	24.7	20.9	21.8	22.6	21.7	21.8	22.6
90	22.4	23.0	25.2	21.1	22.1	23.5	21.9	22.2	23.1
120	22.6	23.2	25.7	21.2	22.4	23.9	22.2	22.4	23.8
150	22.8	23.5	26.4	21.4	22.7	24.6	22.2	22.7	24.3
180	22.8	23.8	27.0	21.6	23.1	25.0	22.4	23.0	24.9
210	23	24.1	27.7	21.8	23.4	25.8	22.6	23.3	25.4
240	23.1	24.3	28.1	21.9	23.8	26.4	22.8	23.7	26.1
270	23.2	24.6	28.7	22.1	24.2	27.1	23.0	24.0	26.7
300	23.4	24.8	29.3	22.3	24.5	27.7	23.1	24.3	27.0
330	23.5	25.2	30.0	22.4	24.9	28.3	23.3	24.7	27.6
360	23.7	25.5	30.5	22.6	25.3	29.0	23.5	25.0	28.1
390	23.8	25.9	31.0	23.0	25.6	29.6	23.7	25.3	28.7
410	24	26.2	31.2	23.1	26.0	30.3	23.9	25.6	29.2
440	24.2	26.5	31.8	23.2	26.4	31.1	24.1	26.0	29.7
470	24.4	26.8	32.3	23.4	26.7	31.8	24.3	26.4	30.1
500	24.5	27.1	32.8	23.7	27.1	32.3	24.4	26.7	30.6
530	24.7	27.5	33.3	23.8	27.5	32.9	24.6	27.1	31.1
560	24.8	27.7	33.9	24.0	27.9	33.5	24.9	27.4	31.6
590	25	28.1	34.3	24.2	28.3	34.1	25.1	27.6	32.0

Table B.3 Temperature rise by the time for 1000 ml dionized water

V=1000ml									
Frequency	582kHz			860kHz			1136kHz		
amplitude	5	6	7	5	6	7	5	6	7
Time(sec)									
0	23.9	23.4	23.5	23.5	23.7	23.7	23.2	21.9	23.4
30	24.1	23.9	24.7	23.8	24.1	24.6	23.2	22.4	23.9
60	24.2	24.3	25.3	23.9	24.5	25.1	23.3	22.7	24.3
90	24.4	24.5	25.7	24.1	24.7	25.6	23.4	22.9	24.7
120	24.5	24.8	26.2	24.2	25.0	26.1	23.5	23.0	25.1
150	24.6	25.1	26.6	24.4	25.4	26.7	23.5	23.2	25.5
180	24.8	25.3	26.9	24.6	25.6	27.2	23.7	23.5	26.0
210	25	25.5	27.4	24.9	25.9	27.9	23.8	23.8	26.3
240	25.1	25.8	27.6	25.0	26.2	28.4	23.9	24.1	26.7
270	25.2	26.0	28.3	25.2	26.4	28.9	24.1	24.4	27.2
300	25.4	26.2	28.8	25.5	26.7	29.4	24.2	24.6	27.6
330	25.5	26.6	29.3	25.6	27.0	30.0	24.3	24.9	28.0
360	25.6	26.8	29.8	25.7	27.4	30.5	24.4	25.2	28.3
390	25.8	27.0	30.2	26.0	27.7	31.0	24.5	25.4	28.7
410	25.9	27.2	30.6	26.2	28.0	31.4	24.7	25.7	29.1
440	26	27.5	31.2	26.3	28.3	32.0	24.8	26.0	29.4
470	26.2	27.8	31.5	26.5	28.6	32.4	24.9	26.2	29.8
500	26.3	28.1	31.9	26.7	28.9	33.0	25.1	26.4	30.1
530	26.4	28.4	32.4	26.9	29.3	33.3	25.2	26.7	30.5
560	26.6	28.6	32.9	27.0	29.5	34.0	25.3	26.9	30.8
590	26.7	28.9	33.3	27.2	29.9	34.4	25.4	27.1	31.2

Table B.4 Temperature rise by the time for 1250 ml dionized water

V=1250 ml									
Frequency	582 kHz			860 kHz			1136kHz		
Amplitude	5	6	7	5	6	7	5	6	7
Time (sec)									
0	21.4	21.1	22.2	21.5	21.7	21.1	20.8	21.1	21.1
30	21.6	21.5	22.5	21.7	22.0	22.0	21.1	21.5	21.7
60	21.7	21.7	22.9	21.7	22.2	22.5	21.4	21.7	22.1
90	21.8	22.0	23.4	21.8	22.5	23.2	21.5	21.9	22.4
120	21.9	22.1	23.7	22.0	22.8	23.6	21.6	22.1	22.8
150	22	22.3	24.3	22.1	23.0	24.0	21.7	22.4	23.2
180	22.1	22.5	24.6	22.3	23.3	24.5	21.9	22.6	23.6
210	22.3	22.7	24.8	22.5	23.5	25.0	22.0	22.8	23.9
240	22.4	22.9	25.2	22.6	23.8	25.3	22.1	23.1	24.2
270	22.6	23.1	25.6	22.7	24.0	25.9	22.3	23.3	24.6
300	22.7	23.4	26.0	23.0	24.2	26.3	22.4	23.5	25.0
330	22.8	23.6	26.3	23.1	24.5	26.7	22.6	23.8	25.3
360	23	23.9	26.7	23.2	24.9	27.1	22.7	24.0	25.7
390	23.1	24.1	27.0	23.4	25.2	27.5	22.8	24.3	26.0
410	23.2	24.3	27.3	23.6	25.4	27.7	22.9	24.5	26.4
440	23.4	24.5	27.6	23.8	25.7	28.1	23.1	24.7	26.7
470	23.5	24.7	28.2	24.0	26.0	28.6	23.2	25.0	27.0
500	23.6	24.9	28.7	24.1	26.1	29.1	23.4	25.2	27.3
530	23.8	25.1	28.9	24.3	26.3	29.6	23.5	25.5	27.6
560	23.9	25.4	29.3	24.4	26.6	29.9	23.6	25.7	28.0
590	24.1	25.5	29.7	24.6	26.9	30.4	23.7	25.9	28.3

APPENDIX C

H_2O_2 DETERMINATION BY THE I_3^- METHOD AND CALIBRATION CURVE

H_2O_2 determination was carried out according to the procedure described by Klassen *et al*., (1994). This method is based on the reaction of (I^-) with H_2O_2 to form the triiodide ion (I_3^-), which has a strong absorbance 351 nm. The analysis of H_2O_2 at concentrations as low as 1 μM is conveniently done by determining the yield of I_3^- formed when H_2O_2 reacts with KI in a buffered solution containing ammonium molybdate tetrahydrate as a catalyst.

Solutions A and B for the I_3^- method were prepared according to the recipe given by Kalssen *et al*., (1994). Solution A consisted of 33 g of KI, 1 g of NaOH, and 0.1 g of ammonium molybdate tetrahydrate diluted to 500 ml with deionized water. The solution was stirred for ~1 h to dissolve the molybdate. Solution A was kept in dark to inhibit the oxidation of I^-. Solution B, an aqueous buffer, contained 10 g of KHP per 500 ml. Various concentrations of H_2O_2 was prepared from reagent grade H_2O_2 (35%), Merck. 2.5 mL of solution A, 2.5 mL of solution B, 1 mL of sample were mixed and diluted to 10 mL by deionized water, and the absorbance at 351 nm was recorded. Blank sample was prepared in the absence of sample. Various concentrations of H_2O_2 and the corresponding absorbance values at 351 nm are recorded for calibration curve, and given in Table C.1. Plot of H_2O_2 concentration versus the corresponding absorbance of the solution, and the calibration curve for H_2O_2 analysis is given in Figure C.1.

Table C.1 H_2O_2 concentration versus absorbance at 351 nm data used for calibration curve preparation

H_2O_2 concentration (mgL^{-1})	Absorbance at 351 nm
0	0.000
3	0.08
5	0.141

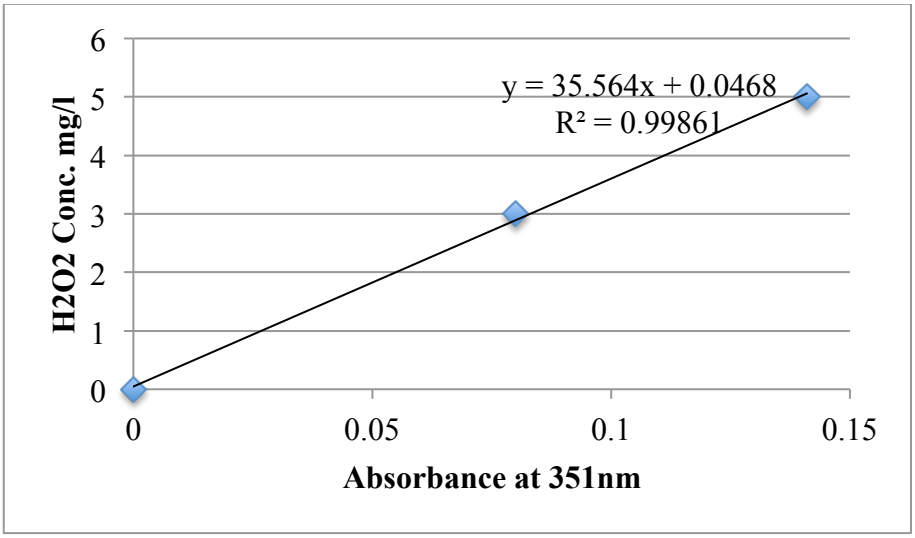

Figure C.1 H_2O_2 Calibration Curve

1 mL of sample was taken at time intervals during sonication of deionized water, and mixed with 2.5 mL solution A and solution B, and then diluted to 10 mL with deionized water. The absorbance at 351 nm was recorded for each sample, and then substituted into H_2O_2 calibration curve equation given in above.

APPENDIX D

HPLC ANALYSIS

The chromatogram of the HPLC analysis has given below at treated samples for 30 minutes by photo-Fenton, US, Ozone, Ozone/US, Ozone/US/H_2O_2.

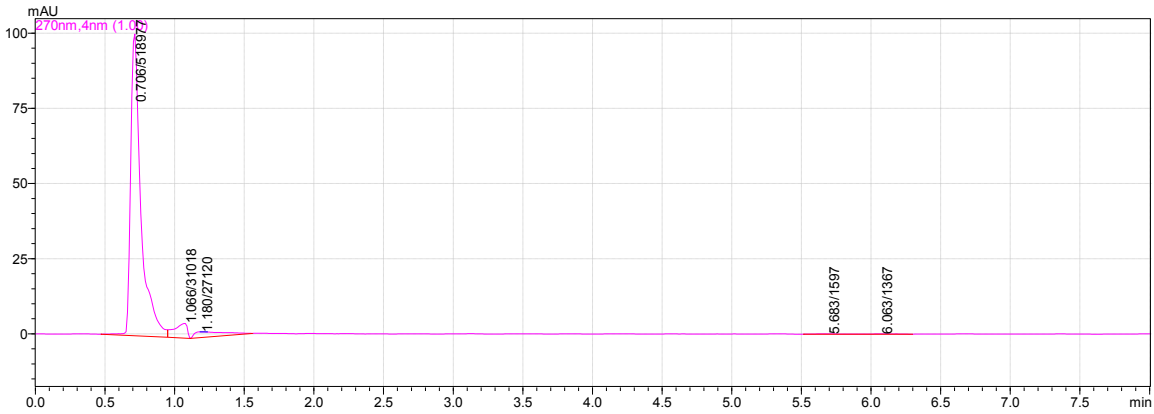

Figure D.1 Chromatogram of the 10 minutes treated sample by photo-Fenton

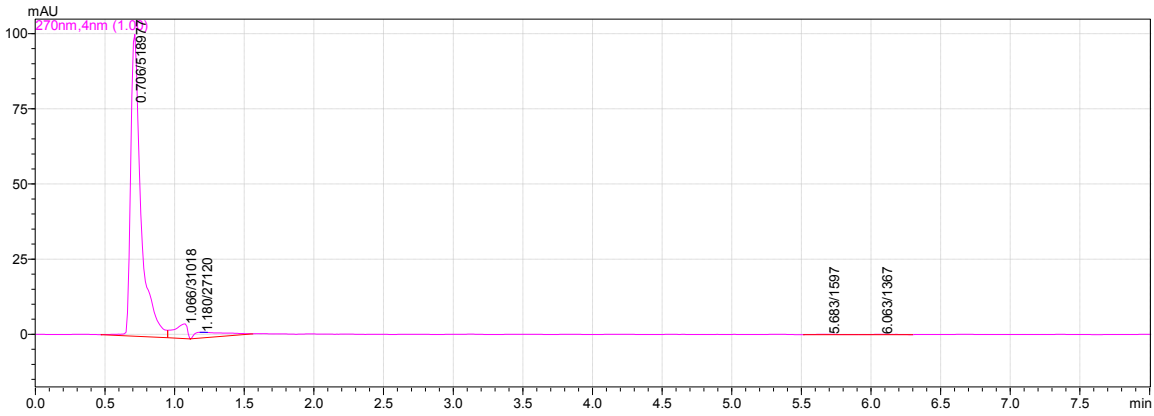

Figure D.2 Chromatogram of the 20 minutes treated sample by photo-Fenton

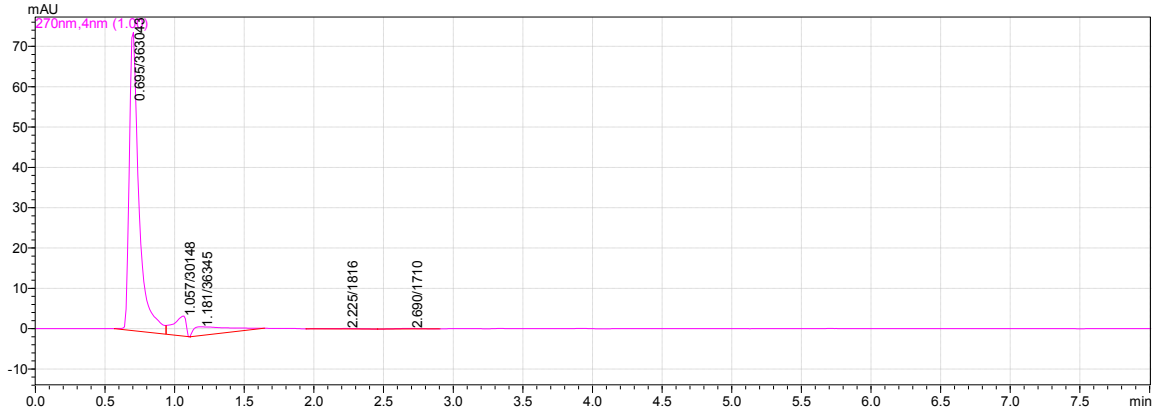

Figure D.3 Chromatogram of the 30 minutes treated sample by photo-Fenton

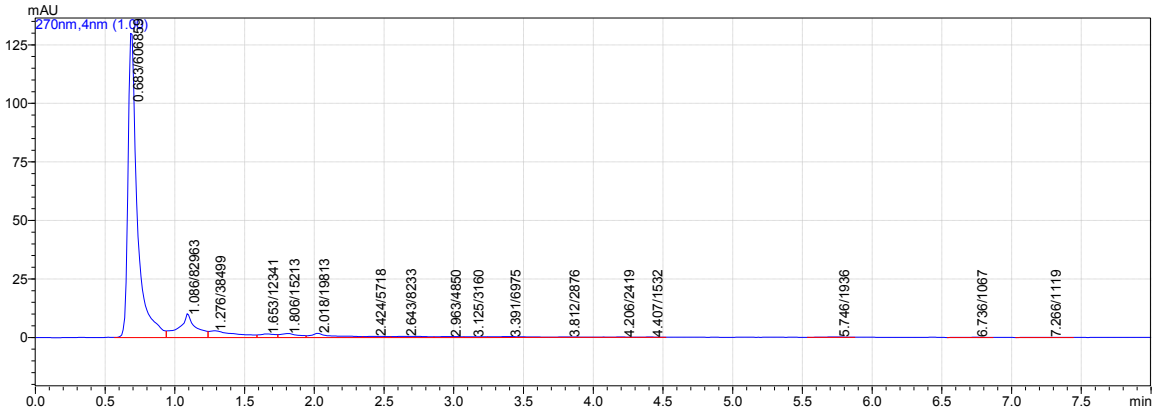

Figure D.4 Chromatogram of the 10 minutes treated sample by Ozone-Alone

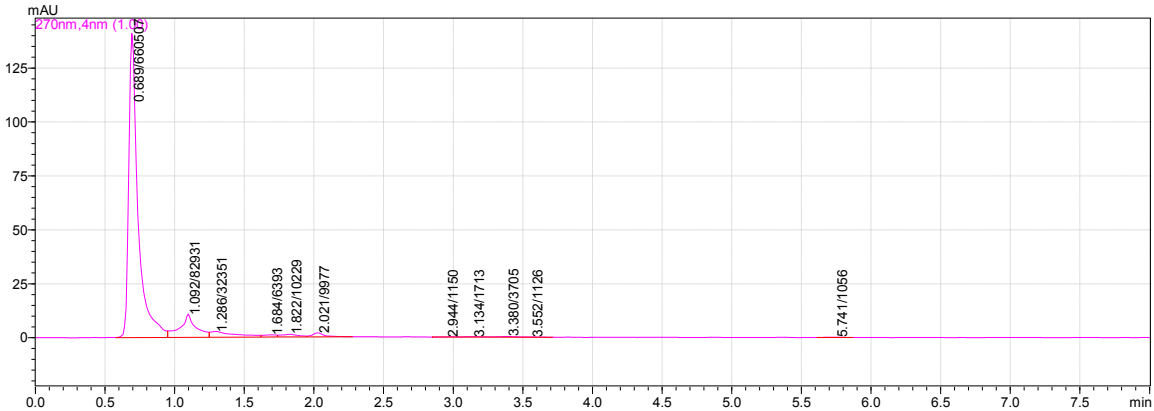

Figure D.5 Chromatogram of the 20 minutes treated sample by Ozone-Alone

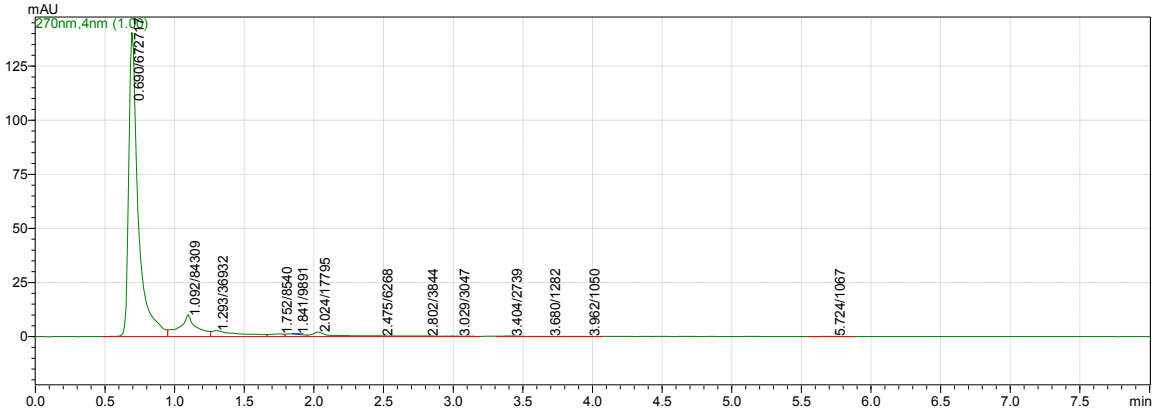

Figure D.6 Chromatogram of the 30 minutes treated sample by Ozone-Alone

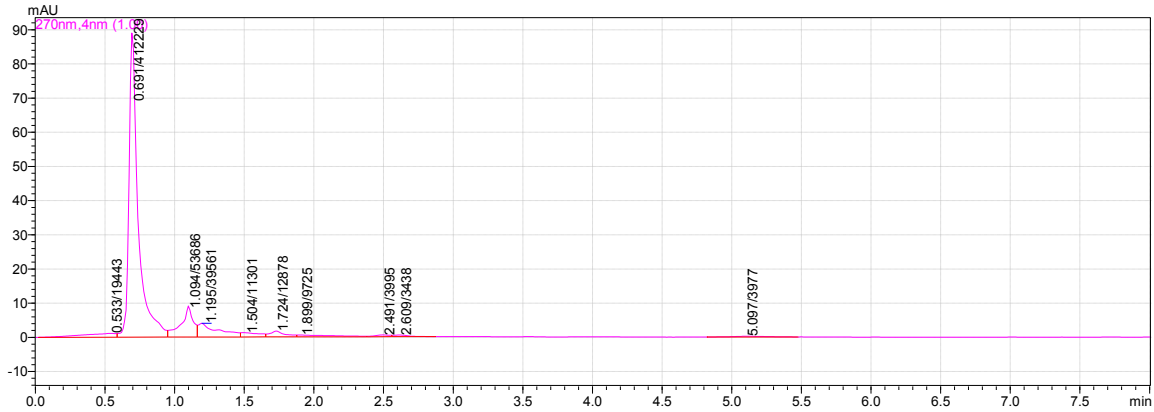

Figure D.7 Chromatogram of the 10 minutes treated sample by US-Alone

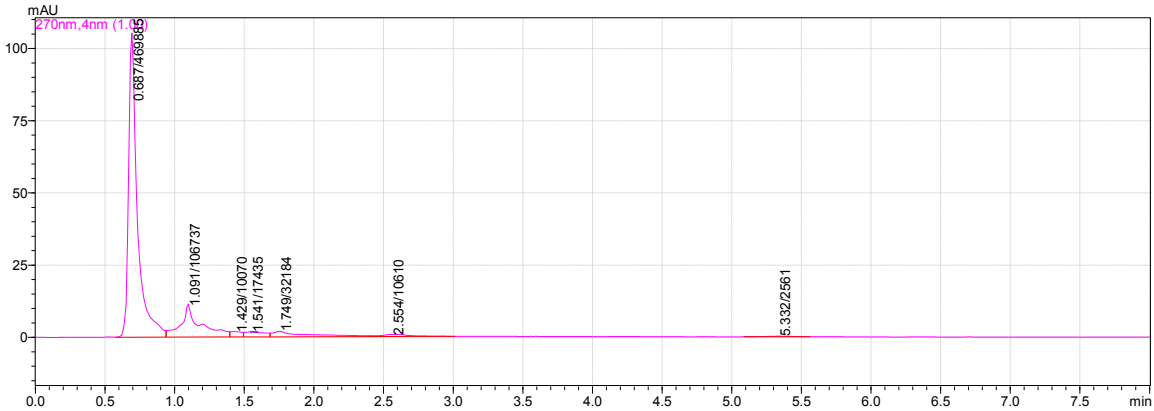

Figure D.8 Chromatogram of the 20 minutes treated sample by US-Alone

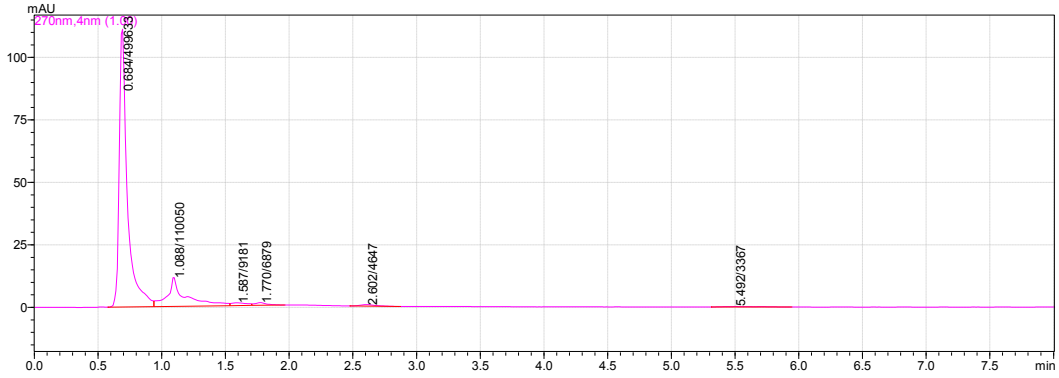

Figure D.9 Chromatogram of the 30 minutes treated sample by US-Alone

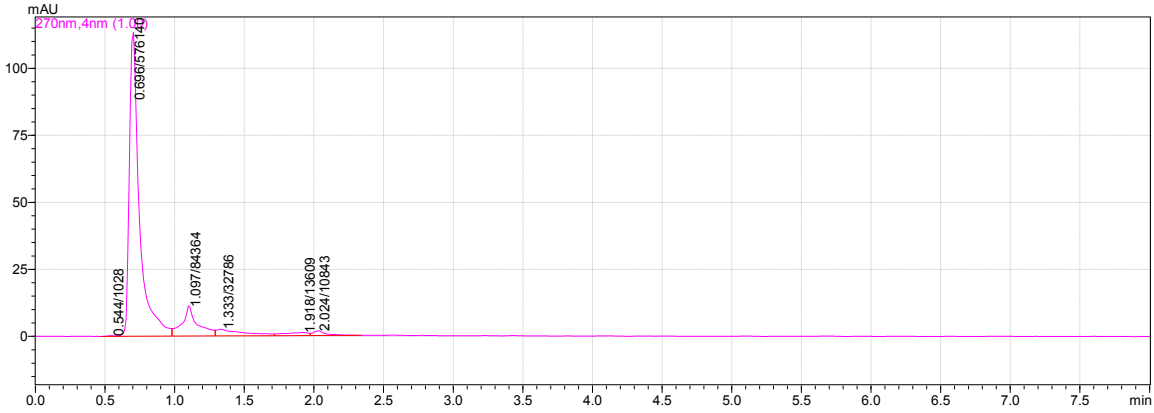

Figure D.10 Chromatogram of the 10 minutes treated sample by US/Ozone

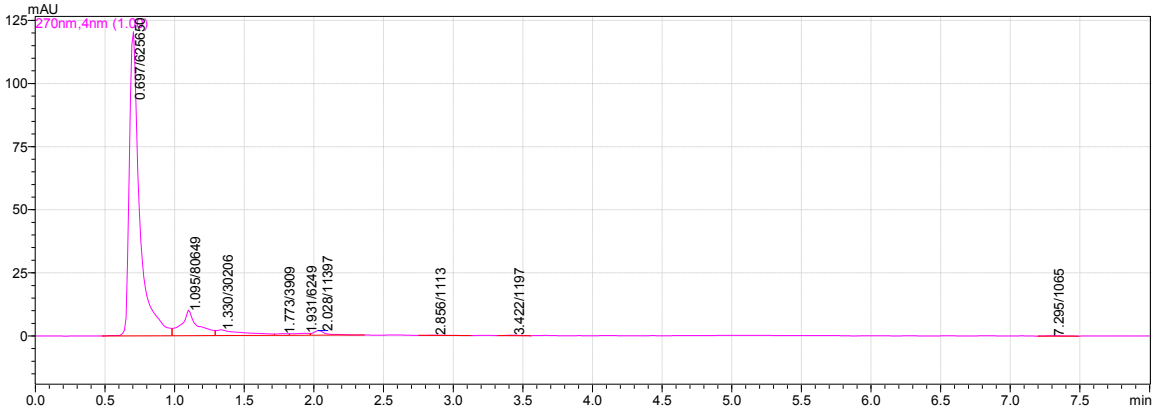

Figure D.11 Chromatogram of the 20 minutes treated sample by US/Ozone

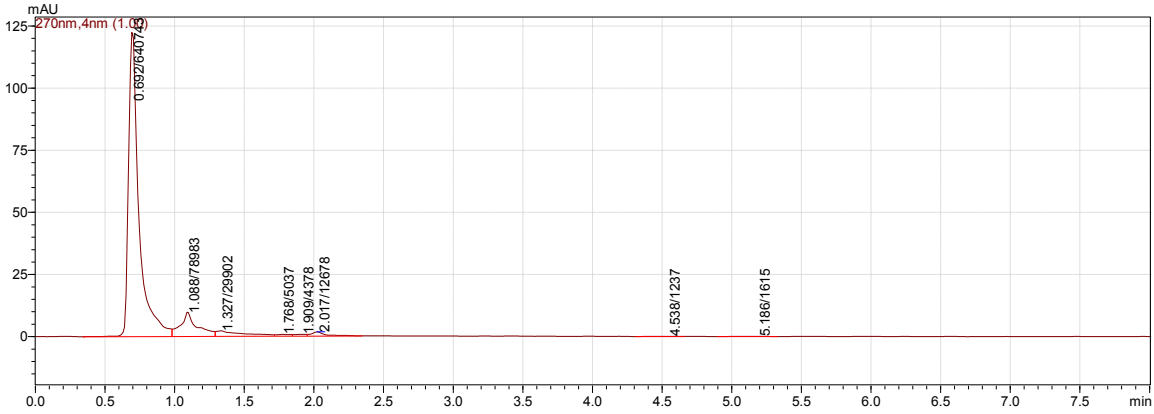

Figure D.12 Chromatogram of the 30 minutes treated sample by US/Ozone

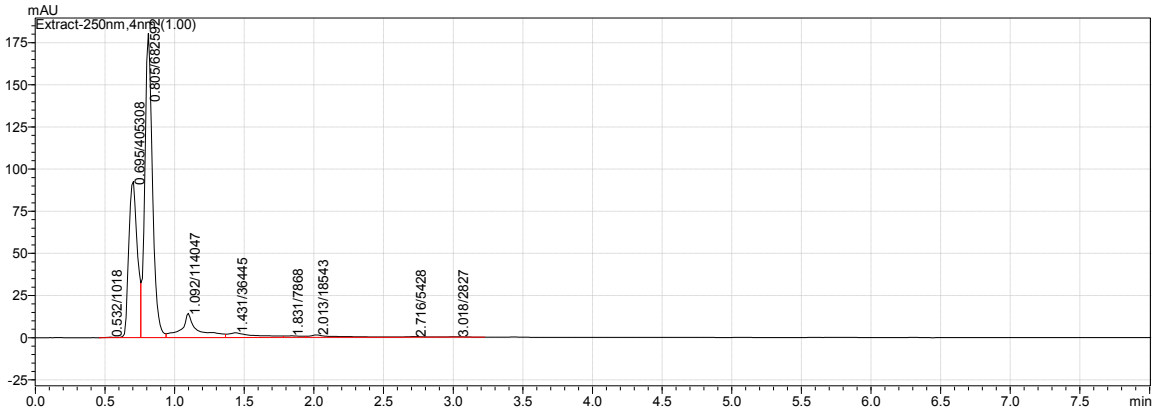

Figure D.13 Chromatogram of the 10 minutes treated sample by US/Ozone/H_2O_2

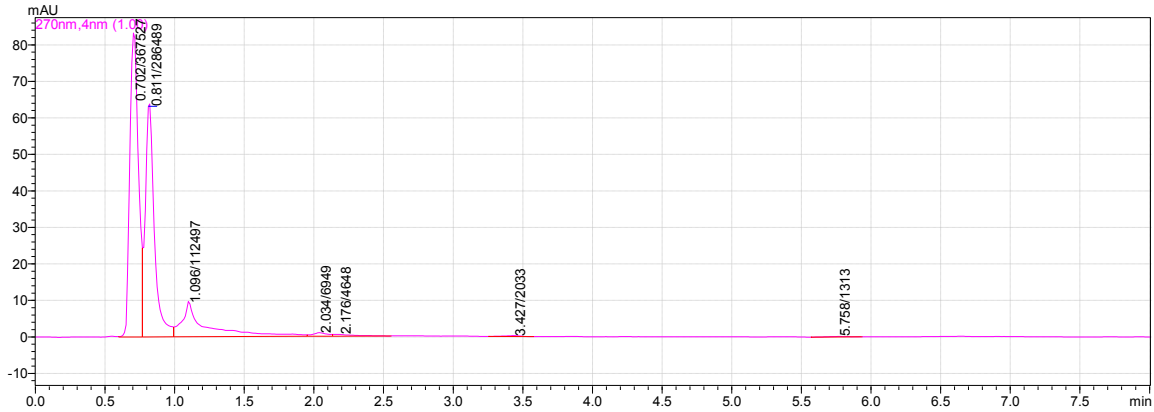

Figure D.14 Chromatogram of the 20 minutes treated sample by US/Ozone/H_2O_2

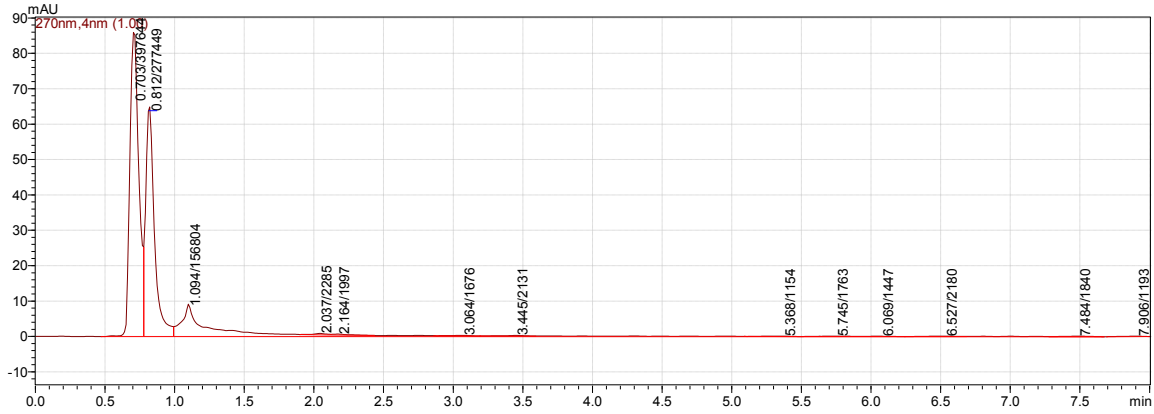

Figure D.15 Chromatogram of the 30 minutes treated sample by US/Ozone/H_2O_2

REFERENCES

AEPA (Australian Environmental Protection Agency) (1998). *Environmental Guidelines for the Textile dyeing and Finishing Industry*. Melbourne: State Government of Victoria

Agarwal, S. (1996). *Industrial environment: Assessment and strategy*. New Delhi, India: APH publishing Corporation

Al-Kdasi A., Idris A., Saed K., Teong C. (2004). Treatment of textile wastewater by advanced oxidation processes - A Review. *Global Nest: The Int. J*, 6 (3), 222-230

Archibald, F. (1997). The use of ozone to decolorize residual diret paper dyes in kraft paper machine whitewater . *Ozone Science and Engineering*, 19 (6), 549-565

Arslan I., Isil A.B., Tuhkanen I.A. (1999). Advanced oxidation of synthetic dyehouse effluent by O_3, H_2O_2/O_3 and H_2O_2/UV processes. *Environmental Technology*, 20, 921-931

Arslan-Alaton, I. (2007). Degradation of a commercial textile biocide with advanced oxidation processes and ozone. *Journal of Environmental Management*, 82 (2), 145-154

Aslam M.M., Baig M.A., Hassan I., Qazi I.A, Malik M., and Saeed H. (2004). Textile wastewater characterization and reduction of its COD & BOD by oxidation. *EJEAFChe*, 3, 804-811

AWWARF (American Water Works Association Research Foundation) (1998). *Development of disinfection guidelines for the installation and replacement of water mains*. Denver: AWWARF

Azbar N., Yonar T., Kestioglu K. (2004). Comparison of various advanced oxidation processes and chemical treatment methods for COD and color removal from a polyester and acetate fiber dyeing effluent. *Chemosphere*, 55 (35)

Balanoskyl, E., Herrera, F., Lopez, A., and Kiwi J. (2000). Oxidative degradation of textile wastewater. Modeling reactor performance. *Water Research*, 34 (2), 582-596

Beltrán, F.J., Ovejero G. and Rivas J. (1996). Oxidation of polynuclear aromatic hydrocarbons in water. *Ind. Eng. Chem. Res*, 35, 883

Bidga R. (1995). Consider Fenton chemistry for wastewater treatment. *Chem. Engineering Progress*, 91 (12), 62

Blesa M.A. (Ed.). *Eliminación de Contaminantes por fotocatálisis heterogénea*. Buenos Aires: Red CYTED VIII-G

Bolton J. R. (1996). Figures of merit for the technical development and application of advanced oxidation processes. *J. Adv. Oxid. Technol.*, 1 (1), 13

Brown, U. P. (1986). The degradation of dyestuffs: part II Behaviour of dyestuffs in aerobic biodegradation tests. *Chemosphere* , 15, 479-491

Buxton G.V. (1988). Critical Review of Rate Constants for Hydrated Electrons, Hydrogen Atoms and Hydroxyl Radicals (OH/O^-) in Aqueous Solution. *Journal Physical and Chemical Reference Data* , 17, 13

Buxton, G. V. (1988). Critical review of rate constants of hydrated electrons, hydrogen atoms and hydroxyl radicals (OH/O^-) in aqueous solution. *J. Phys. Chem. Ref. Data*, 17, 513-886

Calgon AOT Handbook. (1996). Ontario: Calgon Carbon Oxidation Technologies.

Chowdhury P, Viraraghavan T. (2009). Sonochemical degradation of chlorinated organic compounds, phenolic compounds and organic dyes - a review. *Sci Total Environ.*, 407 (8), 2474-2492

Crittenden J. C., Zhang Y., Hand D. W., Perram D. L., Marchand E. G. (1996). Solar Detoxification of Fuel Contaminated Groundwater using Fixed-Bed Photocatalysts. *Water Environment Research*, 68 (3), 270-278

David Yao C.C and Haag W. R. (1991). Rate constants for direct reactions of ozone with several drinking water contaminants. *Water Research*, 25 (7), 761-773

Duguet, J. A. (1989). Application of combined ozone-hydrogen peroxide for the removal of aromatic compounds from a ground water. *Ozone Sci. & Eng.*, 12, 281-284

Dyeing for a change: Current Conventions and New Futures in the Textile Color Industry (2006, July). Retrieved December 2011, from Better Thinking: www.betterthinking.co.uk

Eren Z., Ince N.H. (2010). Sonolytic and sonocatalytic degradation of azo dyes by low and high frequency ultrasound. *Journal of Hazardous Materials*, 177 (1-3), 1019-1024

Ertas, T. (2001). Biological and physical-chemical treatment of textile dyeing wastewater for color and COD removal. *Ozone Science and Engineering*, 23 (3), 199-206

Faroq, S. M. (1991). Activated Carbon Adsorption and Ozone Treatment of a Petrochemical Wastewater. *Environ. Technol.*, 12 (2), 147-159

Fogler, S. (2004). *Elements of Chemical Reaction Engineering*, fourth ed. NJ: Prentice Hall Publications

Gernjak, D. W. (2007). *Solar Photo-Fenton Treatment of EU Priority Substances – Process Parameters and Control Strategies*. University of Natural Resources and Applied Life Sciences, Vienna, Department für Wasser-Atmosphäre- Umwelt, Vienna

Gina Melin (1999). *Treatment Technologies for Removal of Methyl Tertiary Butyl Ether (MTBE) from Drinking Water: Air Stripping, Advanced Oxidation Processes, Granular Activated Carbon and Synthetic Resin Sorbents*. Center for Groundwater Restoration and Protection. Retrieved November, 2011, from http:// www.nwri-usa.org/uploads/Treatment%20Technologies%20Book.pdf

Glaze W.H., Kang. J.W. (1989). Advanced oxidation processes: Test of a kinetic model for the oxidation of organic compounds with ozone and hydrogen peroxide in a semibatch reactor. *Industrial Engineering Chemical Research*, 28, 1580-1587

Glaze, W. H. (1987). The chemistry of water treatment processes involving ozone, hydrogen peroxide and UV-radiation. *Ozone: Sci. Eng.*, 9, 335–352

Gottschalk C., Libra J.A., Saupe A. (2010). *Ozonation of Water and Waste Water*. WILEY –VCH Weinheim

Guendy H. R. (2007). Ozone Treatment of Textile Wastewater Relevant to Toxic Effect Elimination in Marine Environment. *Guendy Egyptian Journal of Aquatic Research*, 33 (1), 98-115

Gulkaya, G. S. (2006). Importance of H_2O_2 /Fe^{2+} ratio in Fenton's treatment of a carpet dyeing wastewater. *J.Hazardous Materials,* 136 (B), 763-769

Hai, Faisal Ibney, Fukushi K., Yamamoto K. (2009) *Hybrid Treatment Systems for Dye Wastewater. Department of Urban Engineering*. Tokyo: Environmental Science Center, University of Tokyo

Hancock, F. (1999). Catalytic strategies for industrial water reuse. *Catalysis Today*, 33, 3-9

Hatanaka S., Tuziuti T., Kozuka T., Mitome H. (2001). *Dependence of sonoluminescence intensity on the geometrical configuration of a reactor cell*. IEEE Transactions on Ultrasonics, Ferroelectrics, and Frequency Control, 48, 28–35

Henglein A., Gutierrez M. (1990). Chemical effects of continuous and pulsed ultrasound: a comparative study of polymer degradation and iodide oxidation. *J. Phys. Chem.*, 94 (12), 5169-5172

Hering, F. M. (1993). *Principles and applications of aquatic chemistry*. New York: Wiley Publishing

Hoigne J., Bader H. (1976). The Role of Hydroxyl Radical Reactions in Ozonation Processes in Aqueous Solution. *Water Research*, 10, 377-386

Hoigne, J. (1998). *Chemistry of Aqueous Ozone and Transformation of Pollutants by Ozonation and Advanced Oxidation Processes*. J. Hrubec, The Handbook of Environmental Chemistry (Vol. 5). Berlin: J.Hrubee (Ed.), Springver-Verlag Publishing

Howard, P. (1989). *Handbook of environmental fate and exposure data for organic chemical. Volume I Large production and priority pollutants*. Chelsea, Michigan, USA: Lewis Publishers

Hu, S.T., Yu Y.H. (1994). Preozonation of chlorophenolic wastewater for subsequent biological treatment. *Ozone Sci. Eng.* , 16, 13–28

Huang C.R., Lin Y.K. and Shu H.Y (1994). *Wastewater Decolorization And TOC-Reduction By Sequential Treatment*. New Jersey Institute of Technology, Chem. Engr., Chemistry And Environmental Science. Newark, NJ: American Dyestuff Reporter

Hung-Yee S. and Ching-Rong H., (1995). Degradation of commercial azo dyes in water using ozonation and UV enhanced ozonation process. *Chemosphere*, 31, 3813- 3825

Hunsberger, J. F. (1977). *Standard reduction potentials Handbook of Chemistry and Physics*. (R. C. In: Weast, Ed.) Ohio: CRC Press

Hyman M., Dupont R.R. (2001). *Groundwater and Soil Remediation: Process Design and Cost Estimating of Proven Technologies*. American Society of Civil Engineers, ASCE Press

Ince, N. H. (1999). "Critical" effect of hydrogen peroxide in photochemical dye degradation. *Water Research*, 33 (4), 1080-1084

J. Bandara, Nadtochenko V., Kiwi J., Pulga C. (1997). Dynamics of oxidant addition as a parameter in the modelling of dye mineralization (orange II) via advanced oxidation technologies. *Water Science and Technology*, 35 (4), 87-93

Jakoba L., Tarek M. (1993). Vacuum-ultraviolet (VUV) photolysis of water: oxidative degradation of 4-chlorophenol. *Journal of Photochemistry and Photobiology A: Chemistry*, 75 (2), 97-103

Kim, S. G. (1997). Landfill leachate treatment by a photoassisted Fenton reaction. *Water Sci. Technol.*, 35 (4), 239-248

Kontronarou, A. M. (1991). Ultrasonic irridation of p-Nitrophenol in aqueous solution. *J. Phys. Chem.*, 95, 3630-3638

Kuo, W. (1992). Decolorizing dye wastewater with Fenton's reagent. *Water Research J.*, 26 (7), 881-886

Langlais, B. D. (1991). *Ozone in Drinking Water Treatment: Application and Engineering*. Boca Raton, FL : AWWARF and Lewis Publishers

Le Marechala A. Majcen, Slokara Y. M., Tauferb T. (1997). Decoloration of chlorotriazine reactive azo dyes with H_2O_2/UV. *Dyes and Pigments*, 33 (4), 281-298

Legrini, O., and Oliveros, E. B. (1993a). Photochemical process for water treatment. *Chemical Reviews*, 93, 671-698

Liu, Robert, Chiu, H.M., Shiau, Chih-Shiuc, Yeh, Ruth Yu-Li, Hung, Yung-Tse (2007). Degradation and sludge production of textile dyes by Fenton and photo-Fenton processes. *Dyes and Pigments Elsevier*, 73 (1), 1-6

Lorimer, T. M. (1988). *Sonochemistry, Theory, Applications and Uses of Ultrasound in Chemistry*. Chichester: Ellis Horwood Series in Physical Chemistry

Malato S., Bianco J. (2002). Photocatalysis with solar energy at a pilot-plant scale: an overview. *Applied Catalysis*, 37, 1-15

Mason T. J. (1999). *Sonochemistry: current uses and future prospects in the chemical and processing industries*. Phil. Trans. R. Soc. Lond. A, 357 (1751), 55-369

Melin G. (2000). *Treatment Technologies for Removal of Methyl Tertiary Butyl Ether (MTBE) from Drinking Water: Advanced Oxidation Processes*. California: National Water Research Institute

Metcalf, Eddy, Inc. (2003). *Wastewater engineering treatment and reuse* (Fourth Edition ed.). New York: McGrawHill Publishing

Michelsen D.L., Woodby P. (1992). *Pretreatment of textile dye concentrates using fentons reagent and ozonation prior to biodegredation*. Preprint for AATCC International Conference and Exhibition. Atlanta

Mitrovic J., Radovic M. (2011). Decolorization of textile azo dye Reactive Orange 16 with UV/H_2O_2 process. *Serb. Chem. Soc.*, 76 (0), 1-22

Molina, V. G. (2006). *Doctoral Thesis: Wet OxidationProcesses For Water Pollution Remediation. Department of Chemical Engineering*. Barcelona: Barcelona University

Morel, F.M.M. and Hering J.G. (1993). *Principles and Applications of Aquatic Chemistry*, New York: John Wiley & Sons Publishing

Munter, A. R. (2001). Advanced Oxidation Processes-Current Status and Prospects. *Proc. Estonian Acad. Sci. Chem.*, 50 (2), 59-80

National Water Research Institue, Advanced Oxidation Report. Retrieved December 20, 2011, from http://www.nwri-usa.org/pdfs/TTChapter3AOPs.pdf

Neppolian, B. S. (2001). Kinetics of photocatalytic degradation of reactive yellow 17 dye in aqueous solution using UV irradiation. *J Environ. Sci. Health Part A., Tox Hazard Subst. Environ. Eng.*, 36, 203-213

Nicholas G. Pace, A. C. (1997). Short pulse acoustic excitation of microbubbles. *Acoustical Society of America*, 1474-1479

O Ecotextiles, What can be considered the "good" chemicals in textile processing. Retrieved December 28, 2011, from O Ecotextiles: http://oecotextiles.wordpress.com/

Olcay Tünay, Kadbasli I. (1996). Color removal from textile wastewaters. *Water Science and Technology*, 34 (11), 9-16

Ollera I., Malato S., and Sanchez-Perez J.A. (2011). Combination of Advanced Oxidation Processes and biological treatments for wastewater decontamination—A review. *Science of The Total Environment*, 409 (20), 4141-4146

Pera-Titus M., Garcia-Molina, V., Banos, M.A., Gimenez, J., Esplugas, S. (2004). Degradation of chlorophenols by means of advanced oxidation processes: a general review. *Applied Catalysis B: Environmental*, 47, 219–256.

Perkowski J., Kos L. (2003). Decolouration of model dye house wastewater with advanced oxidation processes. *Fibres and Textiles in Eastern Europe*, 11, 67-71

Peternel I., Koprivanac N. (2006). UV-based processes for reactive azo dye mineralization. *Water Research* , 40 (3), 525-532

Peyton G. R., Bell O.J., Girin E., LaFaivre M. (1998). *Effect of Bicarbonate Alkalinity on Performance of Advanced Oxidation Processes*. Denver: AWWARF Publishing

Prousek, J. (1996). Advanced Oxidation Processes for Water Treatment. *Chemical Listy*, 90 (4), 229-237

Rauf, M. A. (2005). Photolytic oxidation of coomassie brilliant blue with H_2O_2. *Dyes and Pigments*, 66 (3), 197-200

Rodriguez, C. D. (2002). Photocatalytic degradation of dyes in aqueous solution operating in a fluidised bed reactor. *Chemosphere*, 46, 83-86

Rodriguez, M. (2003). *Doctoral Thesis: Fenton and UV-vis based advanced oxidation processes in wastewater treatment: Degradation, mineralization and biodegradability enhancement*. Department of Chemical Engineering. Barcelona: Barcelona University

Rosario L.C., Abel G.E. (2002). Photodegradation of an azo dye of the textile industry. *Chemosphere*, 48, 393-399

Roy, R. A. (1999). *Cavitation Sonophysic*. In L.A. Crum, Sonochemistry and Sonoluminescence (pp. 25-38). Netherlands: Kluwer Academic Publishers

Savin Irina-Isabella and Butnaru R. (2008). Wastewater Characteristics In Textile Finishing Mills. *Environmental Engineering and Management Journal*, 7 (6), 859-864.

Sheng H. Lin, Chi M. Lin (1993). Treatment of textile waste effluents by ozonation and chemical coagulation. *Water Research*, 27 (12), 1743-1748

Stumm W., Morgan J. (1996). *Aquatic Chemistry: Chemical Equilibria and Rates in Natural Waters* (3rd Edition ed.). New York: A Wiley Interscience Publication John Wiley and Sons Publishing

Suslick, K. S. (1990). Sonochemistry. *Science*, 247, 1439-1445

Suslick, K. S., and Flint, E. B. (1991). Sonoluminescence of Alkali Metal Salts. *J. Phys. Chem.*, 95, 1484-1488

Sychev, A. I. (1995). Iron Compounds and the Mechanisms of the Homogeneous Catalysis of the Activation of O_2 and H_2O_2 and of the Activation of Organic Substrates. *Russian Chemical Reviews*, 64 (12), 1105-1129

Taylor & Francis Group (2007). *Critical Reviews in Environmental Science and Technology,* 1547-6537

Techcommentary: *Advanced Oxidation Processes for Treatment of Industrial Wastewater* (1996). NY: EPRI Community Environmental Center Publ.

Tezcanli-Güyer G. and Ince N. (2004). Individual and combined effects of ultrasound, ozone and UV irradiation: a case study with textile dyes. *Ultrasonics*, 42 (1-9), 603-609

Tezcanli-Güyer G., (1998). *Master Thesis: Reuse of Textile Dyebaths by Treatment With Advanced Oxidation*, Istanbul: Bogazici University

Tezcanli-Güyer G., (2003). *Doctoral Thesis: Degradability of Synthetic Dyestuff With Acoustic Cavitation: Impacts of System Conditions and Physical/Chemical Agents*, Istanbul: Bogazici University

Turhan K., Turgut Z. (2009). Decolorization of direct dye in textile wastewater by ozonization in a semi-batch bubble column reactor. *Desalination*, 242 (1-3), 256-263

USEPA (2006). *Air Quality Criteria for Ozone and Related Photochemical Oxi*dants. National Center for Environmental Assessment-RTP Office, Office of Research and Development, NC, US

Vajnhandl S., La Marechal A.,. (2007). Case study of the sonochemical decolouration of textile azo dye Reactive Black 5. *Journal of Hazardous Materials*, 141 (1), 329-335

Vandevivere P.C., Bianchi R., Verstraete W. (1999) Treatment and reuse of wastewater from the textile wet-processing industry: Review of emerging technologies. *J. Chem. Technol. Biot.*, 72 (4), 289-302

Von Gunten U. (2003). Ozonation of drinking water: Part I. oxidation kinetics and product formation. *Water Research*, 37, 1443-1467

Wu, J.N (2001). Ozonation of aqueous azo dye in a semi-batch reactor. *Water Research*, 35 (4), 1093-1099

Yasar A., Nasir A. (2006). Energy requirement of ultraviolet and AOPs for the post-treatment of treated combined industrial effluent. *Color Technol.*, 122 (201)

Young, L. and Yu J. (1997) Ligninase-catalysed decolorization of synthetic dyes. *Water Research*, 31, 1187-1193

Yusuff R.O, and Sonibare J. (2004). Characterization of Textile Industries' Effluents in Kaduna, Nigeria and Pollution Implications. *Global Nest: the Int. J.*, 6 (3), 212-221

Zapata A., Ollera I., Sirtoria C., Rodríguez A., Sánchez-Pérez J.A., López A., Mezcuae M., Malato S. (2010). Decontamination of industrial wastewater containing pesticides by combining large-scale homogeneous solar photocatalysis and biological treatment. *Chemical Engineering Journal*, 160 (2), 447-456